Fast Characterization of Power Quality Events based on Discrete Signal Processing and Data Mining

Dissertation submitted in partial fulfillment

of the requirements of the degree of

Doctor of Philosophy

in

Electrical Engineering

by

Swarnabala Upadhyaya

(511EE112)

based on research carried out

under the supervision of

Prof. Sanjeeb Mohanty

DEPARTMENT OF ELECTRICAL ENGINEERING

NATIONAL INSTITUTE OF TECHNOLOGY ROURKELA

SEPTEMBER 2016

CERTIFICATE OF EXAMINATION

13/01/2017

Roll Number :	511EE112
Name:	*Swarnabala Upadhyaya*
Title of Dissertation:	*Fast Characterization of Power Quality Events based on Discrete Signal Processing and Data Mining*

We the below signed, after checking the dissertation mentioned above and the official record book(s) of the student, hereby state our approval of the dissertation submitted in partial fulfillment of the requirements of the degree of *Doctor of Philosophy in Electrical Engineering at National Institute of Technology Rourkela*. We are satisfied with the volume, quality, correctness, and originality of the work.

Prof. S. Karmakar	Prof. D.P. Mohapatra	Prof. K.B. Mohanty
(Member, DSC)	(Member, DSC)	(Member, DSC)
Prof. A. K. Panda		Prof. S. Mohanty
(Chairperson, DSC)		(Supervisor)

Prof. D. Das

(External Examiner)

Department of Electrical Engineering
National Institute of Technology, Rourkela
Rourkela-769008, Odisha, India.

Certificate

This is to certify that the thesis entitled *"Fast Characterization of Power Quality Events based on Discrete Signal Processing and Data Mining"* by *Swarnabala Upadhyaya* submitted to the National Institute of Technology, Rourkela for the award of Doctor of Philosophy in Electrical Engineering, is a record of bonafide research work carried out by him in the Department of Electrical Engineering, under my supervision. I believe that this thesis fulfills part of the requirements for the award of degree of Doctor of Philosophy. The results embodied in the thesis have not been submitted for the award of any other degree elsewhere.

Place: Rourkela
Date: 29.09.16

Prof. Sanjeeb Mohanty
Department of Electrical Engineering
National Institute of Technology, Rourkela
Rourkela-769008, Odissa, India.

Dedicated
to
The unseen
and
the seen God

Declaration of Originality

I, Swarnabala Upadhyaya, Roll Number 511EE112 hereby declare that this dissertation entitled *"Fast Characterization of Power Quality Events based on Discrete Signal Processing and Data Mining"* represents my original work carried out as a doctoral student of NIT Rourkela and, to the best of my knowledge, it contains no material previously published or written by another person, nor any material presented for the award of any other degree or diploma of NIT Rourkela or any other institution. Any contribution made to this research by others, with whom I have worked at NIT Rourkela or elsewhere, is explicitly acknowledged in the dissertation. Works of other authors cited in this dissertation have been duly acknowledged under the section "Bibliography". I have also submitted my original research records to the scrutiny committee for evaluation of my dissertation.

I am fully aware that in case of any non-compliance detected in future, the Senate of NIT Rourkela may withdraw the degree awarded to me on the basis of the present dissertation.

Date: 29.09.16
NIT Rourkela

Swarnabala Upadhyaya

ACKNOWLEDGEMENTS

Everywhere there is, at most, only a beginning of beginnings. At, the beginning, I owe thanks to many people whose support, encouragement and motivation, made me capable in this long journey towards Ph.D.

My deepest sincere gratitude goes to my supervisor, Prof. Sanjeeb Mohanty for his inspiring guidance, advice, and unwavering confidence throughout the course of this work. I also thankful to him for his patience, timely help, and gracious encouragement throughout the work. It has been an honour to have work under his guidance. I am truly indebted to him for providing all official and laboratory supports. I also thank him for his insightful comments and suggestions that helped me a lot to improve my understandings.

I expressed my sincere gratitude to my Doctoral Scrutiny Committee members, Prof. A.K. Panda, Prof. S. Karmakar, Prof.K.B. Mohanty of Department of Electrical Engineering; Prof. D.P. Mohapatra of Department of Computer Science and Engineering for taking the time to review my work and providing constructive suggestions. I am very much obliged to the Director, Prof. R.K. Sahoo and Prof. J.K. Satpathy, Head of Electrical Engineering Department for providing all possible facilities regarding my academic requirements. I express my gratitude to the faculty and staff members of Electrical Engineering Department of National Institute of Technology, Rourkela, especially Mr. Jagdish Kar and Mr. Bhanu Pratap Behera for their cooperation and for providing me all the official and laboratory facilities in various ways for the smooth completion of this research work.

I am really indebted to Prof. C.N. Bhende of School of Electrical Sciences, Indian Institute of Technology, Bhubaneswar for his perceptive comments, suggestions and motivations at various point of time of the work. I am extremely grateful to my M.Tech supervisor Prof. M. Tripathy, Veer Surendra Sai University of Technology, Burla for his encouragement in the field of research.

During this long journey of Ph.D, I have been able to cross many huddles due to my great circle of friends and colleagues. First I would like to thank Mr. Abhisek for his inspiration and generous help whenever it was needed. It is my pleasure to have a friend circle, who have inspired and encouraged a lot during the up and down moments of the journey. I am specially indebted to Mr. A.K. Pradhan, Ms. S. Kar, Mr. A. Biswas, Mr. R. Rout, Mrs. S.D. Swain, Mr. P.K. Sahu, Mr. K. Krishna and Mr. S. Mohapatra who helped me in my research work. I also thank to Mr. Avimanyu, Mrs. Prasantini, Ms. Pili, Mr. Dillip for their inspiration and emotional support. I feel blessed to have so many group bodies: Mr. A.K. Nayak, Mrs. T. Dattaroy, Mrs. P.P. Pradhan, Mrs. T. Padhi, Mr. R.N. Mishra, Mr. V.S. Kummkuri, Mr. K. Thakre, Mr. A. Chatterjee, Ms. J. Mishra, Ms. S. Swain, Mrs. D. Pradhan, Ms. N. Kumari, Ms. A. Das, Mr. S. Nayak, Mr. P. Sekhar, Mrs. J. Dalai, Mr. S. Mahapatra. I may be forgiven if a few names have not been mentioned.

I wish to place on record my deep sense of gratitude to my parents (Mrs. S. Upad-

hyaya and Mr. P.C. Upadhyaya), brothers (Mr. J. Upadhyaya, Mr. S. Upadhyaya, Mr. A. Upadhyaya), sisters (Mrs. D. Upadhyaya and Mrs. T. Upadhyaya.) and Sister-in-law (Mrs. A. Upadhyaya, Mrs. S. Upadhyaya) for their kind sacrifice and support without which I could not have reached this place to carry out this research. I would like to express my greatest admiration to all my family members for their caring, love, moral and emotional support during this long journey. I also express my gratitude to my parents in-laws.

I would like to record my warmest feelings of thanks to my family particularly, my husband Mr. Santosh who has endured a lot by tolerating my negligence during this period.

Above all, I would like to thank *The Almighty God* for the wisdom and perseverance that he has bestowed upon me during this research period and indeed, throughout my life.

Swarnabala Upadhyaya

Abstract

The extensive use of solid-state power electronics technology in industrial, commercial and residential equipment causes degradation of quality of electric power with the deterioration of the supply voltage. The disturbances results in degradation of the efficiency, decaying the life span of the equipment, increase in the losses, electromagnetic interference, the malfunctions of equipment and other harmful fallout. Generally, the power quality is the measurement of an ideal power supply. More over the power quality is the continuity and characteristics of the supply voltage in terms of frequency, magnitude and symmetry. The mitigation of power quality (PQ) disturbances requires detection of the source and causes of disturbances. The MODWT is a suitable method for forecasting of further occurrence of disturbance. However proper and quick detection and localization of the disturbances plays a crucial role in the power quality environment. Hence, in this thesis, a fast detection technique has been proposed along with the MODWT in order to provide time-scale representation of the signals by removing the drawback of the traditional methods like DWT and ST. Comparative analysis shows that SGWT is a best technique for localization and detection of distortions than the conventional methods.

During the course of the research, it is found that suitable algorithms are required for the characterization of the disturbances for smooth mitigation of the distortions. So, data mining based classifier has been proposed for discrimination of both single and multiple disturbances. Further, the suitable features are needed for efficient characterization of the disturbances. Hence, the suitable features are extracted in order to

reduce the number of raw data. The data normalization also plays a crucial role for efficient classification. These classification techniques are fast and able to analyze large number of disturbances. In this thesis, large numbers of signals are synthesized both in noisy and noise free environment. In the real time environment, these techniques have been performed satisfactorily. This leads to increase in the overall efficiency of the combination of the detection and classification method.

In recent times, with the advancement of renewable source requires better quality of power. The important issue of the today's distributed generation based interconnected power system is the islanding detection. Non detection zone is a good and reliable measurement of the islanding. However, failure to detect islanding situation sometimes leads to number of serious problem both for the utility and the customers. Hence, this thesis also provides a comparative analysis of the benefits and the drawbacks of aforementioned detection methods which are applied in power quality environment. The voltage signal at the PCC of the renewable distributed generation embedded with IEEE−14 bus system is captured and given as input to the analysis methods in order to extract features from the output of the analysis. The proposed SGWT properly discriminates power quality disturbances from the islanding events by introducing threshold selection. The data mining classifiers are implemented for classification of power quality as well as islanding events captured from IEEE bus system. Similar to the previous cases, the signals of same length are given to all the detection methods in ordered to compare the time of operation of each these methods. Moreover, the proposed techniques have been applied in noise free and noisy environment, bus system embedded with renewable source, real time environment etc.

The overall findings of the thesis could be useful for the industrial and domestic applications. Since the detection methods are simple and faster, they could be useful for power industry and other applications such as medical science etc. Similarly, the classification can be used for application such as stock exchange, medical science etc.

Contents

List of symbols and acronyms

List of symbols

$\mathbb{R}$	:	The set real numbers
a	:	The scale factor
b	:	Translation factor
$g(\cdot)$	:	The mother wavelet
$S(t)$	:	The original time signal
$l\,(n)$	:	Low pass filter
$h\,(n)$	:	High pass filter
$db4$	:	Daubechies wavelet of order 4
j_{max}	:	Maximum Decomposition Level
$p.u$	:	Per Unit
V	:	voltage in volt
$X[n]_{\text{even}}$	:	The set of even index points
$Y[n]_{\text{odd}}$	:	The set of odd index points
$L1, L2, \ldots, L7$	:	Levels of decomposition
$X1$	:	Standard deviation
$X2$	:	Energy of details
$X3$	:	CUSUM
$X4$	:	Entropy
L-G	:	Single line to ground
L-L	:	Line to line
L-L-G	:	Double line to ground
$C1, C2, \ldots, C10$	:	Class Levels

$\%CA$	:	Percentage of classification accuracy
dB	:	Decibel
V_a, V_b, V_c	:	Three phase voltages
r_{hk}	:	Line Resistance
x_{hk}	:	Line Reactance
$b_h = b_k$	:	Half line charging susceptance
m_{tap}	:	Tap setting value
p_l	:	Real power (load)
q_l	:	Reactive power (load)
b_{sh}	:	Susceptance
pv	:	Generator bus
q_G^{max}, q_G^{min}	:	Reactive power load
p_G	:	Real power generation limit
v_G	:	Generator voltage limit

List of acronyms

STFT	:	Short Time Fourier transform
ST	:	S-transform
MODWT	:	Maximal overlap discrete wavelet transform
DWT	:	Discrete Wavelet transform
CWT	:	Continuous wavelet transform
MRA	:	Multi-resolution analysis
WT	:	Wavelet Transform
EMC	:	Electromagnetic Compatibility
IEC	:	International Electrotechnical Commission
AWGN	:	Additive White Gaussian Noise
FFT	:	Fast Fourier Transform
IEEE	:	Institute of Electrical and Electronic Engineers
THL	:	Threshold line
PI	:	Performance indices
PQDI	:	Power quality disturbance with islanding
SMS	:	Slip mode frequency drift
AFD	:	Active frequency drift
OOB	:	Out of bag
CUSUM	:	Cumulative sum
STD	:	Standard deviation
PQ	:	Power Quality
NDZ	:	Non-detection zone
KF	:	Kalman Filter
PA	:	Prony analysis
GT	:	Gaber transform
SNR	:	Signal to noise ratio
CUSUM	:	Cumulative sum

RF	:	Random Forest
DT	:	Decision Tree
MLP	:	Multilayer perceptron
PQD	:	Power quality disturbance
PCC	:	Point of common coupling
PV	:	Photovoltaic
HMMs	:	Hidden Markov Models
MLP	:	Multilayer perceptron
ANN	:	Artificial Neural Network
MATLAB	:	Matrix Laboratory

List of Figures

List of Tables

Chapter 1

Introduction

1.1 Broad area of research

The continuous growth in the application of the microprocessor-based control and the power electronic devices and the adjustable-speed motor drives increases emphasis on the quality of power as these are more sensitive to power quality variations than the traditional equipments. Hence, the term "power quality" has become a prolific buzzword in the power industry since the late $1980s$. Moreover, the power quality (PQ) is like an umbrella which covers various disturbances of the voltage and the current such as the voltage sag, the swell, the harmonics and the oscillatory transients which cause mal-function of the sophisticated equipments. In other words the "power quality" is a nonstop dynamic variation both in time and space. The concern over quality of power has been increasing rapidly as the present life requires a continuous supply of electrical energy. Similarly, the continuous increase of load demand both in the public sectors as well as the industries has made the PQ a serious issue. The presence of disturbances in the loads is responsible for the deviation of the voltage and the current from the ideal waveform. This declines the performance and the lifespan of equipments and also creates instability in the system. Hence, the healthy power system operation requires continues supervision, proper monitoring and the optimum control in terms of power quality improvement.

Moreover, the quality of electricity has become an important issue for both the utilities and the end users. The increased use of non-linear loads has made the PQ a

pressing issue for the power system engineers unlike some years ago when the loads were linear. Hence, the issue of PQ has become more and more important with each passing day. The proper assessment of the active power, the apparent power and the reactive power is a significant issue in many applications such as the industry, the project, public sector etc. Hence, the improvement of PQ requires proper detection and localization of sources and the cause of disturbances. However, it is aimed at improving PQ with a fast detection and classification technology.

1.2 Organisation of the Chapter

The Chapter is organised as follows: Section-1.1 deals with the background of this research work. Power quality issues are described in Section-1.3 along with the cause of initiation and impact of distortions. Similarly, the Section-1.4 deals with the PQ standards. The detection, localisation and classification approaches are introduced in Section-1.5. Similarly, the main influencing factors and the aim of this work is presented in Section-1.6 and Section-1.7 respectively. The work is briefly described in Section-1.8. Section-1.9 provides the scope for future work. Finally, the last Section-1.10 provides the organisation of the thesis.

1.3 Power Quality Issues

The power quality is the interaction of the electrical power with the electrical equipments. In other words, the power quality issue can be defined as "Any power problem manifested in voltage, current or frequency deviations that results in failure or maloperation of the customer equipment" [1]. However, a disturbance in voltage very often causes a disturbance in current. Hence, PQ includes two aspects such as the quality of voltage and the quality of current. As there is no control over the current that particular loads draw, the power supply can only control the quality of the voltage. However, PQ term used to describe the electric power which drives the electrical load and the loads ability to function properly. The insufficiency of the proper power leads either to malfunction or permanent failure of the electrical equipments. The poor quality power also reduces the life span of the electrical equipments. There are many

factors which causes the poor power quality.

According to the International Electrotechnical Commission (IEC), the power quality is the set of parameter which defines the properties of quality of power as delivered to the end users in normal operating condition. In other words the PQ is the continuity and characteristics of the supply voltage in terms of frequency, magnitude and symmetry [2]. Similarly, PQ is the concept of providing power and grounding of the electronic equipment in such a manner that it can be suitable for the operation and comparable with the wiring system as well as other equipments in Institute of Electrical and Electronics Engineers (IEEE) Standard [3].

1.3.1 Main causes of Power Quality Disturbances

There are many factors responsible for creation of poor quality of power. The power quality issues are the consequences of

- Increasing use of solid state switching devices,
- Nonlinear and power electronically switched loads,
- Lighting control,
- Unbalanced power systems,
- Computer and data processing equipments,
- Industrial loads and domestic equipments.

1.3.2 Power Quality Disturbances and its Impact

The quality of power is seriously affected by the use of nonlinear loads as well as the various faults in the power system. However, the electronics equipments as well as the controlling equipments based on the computer implementation requires higher levels of power quality. Such type of devices are sensitive to small change of quality of power. Similarly, short time changes on power quality can cause great economical losses. Due to these reasons, the PQ problems have become an important issue irrespective of customers, power manufacturers and the equipment manufacturer etc. In deregulated

power industry and the competitive market, the price of power directly vary with the quality of power [4].

The PQ disturbances comprises of short duration and long duration voltage variations. According to IEC, the short duration voltage variations are the voltage sag, the voltage interruption and the voltage swell. Similarly, the overvoltage and the undervoltage are long duration voltage variations. However, the harmonics, the interharmonics, notching and the noise are steady−state deviations known as the waveform distortions. The aforementioned issues are more significant in interpreting the actual phenomena which may originate the PQ disturbances. The identification of the disturbances associated with the sources and impacts of these problems to mitigate these disturbance will increase the overall efficiency of the system.

Even though the PQ disturbances lasts only for a fraction of second it causes huge losses and hours of manufacturing downtime in case of industrial applications. Hence, during the last two decades or more, many researchers of different utilities around the world have implemented different power quality monitoring programmes in order to establish a good and healthy environment by providing better service to the end users. The proper monitoring requires detection and localisation of source of the disturbances and the cause of the disturbances. Moreover, continues monitoring requires large number of data. Hence, there is a need for proper collection, analysis and reporting of very large amount of data.

The proper monitoring of PQ requires review of the existing and the developing standards which has been addressed in the next section.

1.4 Power Quality Standards

The power quality monitoring standard needs to be persistent with the existing and the developing international practices. The IEC has defined the Electromagnetic Compatibility (EMC) standardisation, aiming at assuring compatibility between the supply networks and the end users. Most of the materials contained in the IEC series of standards are selected from the guidelines and the standards developed by individual countries. Similarly, other organisations which have developed their own standards are the IEEE, the UIE, the ANSI, CENELEC, and NEMA etc.

Table 1.1: Details of Power Quality Issues

PQ Issues	Definition	Origin	Consequence
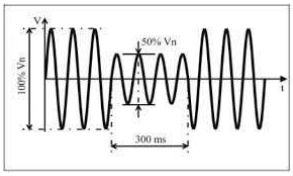 Sag	It is a reduction in the rms voltage between 0.1 to 0.9 pu at the power frequency for duration of 0.5 cycle to 1 minute.	• Abrupt increase of load • Failure of equipments • Ground faults • Lightening • Outages • Faults in transmission and distribution lines • Start-up of large motors	• Equipment shutdown • Malfunction of information technology equipment e.g. stoppage process • Tripping of Electromechanical relays • Disconnection and loss of efficiency of disk drives
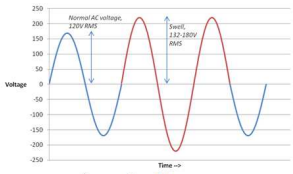 Swell	It is a increment of the rms voltage between 1.1 to 1.8 pu at the power frequency for duration of 0.5 cycle to 1 minute. It is opposite to the voltage dip.	• Shutdown of heavy loads • Badly regulated transformers • System faults • Capacitor switching and load switching • Abrupt power restoration	• Computer damages • Flickering of lighting • Damage or malfunction of power Protection equipment
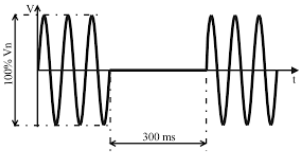 Interruption	An interruption occurs when the supply voltage decreases to less than 0.1 pu for a duration from few milli second to less than 1 minute.	• Opening and closing of automatic recloser of protective devices • Insulation failures of equipment • Lightning and insulator flashover	• Tripping of protective devices • Stoppage of sensitive equipment like PLC, computer, ASD • Tripping of Electromechanical relays • Loss of information
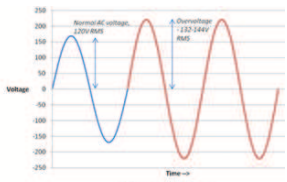 Overvoltage	It is an increment of the rms voltage greater than 1.1 pu at the power frequency for duration more than 1 minute.	• Switching on large load • Energizing of large capacitor bank • Incorrect tap settings on transformer	• Flickering of lighting and screen • Damage or malfunction of sensitive equipments

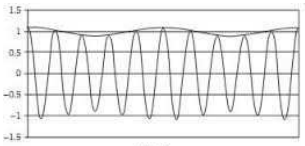 Flicker	Flickering occur when the amplitude varies between 0.1% to 7% of the nominal voltage at frequencies below 25 Hz.	• Arcing in power system • Small power loads variation such as power regulators, welders, boilers, cranes and elevators etc • Arc furnaces • Power electronic devices like cycloconverters and Static frequency converters • Starting of large motors • Oscillating load	• Flickering of lighting and screen • Maloperation of relays and contactors • Problem creates in sensitive equipments e.g medical laboratories. • Unsteadiness in visual impression
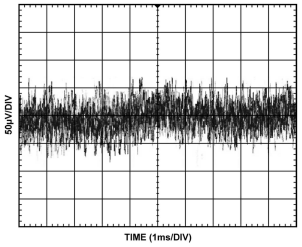 Noise	Noise is defined as the as unwanted electrical signal super imposed upon the power system signal.	• Power electronic devices • Control circuits • Solid−state devices and Switching power supplies • Arcing equipments	• Malfunction of microcomputer and programmable controller • Disturbances in sensitive electronic equipment • Maloperation of relays and contactors • Data loss
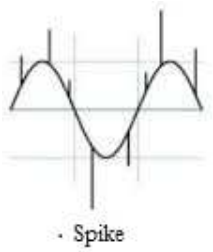 Spike	Spike is occurs when voltage varies very fast for duration of a several microseconds to few milliseconds.	• Disconnection of heavy loads • Lighting • Switching of power factor correction capacitor	• Damage of electronic components • Electromagnetic interference • Data loss • Destruction of insulation material

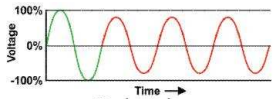 Undervoltage	It is a reduction in the rms voltage less than 0.9 pu of nominal value at the power frequency for duration greater than 1 minute.	• Switching on large load • Insulation failures of equipment • Switching off large capacitor bank	• Flickering of lightning • Flickering of lighting and screen • Stoppage of sensitive equipment like PLC, computer, ASD • Malfunction of information technology equipment e.g. stoppage process
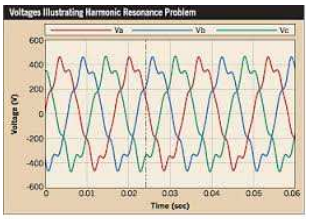 Harmonic	Harmonics are the periodic distortion of supply voltage in which frequencies are integer multiple of the supply frequency.	• Non-linear loads like power electronics devices, switched mode power supplies • Data processing equipments • Welding machines, rectifiers and DC brush motors.	• Over heating of transformer, cables and equipments • Electromagnetic interference with communication systems • Occurrence of resonance • Malfunction of the protective devices • Losses in power system • Distortion in transformer secondary voltage.

1.4.1 IEC Standards on Electromagnetic Compatibility (EMC)

Electromagnetic Compatibility of the systems or the equipments is to operate appropriately in the electromagnetic environment without producing overwhelming disturbances to any object in that environment [5]. The compatibility levels are based on 95% cumulative probability levels of the entire system considering the disturbances space and time variations.

The IEC standards and the technical reports are divided in to six parts.$610000-1-X$ working group has defined the PQ issues. $610000-2-X$ working group has concentrated on emission limits as well as the susceptibility of a particular type or class of appliances or equipments under certain environmental conditions. However $610000-3-X$ deals with the source and the impact of harmonics. Similarly, the $610000-4-X$ working group has contributed on the testing and the measurements of PQ (e.g. $61000-4-30$ is power quality measurements). The installation of protective devices in order to mitigate the disturbances are the contribution of $610000-5-X$ working group. The $610000-5-X$ standard is based on the Generic immunity and emissions. Moreover, $IECSC77A$ working group has concentrated on low frequency EMC Phenomena which is essentially equivalent of "power quality" in American terminology.

1.4.2 IEEE Standards

IEEE Standard 1152 provides standard definitions for the different kind of power quality (PQ) problems and the general guidelines for the power quality monitoring [3]. The working group of the IEEE Standard 1152.2 has developed the guidelines for the characterisation of different PQ problems which includes minimum magnitude, phase shift, duration etc for disturbances such as sag.

Similarly, another group has specified the exchange of power quality monitoring information in IEEE 1159.3 standard. Moreover, SCC−22 sponsored task group has developed IEEE Standard 1159 for monitoring of power quality. IEEE Standard 519 working group has concentrated on control of harmonics in Electrical power system such as the harmonic limits on the power systems, limit and consequence single phase harmonic and philharmonics.

These standards can provide proper guidance to understand the PQ disturbances and take adequate efforts in order to avoid the economic loss due to it. So in this process the efficient and the simple detection as well as the classification techniques are required for the proper discrimination of the disturbances. In this thesis, the proper and the quick detection and localisation of different PQ distortions along with the feature extraction and classification has been taken up.

1.5 Approaches for Detection, Localisation and Classification of PQ Disturbances

The mitigation of PQ disturbances requires proper localisation of the source and the cause of disturbances. The detection and identification of PQ disturbances are important aspects in order to resolve the power associated equipments or the facility problems. The characterisation of power quality disturbances involve following steps

- Collecting different type of power signals
- Analysing the signals passing through the transformation
- Extracting features from the out put of the analysis methods
- Inspecting the features by classifiers in order to discriminate the disturbances.

Power quality disturbance localisation is the key word in order to detect the distortions. In this thesis, the adopted detection and the classification techniques of PQ disturbances are the Wavelet Transform (WT) and the Data Mining (DM) respectively.

1.5.1 Wavelet Transform (WT)

In this thesis, the Wavelet transform has been utilized in order to analyze different synthesized and real time voltage signals. The Wavelet Transform employs small wavelets. The Wavelet can be defined as an oscillatory function having a zero mean (no d.c component) and decaying to zero. The WT uses the basis function known as the mother wavelet unlike the Fourier transform (FT). The analysis of the WT provides the time-scale representation by using the shifted and the dilated version

of the mother wavelet. The signal is decomposed into different frequency levels and presented as the wavelet coefficients. The signal components which are overlap both in the time and the frequency are separated in wavelet expansion. In this case, the signal is decomposed in to different resolution levels providing coefficients such as the detail and the approximation coefficients. The detail coefficients contain high frequency components and the approximation contains low frequency components. Generally, the distortions are present in detail coefficients. Any change in the smoothness of the signals or in wave shape can be detected at the finer decomposition levels. The variants of the wavelet transforms are the continuous wavelet transform (CWT), the discrete Wavelet transform (DWT) etc. The phasor representation of WT known as the S-transform (ST). The ST also has good multiresolution capability.

1.5.2 Data Mining (DM)

Data mining is a process by which the data is analyzed from different aspects and summarized into useful information i.e decision. Moreover, the Data mining software is a analytical tool which analyzes data by finding the correlations and the patterns among dozen of fields in the large relational database. Similarly, this tool extracts hidden predictive information from large databases. Hence, it is a computational process of discovering patterns from the large data sets by employing methods at the inspection of the machine learning, the artificial intelligence, the statistics and the database systems. However, the actual data mining is the semi-automatic or automatic analysis of the large data in order to extract the previous knowledge, interesting patterns (clustering analysis) and the dependencies (association rule mining). Six steps within a typical data mining process

1. Problem Understanding
2. Data Understanding
3. Data preparation
4. Modelling
5. Evaluation

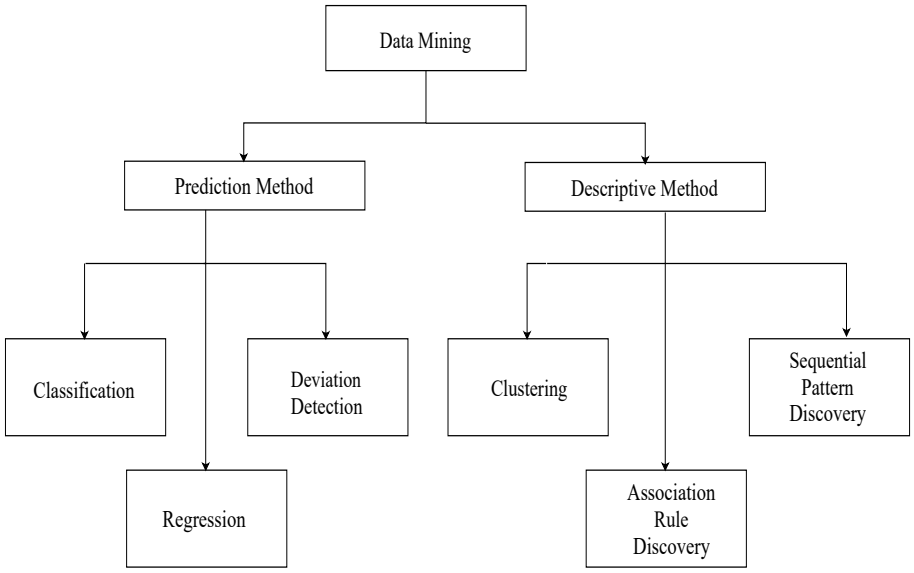

Figure 1.1: Categorisation of Data mining

6. Deployment

The function of the data mining is divided in to two categories such as predictive and the descriptive. The predictive method and the descriptive method again is divided in to different sub category presented in Figure 1.1

Classification method predicts the categorial class labels and the prediction method predicts continuous valued function. The classification is the discovery of a model which is interpreted from the knowledge of the data set. This model predicts the class label from the unknown data. The data mining based classification approaches are implemented in this thesis work for the discrimination of power system abnormality like different types of power quality disturbances and faults etc.

1.6 Motivation

There are several reasons for being motivated to work on the characterisation of synthesised, real time and renewable distributed generation based PQ disturbance using using discrete wavelet transform and data mining classifiers. Some of the reasons are mentioned below

1. The Implementation of the modern power electronics devices and the propaga-

tion of the nonlinear loads are the causes of creating distortions in the voltage and the current signals in terms of PQ disturbance which results in harmful consequence and economic losses. The mitigation of these disturbances require proper localisation of the source and the cause of disturbance. The traditional frequency analysis techniques have several draw backs.

- The Fourier transform (FT) only provides frequency components of the signal.
- The advance Fourier transform is Short Time Fourier transform (STFT) suffers from the fixed window and only suitable for the stationary signals.

2. The time scale based discrete wavelet transform (DWT) suffers from the processing time.

3. The widely used S-transform (ST) makes the system sluggish as it requires high computation.

4. The modified version of DWT has implemented for analysis of signal of any length and future prediction.

5. The lifting based Wavelet Transform (WT) known as the Second Generation Wavelet Transform (SGWT) has been preferred for the implementation in the detection and the localisation of PQ disturbances due to its fast processing and simplicity.

6. The establishment of a healthy power system needs proper and automatic discrimination of the PQ disturbances. The conventional classification methods have some disadvantages as mentioned below.

   - The Artificial Neural Network (ANN) based classification method suffers from several draw backs like retraining with addition of more data, increase of training time with increase in data size.
   - The Hidden Markov Model (HMMs) fails to classify slow disturbances.

   A nano-second of a power quality disturbance demands a very efficient and a simple power quality classification algorithm which is the need of the day. Hence,

data mining based classifiers have been adopted for the discrimination of both the single and the combined signals. These automatic classifiers have been selected for the discrimination of large number of data sets.

7. More over, the integration of the renewable sources along with the conventional resources is growing in order to meet the increasing demand for good quality of power and the reliable supply. Although advancement in renewable sources reduces environmental pollutions, the high level of penetration of DGs sometimes require proper control and protection. However, in case of the photovoltaic (PV) system, the variation in the environmental factor such as the solar radiations creates PQ problems. The grid integration of renewable energy sources create serious problems which needs to be removed. The removal of all these distortions depends upon proper and quick detection and the discrimination of the variation. Hence, the aforementioned detection techniques have been implemented on the voltage signal in order to validate the suitability of the method in any environment.

1.7 Objective

- To synthesize different types of power quality disturbance signals and propose simple, suitable and fast analysis technique in order to detect and localize the disturbances.

- To extract suitable features from the signal analysis and propose a fast automatic classifier in order to classify large classes of data set. The testing of the proposed method in the noisy environment.

- To implement the proposed detection and the classification methods in real time environment for validating its suitability.

- To develop IEEE−14 bus system model embedded with renewable source and inject different power quality disturbances into the bus by varying loads. Islanding situation is created within the PQ disturbances.

- To implement the aforementioned detection methods for analysis of PCC voltage signal and extract suitable features from the detail coefficients in order to discriminate the PQ events from the islanding events. Implementation of proposed classifiers for classification of PQ and the islanding events.

1.8 Brief Work done

In this research work, different type of power quality disturbance (PQD) signals have been synthesized. The variants of the WT and the ST have been applied on the synthesized signals for the localization of the distortions within the signals. The signals have been decomposed up to finer levels with the variants WT in order to localize the disturbances. From out put of the WT variants, suitable features have been extracted and given as input to the different classifiers in order to discriminate the disturbances. Moreover, the noisy signals have also been classified with these classifiers.

Similarly, both the single phase and three phase PQD signals have been captured from two different transmission panels. These signals have been fed for the decomposition with the transformations like the previous cases. The extracted features from the output of transformations have been given to the classification block. Moreover, different types of fault have been classified with the classifier in order to test the suitability of the techniques.

The variants of the WT have been applied on the IEEE−14 bus system in order to verify the efficacy of the proposed techniques. The IEEE−14 bus system has been connected with the photovoltaic system after removing a synchronous generator at that location. Different PQ disturbances have been injected at the adjacent bus of PV connected bus and during the PQ disturbances the islanding events are created artificially in order to discriminate pure events from the islanding events. The voltage signals captured at the PCC have been fed to these transformations in order to localize the distortions and suitable features are extracted from the detail component of the WT variants. The extracted feature values help in discriminating between the PQ and the islanding events. The proposed classifiers have been implemented for classification purpose.

1.9 Contribution and Scope of the Thesis

1. Synthesis of ten types of distorted voltage signals along with the normal voltage waveform using MATLAB Simulation. The analysis of these signals in order to localise the distortions by analyse the
   - Detail coefficients of the discrete wavelet transform
   - Contours of the S-transform
   - Detail coefficients of the Maximum overlap discrete wavelet transform (MODWT)
   - Detail coefficients of the second generation wavelet transform
2. Comparison of effectiveness of the above analysis methods.
3. Extraction of suitable features from the coefficients of above mentioned wavelet variants and S-transform contours
4. Characterisation of different PQ signals by processing the features through the classifiers such as
   - Multilayer perceptron (MLP)
   - Hidden Markov Model (HMMs)
   - Decision Tree (DT)
   - Ensemble decision tree i.e. Random Forest (RF)
5. Comparison of the efficiency of the aforementioned classifiers both in the noisy and the noise free environment.
6. Classification of both real time single phase and the three phase voltage signals captured from the transmission panels. Similarly, discrimination of different type of real time fault signals.
7. The injection of the PQ disturbance to the adjacent bus of the renewable source connected $IEEE-14$ bus system. The disconnection of the renewable source during the PQ events in order to observe the consequence of islanding within the PQ environment.

8. The discrimination of the PQ events from the islanding events by selecting threshold of the performance indices.

9. Classification of the distortions by the classifiers.

1.10 Organisation of the Thesis

The entire thesis is divided in to seven chapters. This subsection gives a brief description of the contents of the various chapters in the thesis.

- Chapter 1 has provided the brief idea about the PQ disturbances. The details such as the structure, the origin and the consequence of different types of voltage signals are presented. The purpose of choosing this work has been reported. Similarly, the objectives, the scope and finally the organization of thesis are outlined.

- Chapter 2 presents a detailed literature survey on different techniques for the localisation, the feature extraction and the classification of power quality disturbances. Moreover, techniques related to the thesis also reported are illustrated in this chapter. Remark related to the thesis are outlined.

- Chapter 3 proposes techniques for the detection and the localisation of different PQ signals known as Maximal Overlap Discrete Wavelet Transform and Second Generation Wavelet Transform. The synthesized signals are decomposed up to four finer levels with the DWT, the MODWT and the SGWT. These signals are also analyzed with the contours of S-transform. These analysis methods are compared in terms of the processing time and the structure of out put waveform.

- Chapter 4 presents suitable classifier for the classification of large class of data set. Large number of voltage signals are synthesized and decomposed up to seventh decomposition levels. Four features are extracted from the coefficients of the WT variants and fed to the classifiers such as the MLP, the HMM, the DT and the RF in order to classify the disturbances. More over, the Additive White Gaussian Noise (AWGN) with different signal to noise ratio (SNR) level

is added to the pure PQ signals in order to get noisy PQ signal. The efficiency of these classifiers are compared both in the noisy and the noise free environment.

- The comparison of the above classifiers in real time environment has been carried out in Chapter-5. For the classification of the real time signal, different voltage signals are collected from both the single phase and three phase transmission panels. These signals are passed through the DWT, MODWT, SGWT, ST and the features are extracted from the output of these transformations and given as inputs to the aforementioned classifiers. The discrimination of the fault signals have been carried out with aforementioned techniques.

- In Chapter 6 The discrimination of the PQ disturbances from the islanding events has been carried out with signals captured from $IEEE-14$ bus system embedded with renewable source. The PQ disturbances are injected in to a bus. During the PQ event, the renewable source disconnected in order to realise the consequence of the islanding within the PQ environment. The captured PCC voltage signal is fed for the analysis. Suitable features are extracted and threshold line is drawn from these feature values in order to discriminate the islanding events from the PQ disturbances.

- Chapter 7 provides the concluding remarks by summarizing the contribution and conclusion of all the chapters. Finally, future scope of work is discussed.

Chapter 2

Review of Literature

2.1 Introduction

The proper and the continuous monitoring of the power quality disturbances has become a significant issue both for the utilities and the end-users. The operation of the power system can be improved by analyzing the PQ disturbances consistently. Hence, the development of the techniques and the methodologies in order to diagnose the power quality disturbances has acquired great importance in research. The PQ is actually the combination of quality of the voltage and the quality of current [6], [7] but in most of the cases, it is generous with the quality of voltage as the power system can only control the voltage quality. Hence, the yardstick of the power quality area is to preserve the supply voltage within the tolerable limits [8], [9]. The maintenance of quality of power in terms of voltage requires proper selection of the suitable detection and the characterisation methods. These are the crucial steps for maintenance of healthy power system by mitigating the PQ disturbances.

This chapter provides an over all survey on the existing work of the power quality detection and the characterisation. The performance of these detection and classification methods is illustrated in the power quality and the islanding environment. Most of the events in power system are discriminated according to appropriate standards such as IEEE 1159, IEC 61000 [10].

In order to gain a healthy power system operation, it is crucial to choose efficient and fast disturbance detection methods. The characterisation of the different

PQ signals is followed by the extraction of suitable features. Several detection and classification methods have been reported in the literature for improving the quality of power which are briefly surveyed below.

2.2 Organisation of the Chapter

This Chapter is organized as follows: Section-2.1 introduces the significance of power quality. Section-2.3 provides idea about different localisation techniques of the PQ disturbances. The Section-2.4 deals with the importance of different features. The Section-2.5 provides significance of different classifications methods. Similarly, the different islanding detection methods are discussed in the Section-2.6. Finally, the Section-2.7 provides the concluding remark of the literature review.

2.3 Techniques implemented for the signal analysis

The power system operation some times requires virtual estimation of the non periodic and time varying variations in terms of the duration evaluation and the localisation of the propagation of disturbances. Ultimately, both the time and the frequency analysis are in great demand. The widely used techniques for the analysis of both the stationary and the non stationary such as the FT, STFT, WT, Gaber transform (GT), ST, Prony analysis (PA), Kalman Filter (KF) and Cohen class etc provide information in frequency and the time domain.

2.3.1 Fourier Transform based Methods

The fast technique for the frequency domain analysis is the Fourier transform. However, it is suitable only for the stationary signals as it only provides information in frequency domain [11], [12]. It correlates the signal with the sine and the cosine functions. But it fails to give any information in time domain. This single domain analysis problem of FT is resolved by STFT which divides the signal into small segments with fixed window length [13]. On the other hand, the time frequency information related to the disturbance waveform can be obtained in STFT [14]. So, this spectral analysis is

suitable for the stationary signals [15] and not for the transient signals [16]. The fixed window property of STFT limits its application within stationary signals [17], [18], [19]. Moreover, the WT is a popular technique which provides information about signals both in the time and the frequency domain.

2.3.2 Discrete Wavelet Transform (DWT)

The most popular WT based on the multiresolution analysis (MRA) is established by Mallat in 1988 [20]. In MRA, the signal being analysed is decomposed into two distinct representation such as the low frequency and the high frequency component by passing though the low and high pass filters. These low and high pass filters are called the Quadrature mirror filters. This decomposition process is followed by down sampling with reduction of samples and provides details and approximations. The approximations at the first level of decomposition are used to iterate the process [21], [22]. The Continuous Wavelet Transform (CWT) is adopted for the continuous signal and DWT for discrete signals. Similarly, the MRA based DWT is widely used in various non stationary signal analysis in the area of power quality [23], [24], [25]. Some times, this technique is implemented for the separation of the fundamental frequency component and the distorted signal components. A.M Gaouda et.al. have implemented the DWT for the discrimination of the PQ disturbances with the standard deviation curve [26]. Although the DWT is the most commonly used method, the down sampling of the DWT may lose some important information and requires extra time [27], [28]. Hence,the extension of the DWT has been presented in next subsequent subsection.

2.3.3 S-Transform (ST)

The time-frequency representation of a time series has been introduced by R.G. Stockwell through the S-transform. The ST is the phase correction of the WT and is a good candidate for the analysis of signals. Due to the excellency of the time-frequency resolution, the S-transform has been implemented in [29] for the analysis of the different type of PQ disturbances. Bhende et.al. have preferred ST for the analysis of PQ signals as well the feature extraction from the contours [30]. Similarly, the ST has been implemented in [31], [32], [33], [34] and [35] in order to provide time resolution

both in terms of real and imaginary components of the spectrum. Although the ST is a suitable approach for the analysis of signals it suffers from the computational complexity. Hence, extra memory requirement makes the system sluggish. Ultimately, the time requirement is high in ST operation [36], [37]. Hence, a modified version of the wavelet transform has been discussed in the next subsequent subsection.

2.3.4 Maximal Overlap Discrete Wavelet Transform (MODWT)

The modified version of the DWT, known as Maximal Overlap Discrete Wavelet Transform (MODWT) or Modified Discrete Wavelet Transform. The down sampling free MODWT has an advantage of being able to process any sample size. The DWT implementation is limited by the sample size of multiple of $2s$ [38]. The MODWT has been implemented [39] as the 'undecimated DWT' with the context of infinite sequence. Similarly, the MODWT has implemented as the 'translation invariant DWT' [40], and the 'time-invariant DWT' [41]. Moreover, the free choice of the starting point is another advantage of the MODWT method [42]. The shifting property of the MODWT makes its application suitable for the prediction of subsequent disturbances in the power quality area [43], [44] as well as other areas [45], [46]. Thus the MODWT has been preferred for the analysis PQ disturbances.

Similarly a fast wavelet method has been chosen for the analysis of the signals, discussed below.

2.3.5 Second Generation Wavelet Transform (SGWT)

The Lifting scheme based SGWT introduced by Wim Sweldens is similar to the traditional DWT [47]. This variant of the WT is down sampling free method. The time domain analysis based SGWT is faster than the frequency domain analysis. Moreover, the convolution free SGWT requires half the number of computation [48]. The in place replacement property of the SGWT consumes less memory [49]. A. Serdar Yilmaz et.al. have discussed the lifting Based Wavelet Transforms (LWT) known as the Second Generation Wavelet Transform (SGWT) for the characterisation of five different types of PQ events in the distribution level. The magnitude of transient PQ events has been located through the width of the signal. According to the simulation

results, they concluded that SGWT is more efficient and faster than the convolution based traditional wavelet transforms. The SGWT has been chosen as a suitable means in different fields due to its simplicity and fast processing nature [50]. Both the analysis and synthesis of the image has been carried out successfully.

Out of these four analysis methods, the SGWT is preferred for the localisation of disturbances in this work because of the advantages such as

1. It is a time domain analysis.
2. Requires half number of calculations.
3. Simpler and easy to handle.
4. Less memory consumption.
5. Fast method.

2.4 Feature Extraction

The extracted features are given as for input to the classifiers instead of giving the raw data so that memory consumptions is reduced. The optimal feature extraction has played crucial rule in discrimination of PQ signals. According to Zhu et.al. in [51] energy is a suitable parameter. Gaouda et.al. have implemented the standard deviation curve for the characterisation of different PQ signals by comparing the magnitude at different decomposition levels [26]. Similarly, the entropy has been considered in [52]. Panigrahi et.al. have considered some more features such as the Mean, Kurtosis, Skewness etc [53]. Similarly, the other features such as the RMS, the Form factor, Crest factor, Interquartile range etc are extracted along with the above mentioned features in the power quality environment [54]. Moreover, the authors in [55] have extracted 62 candidate features from the S−matrix. By the implementation of the optimisation method (smoothing parameter matrix H), less influential features were eliminated gradually and only six features were selected.

2.5 Classification Methods

The characterisation of the PQ disturbance signals requires proper pattern recognition techniques for proper classification. The automatic pattern recognition methods includes the artificial intelligence techniques such as the artificial neural network (ANN), the fuzzy logic (FL), and the adaptive fuzzy logic etc for the discrimination of PQ disturbance signals. The probabilistic methods such as the Hidden Markov models, the Dempster-shafer theory etc have been recently developed.

2.5.1 ANN

The artificial neural networks are the oldest methods consisting of the training and the testing methods for the pattern recognition [56], [57], [58]. The advantages of ANN is that it is assumption free. The recognition of ANN depends on the training session. The network adjusts its internal parameters according to the rules during the training session. The disadvantages of the ANN is that training process requires a lot of time. More over, the ANN requires retraining when a new phenomenon is added. The ANN has other disadvantages like the local optimal and the poor convergence.

The fuzzy logic is the next approach in the process of pattern recognition [59]. It is based on the concept that human brain don't make any decisions based on the sharp decision boundary. The FL uses either 0 or 1 unlike the classical digital logic. This FL uses a decision boundary which smoothly transitions between the stages through the membership function. A higher membership value means that a particular PQ disturbance signal is more dominant in the test signals. The classification process is carried out with a fixed set of fuzzy logic rules which involves the fuzzification, the inference, the composition and the defuzzification. The combined approaches of the neural network and the fuzzy logic, an efficient and robust method has been implemented in [60], [61], [62], [63]. In these cases the ANN is used to tune, refine the FL system and finally, adjusting the rules as the system is running. Similar to the ANN, FL requires a huge computation time. Moreover, the fuzzy export system uses a collection of fuzzy sets and rules instead of Boolean sets for the reasoning [13].

The support vector machine is a machine learning algorithm. The supervised learning based SVM uses a hyperplane as a decision surface for the classification of

PQ signals. The proper classification depends on the optimal structure of hyperplane. The SVM has been compared for the classification of voltage signals in [7]. Some times it fails to classify multiclass data.

2.5.2 Hidden Markov Models (HMMs)

The HMM is defined as a double stochastic process. The HHMs comprise of an underlying stochastic process that is not directly observable but can only be visualized through another set of stochastic processes that produce a sequence of observations. In HMMs, a model is formed with the training data and the testing data are tested with the model. Moreover, the the Hidden Markov Model (HMMs) classifier is not suitable for classifying the slow phenomena like interruption,sag etc [64], [65]. Moreover, Dampster-Shafer theory of the evidence provides a partial belief of the accepted hypothesis. It pools several pieces of evidence bearing on a hypothesis under consideration in order to assess the truth of the hypothesis [66].

2.5.3 Decision Tree (DT)

The decision tree (DT) is a data mining based classifier. The DT is a tree like structure, simple to understand and interpret. The algorithms are robust to noisy data. The DT generally is based on the splitting criteria. The main advantage of the DT is that its ability to break down a complex decision making process into a collection of simpler decisions [67]. In the conventional single stage classifier each data sample is tested against all classes where as in the DT a sample is tested against only certain subsets of classes by reducing the unnecessary computations. The DT has been implemented for the classification of both single as well as the combined signals in [68], [69] and [70]. In [68], the extracted features from the S-transform have been fed as input to the DT-fuzzy classifier. From the boundaries of the DT classification, the fuzzy membership functions and the corresponding fuzzy rule have been developed for the final classification. Similarly, in [69] the DT has been used for the features extraction using the fuzzy classifier.

2.5.4 Ensemble Decision Tree

The ensemble decision tree known as the Random forest (RF) is a good candidate for the classification algorithm and classifies large number of classes simultaneously. Random forest is developed by Leo Breiman [71]. The RF properly classifies both the fast and the slow phenomena as it is based on classification, clustering, rule generation and knowledge discovery. Out of these classification methods, the RF has been preferred for the discrimination the PQ disturbances and the fault. In this work due to the following advantages have been discussed in Chapter-4.

1. The instability of individual trees is eliminated in RF [72].
2. The RF is a very fast tool for the classification.
3. The RF has the ability of classification of the multi−class.
4. It can implemented for the discrimination of large number of classes as it is free from over fitting problem.
5. The training and testing algorithms of the RF is very simple.

2.6 Discrimination of the Power Quality (PQ) Disturbances from Islanding Events

The islanding is the state of the electric power system that occurs when part of the network is disconnected from the rest of the system and the remaining parts energized by the distributed resources. However, this islanding introduces negative impacts on the DG itself and also on the utility. On the other hand, the PQ problems generated due to the increment or decrement of the voltage and salvation of harmonic from the nonlinear load and solid state devices creates serious problem to the customers and the connected DG, needs to be addressed properly. In some cases, the voltage unbalance and the harmonic distortion detection methodology also creates undesirable trip signal that may be misinterpreted as islanding [73]. Similarly, the variation of the real and the reactive power imbalance have been considered for the islanding detection leading to the non-detection zone (NDZ) [74]. Thus, the discrimination of the PQ from the

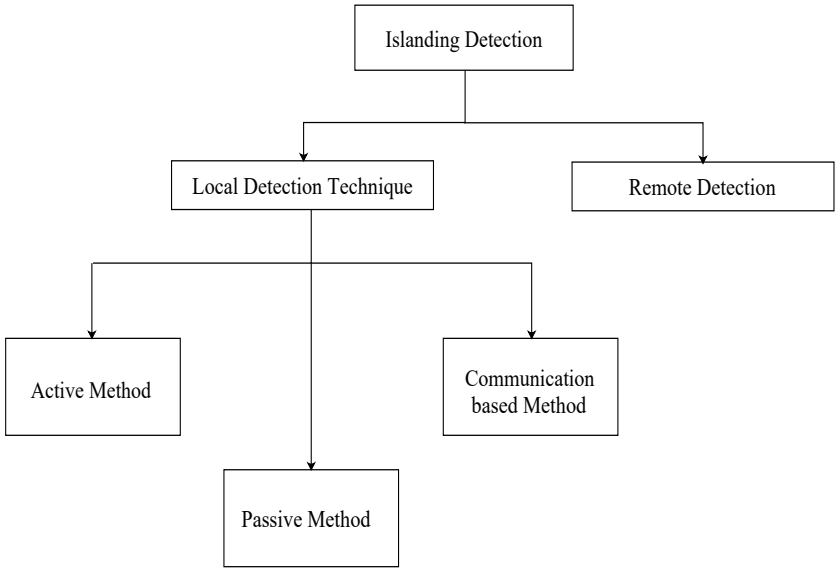

Figure 2.1: Islanding detection methods

islanding requires precise observation with proper methodology. In recent years, the various techniques have been implemented for the PQ disturbance and the islanding event detection. The islanding detection methods are categorized as remote and local techniques. Again, the local techniques categorized as the active, the passive and the communication methods are shown in Fig. 2.1.

2.6.1 Active Methods

In case of active methods, the small disturbances injected into the system and the subsequent results are observed in terms of change in the output parameter. Some of the universal used active detection methods are the active frequency drift (AFD) [75], the Sandia frequency shift (SFS), the automatic phase shift (APS), and the slip mode frequency drift (SMS) [76]. The SMS method uses positive feedback for the detection of the islanding condition. In this case, the grid frequency remains the same. The SMS, APS and AFD may suffer from the high non-detection zone (NDZ) with the increase of reactive power. The SFS though provides less NDZ, may produce poor PQ [77]. The system stability reduces due to the positive feedback.

2.6.2 Passive methods

The Passive scheme is a low cost method which makes decision based on the local measurement of the voltage and the current signals. The algorithms of under voltage or the over voltage, under or over frequency, Rate of change of frequency (ROCOF), rate of change of power [78] etc. are extensively implemented for the islanding. The under voltage or over voltage is a slow detection method. The passive methods suffer from the non-detection zone (NDZ) [79]. As the methods suffers from the NDZ, it is difficult to set the threshold.

2.6.3 Communication based Methods

Communication based islanding detection is also universally accepted approach but somewhat cost effective than the traditional passive methods. In order to minimize the NDZ, signal processing techniques such as the Fourier transform (FT), the short term Fourier transform (STFT), the discrete wavelet transform (DWT), the S-transform (ST) [80], [81], [82], [83] have been implemented in order to enhance detection quality. The FT is the fast analysis approach that only yields the frequency component. Similar to the PQ disturbance case, the STFT provides the time-frequency components but it has limited application with the fix window. The transient signals are properly analyzed with the multiresolution analysis of the WT. Moreover, the commonly used, DWT is a suitable technique for the analysis of both the stationary and the non-stationary signals, but it suffers from the computational complexity. The extension of the WT with the phaser information, known as the S-transform has been implemented widely for the detection of various PQ disturbances and the islanding events. However, in some cases, the capability of the ST degrades during the analysis of the nonstationary signals with transients [37]. But the main limitation of the ST is its computational complexity which requires large memory [84]. Hence, SGWT is preferred for the islanding detection in this work due to its simplicity and fast processing nature.

2.7 Remark from Literature Review

From the above research literature survey, the following remarks can be reported.

- The ST is a good candidate for the signal analysis. But the major draw back of ST is the computational complexity. The ST requires more time and extra memory which makes the system sluggish.
- The Modified version of DWT i.e Maximum overlap discrete wavelet transform (MODWT) is suitable for future forecasting.
- The lifting based SGWT is faster and simpler for the implementation as compared to the traditional methods.
- The ANN based classifiers although widely used, requires a lot of time and requires retaining when new phenomena is added. The HMMs classifier is only suitable for the fast disturbances such as the transients.
- The data mining based DT classifier is faster than the ANN and the HMMs. It can classify all types of disturbance irrespective of fast or slow, single or combined signal.
- The ensemble DT i.e RF is faster and can classify large number of classes.
- In the subsequent Chapters the discrete signal processing transforms and the data mining classifiers have been utilized in order to carry out the detection and the classification process respectively.

Chapter 3

Detection and Localization of the Synthesized PQ Disturbances using Different Discrete Wavelet Transform and S-Transform

3.1 Introduction

In Chapter-1, the overview of the Power Quality characterization has been discussed. The various steps carried out in the PQ characterization is also presented. A brief introduction to the signal processing and the data mining techniques is also given. Further a detailed literature review is discussed in Chapter-2.

As discussed in Chapter-1, one of the important steps for the PQ characterization is the detection and the localization of the disturbances. These processes lead us to know the causes and the sources of the disturbances. The monitoring of the power system in terms of mitigation of PQ problems requires detection and localization of source of disturbances [26].

In recent years, several researchers have adopted different signal processing techniques for the detection and identification of the PQ disturbance signals. The Fourier Transform is a fast technique which provides information regarding the frequency component, but fails to provide any information regarding the time of occurrence and the

duration of the disturbance. Hence the implementation of the FT is limited to the stationary signals. The Short Time Fourier transform (STFT) overcomes the limitations of FT by providing the time-frequency information [14]. However, this commonly used STFT is unable to track the transient signals due to it's fixed window property [69]. The Multi Resolution Analysis (MRA) introduced by Mallet [20] is suitable for the transient signals as it provides a long window at low frequency and a short window at high frequencies. The MRA of the WT resolves the signal into time scale rather than the time frequency scale in STFT. The WT uses the wavelet as the basis function instead of an exponential function in FT and STFT. The WT decomposes the signal into different frequency levels as the wavelet coefficients. According to the type of signal, the continuous wavelet transform (CWT) and the discrete wavelet transform (DWT) are adopted. The CWT is employed for the continuous signals and for the discrete time signal analysis DWT is adopted. From the discussion in the above paragraph, it is quiet obvious that for carrying out the process of detection and the localization of the PQ disturbances, the Wavelet Transform is the most suitable transform used for these two processes. The modified wavelet transform known as Maximal Overlap Discrete Wavelet Transform (MODWT) has chosen for localisation of power quality disturbance with forecasting. Moreover, the Second Generation Wavelet Transform has been implemented for quick detection and localisation of the disturbances.

3.2 Important Steps carried out in this Chapter

- Decomposition of ten types of different power quality disturbances up to four decomposition levels with the variants of Wavelet Transform.
- Application of S-Transform on signals.
- Analysis of different decomposition levels of different WT and contours of ST.
- Measurement of precessing time of aforementioned methods for localisation of disturbances.

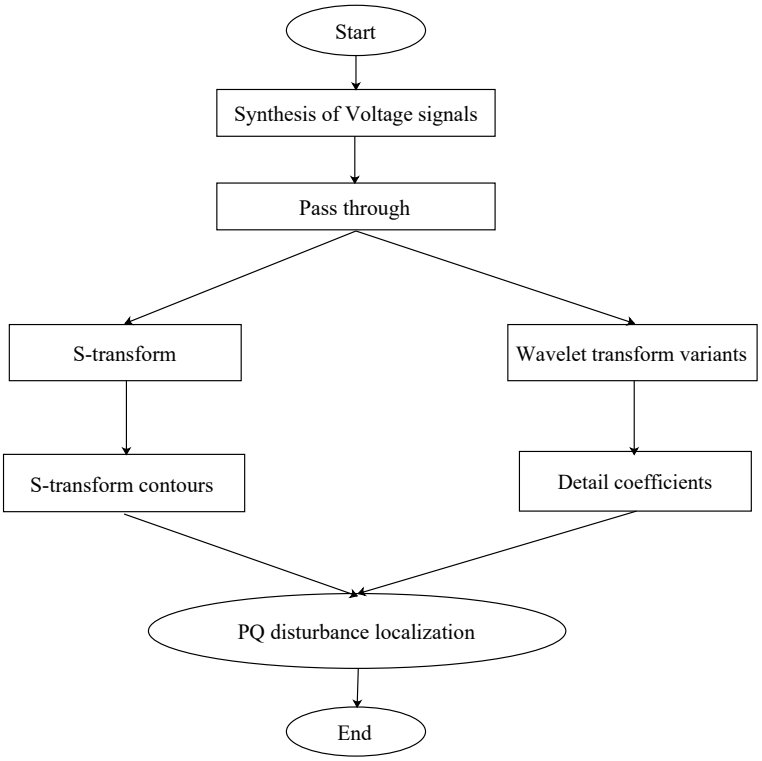

Figure 3.1: Flow chart presentation of the Chapter work

3.3 Organisation of the Chapter

In this Chapter, initially a brief theory of the Continuous Wavelet Transform is given for analyzing a continuous signal is given. Then three different types of Wavelet Transforms, namely the Discrete Wavelet Transform, the Modified Discrete Wavelet Transform, the Second Generation Wavelet Transform (SGWT) have been utilized along with the S-Transform for the detection and the localization.

This Chapter is organized as follows: Section-3.4 presents the brief theory of the DWT. Similarly the theory for the S-transform, MODWT and SGWT are given in Section-3.6, Section-3.7 and Section-3.8 respectively. Section-3.9 discusses the detection and the localization results using these three types of Wavelet Transform. The concluding remarks are provided in Section-3.10. All these procedures have been presented in the form of flow chart shown in Figure 3.1.

3.4 Wavelet Transform

The WT presents the signal as a combination of wavelets at different location (amplitude) and the scales (duration or time). WT is a powerful tool in signal analysis.

3.4.1 Continuous Wavelet Transform (CWT)

The continuous wavelet transform is adopted for the continuous signal analysis. The translated and scaled version of mother wavelet are multiplied with signal to be analysis in order to generate the wavelet coefficients at different resolution levels. Mathematically, the CWT of a signal $S(t)$ is defined in (3.1) as

$$CWT(a,b) = \frac{1}{\sqrt{a}} \int_{-\infty}^{\infty} S(t) g\left(\frac{t-b}{a}\right) dt \tag{3.1}$$

where, $g(\cdot)$ is the mother wavelet, a is the scale or dilation factor and b is the translation factor and both the variables are continuous in nature. The matching of the original signal $S(t)$ with the scaled and translated mother wavelet is represented by WT coefficient $CWT(a,b)$. The scaling factor a is inversely proportional with the frequency. That implies when the frequency under analysis is small, the scaling factor expands and viceversa. By the implementation of WT, the one-dimensional original time-signal $S(t)$ is mapped into two dimensional function space across the scale and translation factor. The scaling factor a changes with the decomposition levels in order to decompose the signal to corresponding frequency level. The signal translates at a particular scale a over continuous time to provide the wavelet coefficients. The efficiency of the WT depends on the attribute of the mother wavelet chosen. The commonly used wavelets present in the wavelet library are Daubechies, Haar, Symlet and Morlet etc. For the power system application, the most widely used mother wavelet is the Daubechies [85]. However, the CWT is computationally expensive which generate a lot of redundant data. In order to circumvalent these demerits an effective implementation applicable for discrete signal analysis known as discrete wavelet transform (DWT) has discussed below [86].

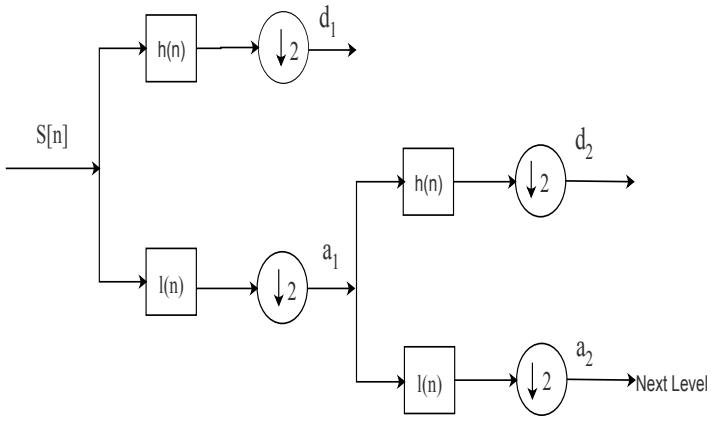

Figure 3.2: Block diagram representation of DWT decomposition

3.4.2 Discrete Wavelet Transform (DWT)

The DWT is implemented for analysis of discrete signal. By the substitution of $a = a_0^m$ and $b = nb_0a_0^m$, the DWT is derived from the CWT. The expression of DWT for a time signal $S(n)$ with the mother wavelet $g(\cdot)$ is present in (3.2) as [85]

$$DWT(m,k) = \frac{1}{\sqrt{a_0^m}} \sum_n S(n) g\left(\frac{k - nb_0a_0^m}{a_0^m}\right) \tag{3.2}$$

where k is the integer that refers the sample. Both a and b are discrete variables. With the interchanging of the variables n, k and rearranging (3.2), equation (3.3) can be written

$$DWT(m,n) = \frac{1}{\sqrt{a_0^m}} \sum_k g\left[a_0^{-m}n - b_0k\right] \tag{3.3}$$

By observation, it is seen that the (3.3) is resembles the convolution equation of the impulse response of the FIR filter as

$$Y[n] = \frac{1}{C} \sum S[k]h[n-k] \tag{3.4}$$

where $h[n-k]$ is the impulse response of the FIR filter. From the (3.3) and (3.4), it is observed that the $g\left[a_0^{-m}n - b_0k\right]$ is the impulse response of the DWT filter.

With $a_0 = 2$ or $(a_0^{-m} = 1, \frac{1}{2}, \frac{1}{4}, \frac{1}{8} \dots)$ and $b_0 = 1$ the DWT can be applied with a low pass filter $l(n)$ and the high pass filter $h(n)$ as shown in Figure 3.2.

A signal $S[n]$ is fed to the low pass and the high pass filter known as Quadrature mirror filters which is shown in Figure 3.2. The outcomes of the two filter undergoes down sampling by a factor 2. The output achieved by passing through the high pass filter and after down sampling is called the detailed coefficients. Similarly, when the output is passed through low pass filter and down sampled by factor 2, the approximation coefficients are obtained. The low pass and the high pass filter are related by (3.5)

$$h[L-1-n] = (-1)^n l(n) \tag{3.5}$$

where L is the length of filter.

The signal decomposed into the detailed and the smooth part at the first level of decomposition is passed through the quadrature mirror high pass $h\,(n)$ and low pass filters $l\,(n)$ respectively. Thus the detail version consists of the high frequency components than the smooth version. Mathematically, they are defined as (3.6) and (3.7)

$$c_1\,(n) = \sum_k h(k-2n)c_0(k) \tag{3.6}$$

$$d_1\,(n) = \sum_k g(k-2n)c_0(k) \tag{3.7}$$

The coefficients representing low frequency contents known as signals approximations and similarly, the coefficients represents the high frequency contents are known as its details. The approximations of the signal keep the global feature content of a signal considered for analysis whereas the details tell us the irregular and transient content of the signal under analysis. So in this work, details are used for detection of distortions within the voltage signals.

3.4.3 DWT Approach in Power Quality Environment

The MRA of the DWT involves the decomposition of the signals in to the different frequency levels. The proper analysis of signal care for some factors. The choice of the mother wavelet according to the structure of the signal plays a vital rule. Similarly, the

section of maximum decomposition level is another parameter in the DWT analysis. The precise selection of the aforementioned two parameters enhances the analysis efficiency. They have been discussed shortly.

3.4.3.1 Selection of the Mother Wavelet

An authentic analysis of the PQ disturbance signal depends upon the selection of the mother wavelet. At lower scale, the mother wavelet is most localized in time and oscillates most rapidly within a very short period of time. As the wavelet goes to higher scales, the analyzing wavelets become less localized in time and oscillate less due to dilation nature of the wavelet transform analysis. As a result of higher scale decomposition, fast and short transient disturbances will be detected at lower scale whereas the slow and the long transient disturbances will be detected at higher scale. So both the slow and fast transients can be detect with a single type of analyzing wavelet.

The WT provides a successful detection and localization of the disturbance signal when the structure of mother wavelet similar is to the signal structure considered for the analysis.

The mother wavelet can be of two types, the scale dependent and the scale independent. A single wavelet is implemented for all the decomposition levels for the level independent mother wavelet selection. Where as for the level dependent wavelet selection, the appropriateness of a wavelet as the mother wavelet is tested for each level. The wavelet transforms are performed by dialing a mother wavelet in course of analysis, rather than by contracting the mother wavelet. For slow and long transient disturbances, db8 (Daubechies wavelet of order 8) and db10 (Daubechies wavelet of order 10) are preferable. Similarly, db4 and db6 are preferable for the fast and the short transient disturbances. However, db4 is selected as a suitable mother wavelet for the detection of both the slow and fast transient disturbances due to its localization property [87]. In this Chapter, one type of mother wavelet is selected for detection of all type voltage disturbance signals. At the higher scale of signal decomposition, the slow and long transient disturbances are detected at higher scales where as the fast and the short transient disturbance signals are detected at the lower scale. Hence, single analyzing wavelet has been chosen to detect both the slow and the fast transient

signals.

3.4.3.2 Selection of Maximum Decomposition Level

The maximum number of level up to which a signal can be decomposed is determined according to the expression $j_{ful} = fix(log_2 n)$. Where the n is the signal length and fix is to round the value of the parameter in the bracket to its nearest integer. According to the MATLAB wavelet toolbox, the length of the signal at the highest level of decomposition should not be less than the length of the wavelet filter considered for use [88]. Hence, the signal can be decomposed up to the maximum level as expressed in [89] and is given by equation (3.8)

$$j_{max} = fix(log_2(\frac{n}{n_w} - 1)) \tag{3.8}$$

where n is the length of the signal and the n_w is the length of the filter of the mother wavelet considered. The decomposition of a signal more than the j_{max} level is time-consuming and meaningless.

3.5 Power Quality Disturbance Model

The PQ analysis comprises of various electrical disturbances such as the voltage sag, the voltage swell, harmonic distortions and so on. Simulation of various waveforms are presented in this Section. The pure sine wave and ten types of different disturbances are considered for analysis. These PQ disturbances are considered in ten cycles of a waveform with 50 Hz fundamental frequency. The sampling frequency is 3.2 kHz. The signals are generated based on the model [55] given in Table 3.1.

The unit step function $u(t)$ in the whole Table 3.1 provides the duration of disturbances present in the pure sine waveform.

3.5.1 DWT Implementation in PQ Disturbance Localization

The signals have been decomposed up to four finer levels. The vertical axis has been presented with the amplitude of the voltage in volt V p.u and the horizontal axis with the time (in second) in terms of samples.

Table 3.1: Power quality Disturbance Models

PQD events	Class	Equations	Parameter
Normal Voltage	C0	h(t)=sin(wt)	$w = 2\pi 50 rad/s$
Sag	C1	h(t)=$[1 - \alpha(u(t-t_1) - u(t-t_2))]$ $sin(wt)$	$0.1 \leq \alpha \leq 0.9$, $T \leq t_2 - t_1 \leq 9T$
Swell	C2	h(t) =$[1 + \alpha(u(t-t_1) - u(t-t_2))]$ $sin(wt)$	$0.1 \leq \alpha \leq 0.8$, $T \leq t_2 - t_1 \leq 9T$
Interruption	C3	h(t) =$[1 + \alpha(u(t-t_1) - u(t-t_2))]$ $sin(wt)$	$0.9 \leq \alpha \leq 1$, $T \leq t_2 - t_1 \leq 9T$
Oscillatory transient	C4	h(t)= $sin(wt)+$ $\alpha\ exp(-(t-t_1)\tau)(u(t-t_1) - u(t-t_2))$ $sin(2\pi f_n t)$	$0.1 \leq \alpha \leq 0.8$, $0.5T \leq t_2 - t_1 \leq 3T$, $300Hz \leq f_n \leq 900Hz$, $8ms \leq \tau \leq 40ms$
Flicker	C5	h(t)=$[1 + \alpha sin(2\pi\beta t)]$ $sin(wt)$	$0.1 \leq \alpha \leq 0.2$, $5Hz \leq \beta \leq 20Hz$
Harmonics	C6	h(t)=$\alpha_1 sin(wt) + \alpha_3 sin(3wt)+$ $\alpha_5 sin(5wt) + \alpha_7 sin(7wt)$	$0.05 \leq \alpha_3$, $\alpha_5, \alpha_7 \leq 0.15$, $(\alpha_i)^2 = 1$
Sag + Harmonics	C7	h(t)= $[1 - \alpha(u(t-t_1) - u(t-t_2))]$ $(\alpha_1 sin(wt) + \alpha_3 sin(3wt) + \alpha_5 sin(5wt))$	$0.1 \leq \alpha \leq 0.9$, $T \leq t_2 - t_1 \leq 9T$, $0.05 \leq \alpha_3, \alpha_5$, $\alpha_7 \leq 0.15$, $(\alpha_i)2 = 1$
Swell + Harmonics	C8	h(t)= $[1 + \alpha(u(t-t_1) - u(t-t_2))]$ $(\alpha_1 sin(wt) + \alpha_3 sin(3wt) + \alpha_5 sin(5wt))$	$0.1 \leq \alpha \leq 0.9$, $T \leq t_2 - t_1 \leq 9T$, $0.05 \leq \alpha_3$, $\alpha_5, \alpha_7 \leq 0.15$, $(\alpha_i)^2 = 1$
Notch	C9	h(t)= $sin(wt) - (sign(wt))$ $\{9k = 0k[u(t-(t_1+0.2n)) - u(t-(t_1+0.2n))]\}$	$0.1 \leq k \leq 0.4$, $0 \leq t_1, t_2 \leq 0.5T$, $0.01T \leq t_2 - t_1 \leq 0.05T$
Spike	C10	h(t)= $sin(wt) + (sign(wt))$ $\{9k = 0k[u(t-(t_1+0.2n)) - u(t-(t_1+0.2n))]\}$	$0.1 \leq k \leq 0.4$, $0 \leq t_1, t_2 \leq 0.5T$, $0.01T \leq t_2 - t_1 \leq 0.05T$

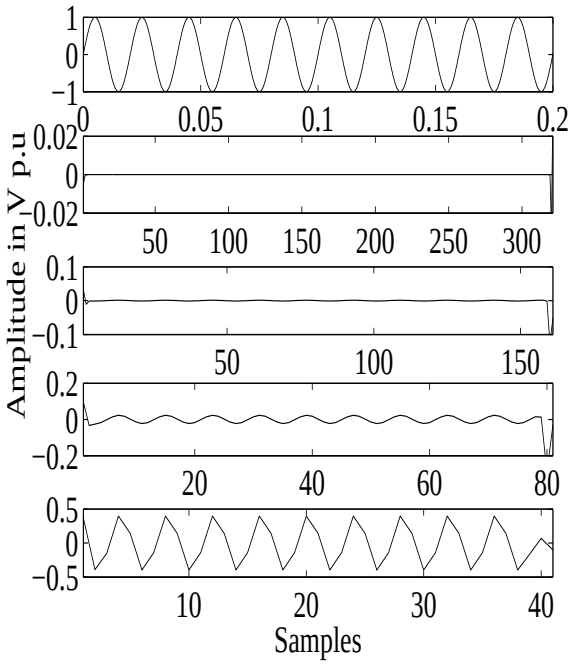

Figure 3.3: Localization of the pure sine wave in DWT decomposition

The original sinusoidal voltage signal has been presented along with decomposition levels as shown in Figure 3.3. As it is distortion free, so there is no deviation in the decomposed levels wave form.

The sinusoidal voltage signal with sag is considered in Figure 3.4. The deviation in voltage due to sag has been properly detected by the decomposition levels. The inception as well as the end point of sag is clearly localized by the finer levels.

Similarly, the swell in sinusoidal signal is considered for the analysis and presented in Figure 3.5. The start and end point of swell have been clearly detected in the finer decomposition levels.

The analysis of the interruption in voltage signal is given in Figure 3.6. The deviation due to the interruption has been localized in all decomposition levels.

Notch in each cycle of the sine wave is considered Figure 3.7. The notches are clearly detected and localized by the decomposition levels. Similarly the spike in each cycle is considered for analysis shown in Figure 3.8.

Harmonics in the sine wave have been considered for the analysis and shown in Figure 3.9. The harmonic is considered as stationary in power system. By comparing

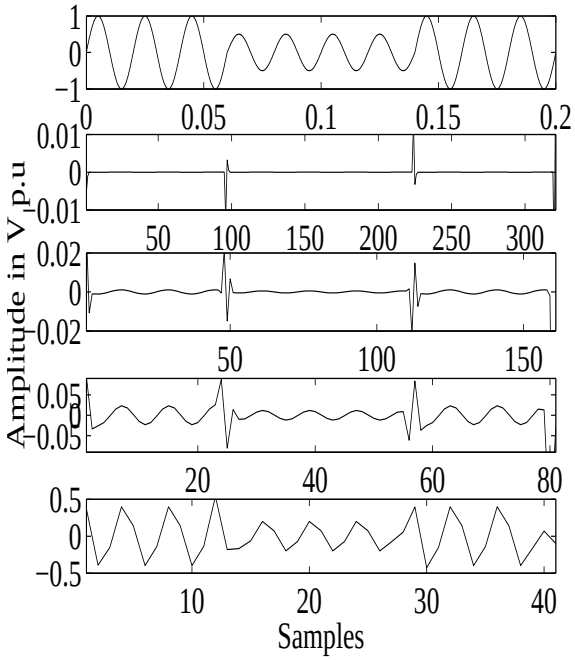

Figure 3.4: Localization of the sag in pure sine wave

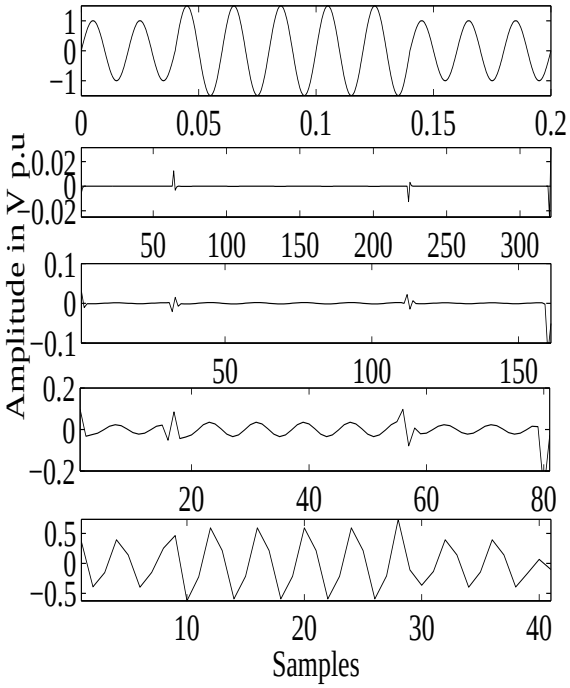

Figure 3.5: Localization of the sine wave with swell

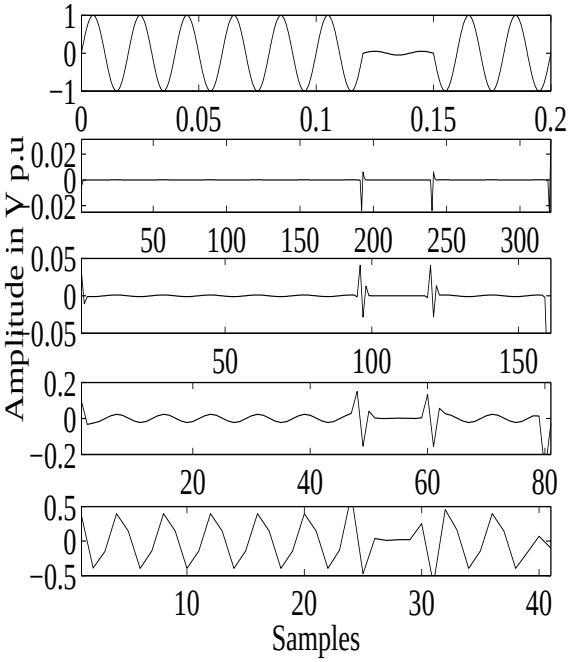

Figure 3.6: Localization of the sine wave with interruption

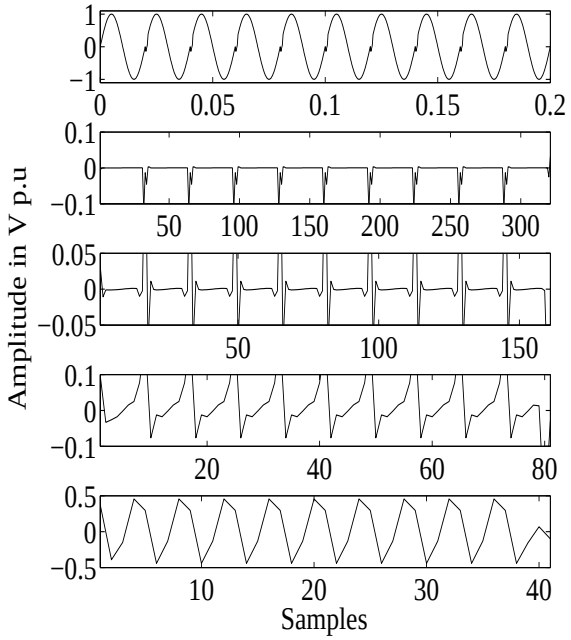

Figure 3.7: Localization of the sine wave with notch

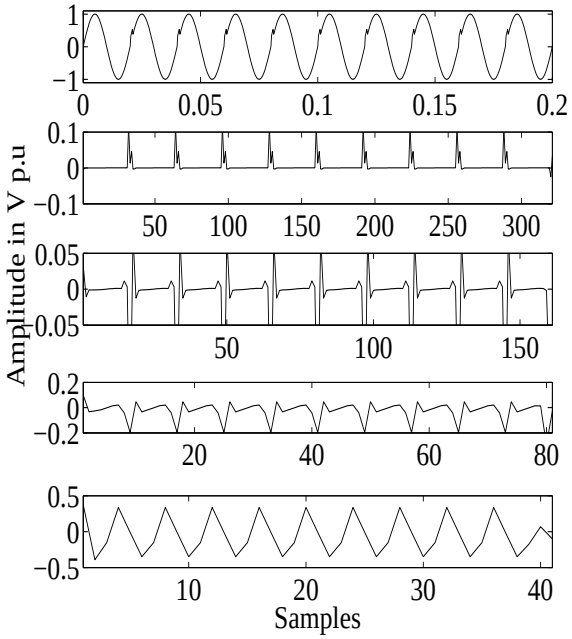

Figure 3.8: Localization of the sine wave with notch

the magnitude of the decomposed waveform of Figure 3.3 and Figure 3.9, it can be observed that there is some magnitude of the decomposed waveform of harmonic signal where as normal sine wave posses zero magnitude at their respective decomposition levels. Similarly, considering the pure swell signal in Figure 3.5 and the swell with harmonic Figure 3.10. The magnitude of the decomposed waveform of pure swell signal differs from the harmonic doped signal.

By comparing the pure sine wave signal with other distorted signals it is observed that, magnitude of wavelet coefficients associated with disturbance events are much larger than that of disturbance free coefficient. The DWT decomposition provides the time scale representation. The extension of the wavelet idea is based on a moving and scalable localizing Gaussian window known as the S-transform.

3.6 S-Transform

The S-transform is the derived form of the continuous wavelet transform with a phase correction factor. In other words, the S-transform is the combination of the WT and

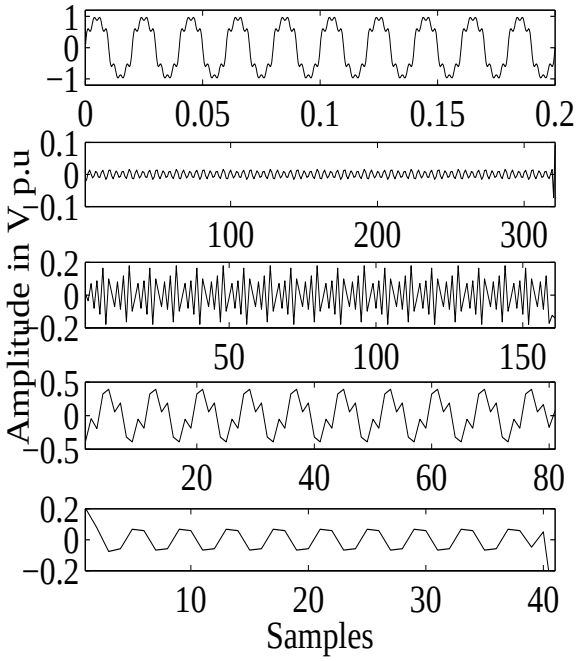

Figure 3.9: Localization of sine wave with harmonics

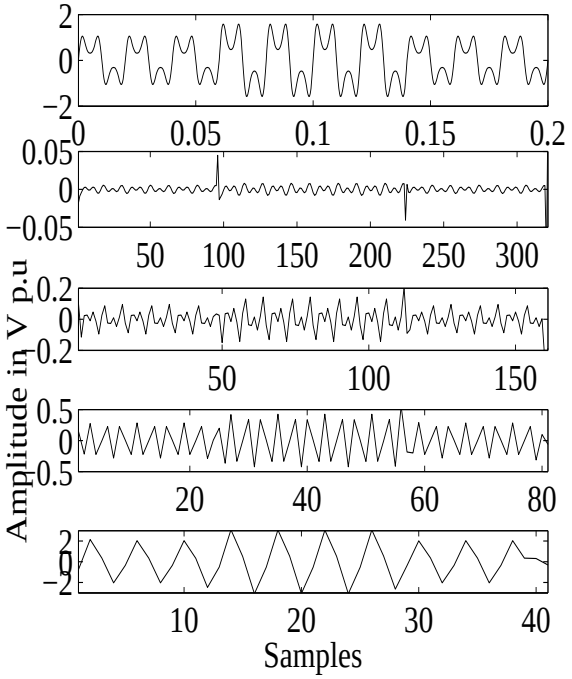

Figure 3.10: Localization of sine wave with harmonics and swell

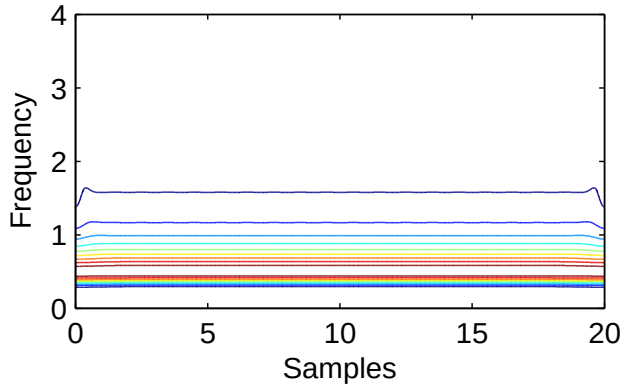

Figure 3.11: Localization of pure sine wave using S-transform

short time Fourier transform that provides the time-frequency spectral localization of the signals. The frequency dependent variable window provides multiresolution analysis (MRA) while retaining the absolute phase of each frequency. So, the S-transform provides proper detection and identification of time series signal of PQ.

3.6.1 S-transform Approach in Power Quality Environment

The MRA of the S-transform makes it as a suitable tool for time series analysis in power system environment [90]. Mathematically, the S-transform of a continuous time signal $h(t)$ has been presented in (3.9) as

$$S(\zeta, f) = \int_{-\infty}^{\infty} h(t) \frac{|f|}{\alpha\sqrt{2\pi}} . exp(\frac{-f^2(\zeta - t)^2}{2\alpha^2}) \tag{3.9}$$

where f is the frequency, t is the time and the ζ is the control parameter that controls the Gaussian window position on the t-axis. The factor α controls the time and the frequency resolution. As a result the frequency resolution increases, when the parameter α value is above 1. Similarly, if α decreases below 1, the time resolution improves [31]. In this work, the α is taken as 0.5 for analysis of all these aforementioned signals.

A power signal $h(t)$ in discrete form is expressed as $h(kT)$, for $k = 1, 2, \ldots, N-1$ and the sampling time interval T. Mathematically, the discrete version of Fourier

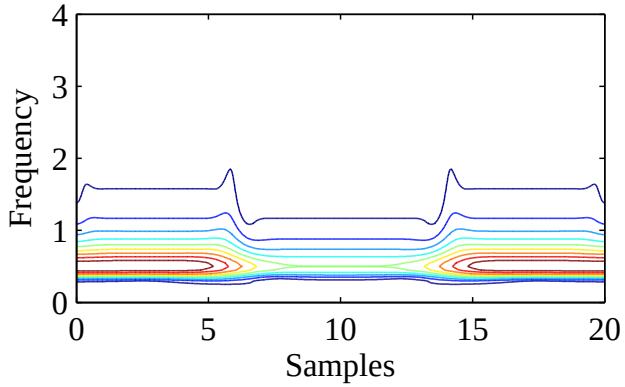

Figure 3.12: Localization of sag in pure sine wave

transform of the $h(kT)$ has been expressed [29] by (3.10)

$$H[\frac{n}{NT}] = \frac{1}{N}\sum_{k=1}^{N-1} h(kT) \cdot exp\left(\frac{-i2\pi k}{N}\right) \tag{3.10}$$

where $n = 0, 1, 2 \ldots, N-1$

The S-transform of a discrete time series $h(kT)$ is expressed by assuming $f \rightarrow \frac{n}{NT}$ and $\zeta \rightarrow jT$ is represented as

$$S[jT, n/NT] = \sum_{m=0}^{N-1} H[\frac{m+n}{NT}]G(m,n)e^{\frac{i2\pi mj}{N}} \tag{3.11}$$

and the $G(m,n) = e^{\frac{-2\pi^2 m^2}{n^2}}$, $n \neq 0$, where $j, m = 0, 1, 2, \ldots, N-1$ and $n = 1, 2, \ldots, N-1$. By assuming $n = 0$, equation (3.11) is given as in equation (3.12) as

$$S[jT, 0] = \sum_{m=0}^{N-1} h[\frac{m}{NT}] \tag{3.12}$$

The equation (3.12) provides zero frequency voice. The output of the S-transform is an $N \times M$ matrix is known as S-matrix. The row of the S-matrix represents the frequency and the column represent the time. Moreover, each element of the matrix is a complex value. The averaging of the amplitude of the S-matrix over time results

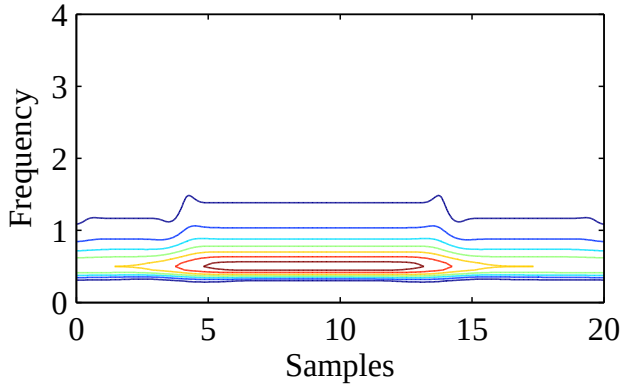

Figure 3.13: Localization of swell in pure sine wave

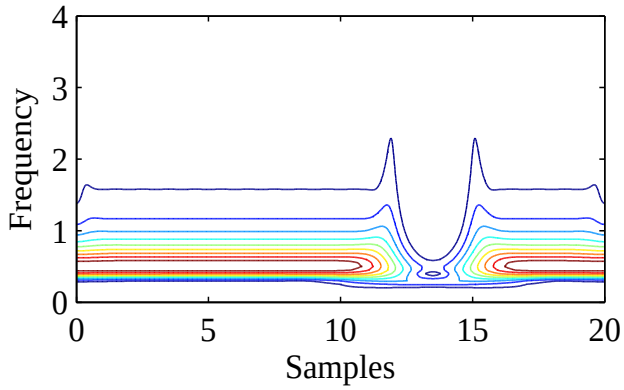

Figure 3.14: Localization of interruption in pure sine wave

in Fourier spectrum [30]. In this work, the α value is .5 for localization of both the stationary and the non stationary signals.

3.6.2 S-Transform Implementation in PQ Disturbance Localization

The S-transform provides high frequency resolution at low frequency and high time resolution at high frequency. The MRA based S-transform is employed on the same PQ signals in order to localize the disturbance. The equation(3.9) to equation(3.12) have been implemented to detect ten types of PQ disturbances using ST.

The pure sine wave voltage signal has been considered for analysis in Figure 3.11. The vertical axis presents the frequency in kHz and the horizontal axis presents the

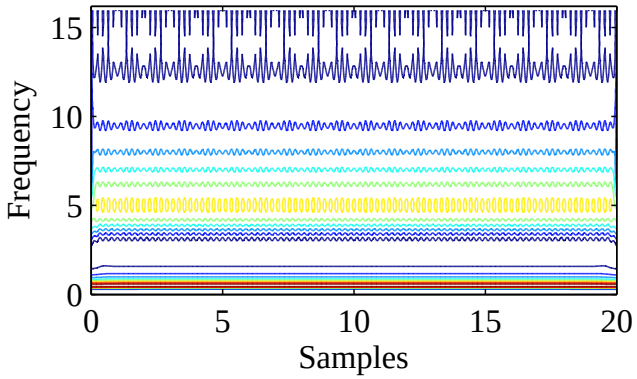

Figure 3.15: Localization of oscillatory transient in pure sine wave

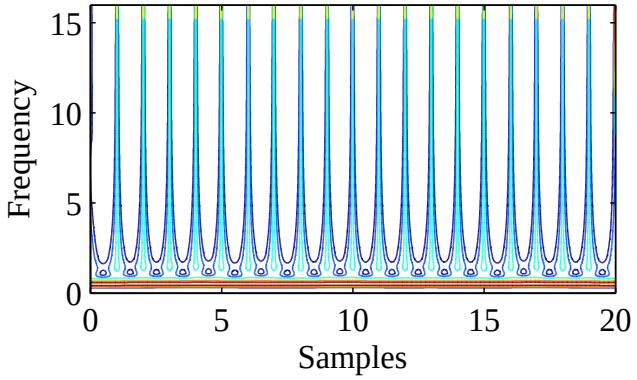

Figure 3.16: Localization of notch in pure sine wave

time (in second) in terms of samples.

The voltage signal with Sag is considered in Figure 3.12. The voltage dip has been properly detected from the time frequency plot of the S-transform contours. The sag is clearly localized by the contours. The contours show a decline in magnitude during the disturbance similar to the sag in the voltage signal.

Similarly, the swell in the sinusoidal voltage signal is localized by the increased magnitude of the contours. The patters produces a swell in the magnitude during the distortion and is given in Figure 3.13.

The huge reduction in the magnitude of the contours similar to the interruption in the voltage is shown in Figure 3.14.

The S-transform is implemented on the oscillatory transient signal and the Figure 3.15 shows that the distortion properly localized in the S-transform contours.

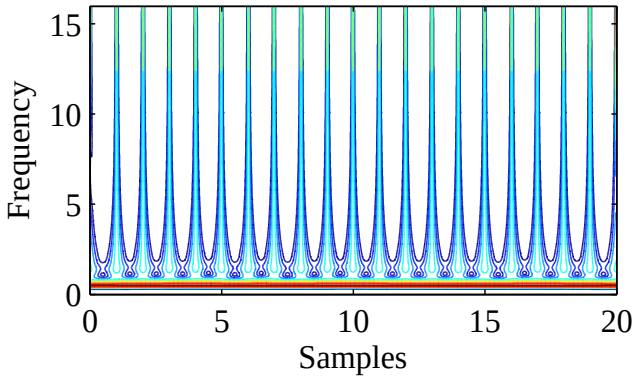

Figure 3.17: Localization of spike in pure sine wave

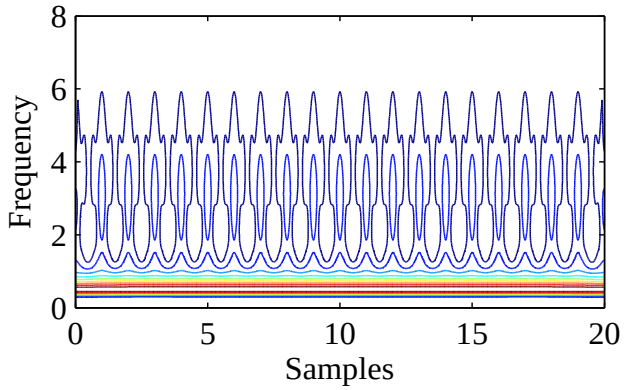

Figure 3.18: Localization of harmonic in pure sine wave

The signal with notch in each cycle has been localized by the highly increased magnitude of contour and shown in Figure 3.16. Similar phenomena has been applied for the spike given in Figure 3.17.

The sine wave with harmonic has been analyzed in ST implementation presented in Figure 3.18. The harmonic has been identified by the contours of the ST.

The swell with harmonic in sine wave has been properly detected by the increased magnitude of the contours presented in Figure 3.19. Similarly, the reduced magnitude contours corresponds to the sag in voltage shown in Figure 3.20.

From Figure 3.12 to Figure 3.20, it is quiet clear that the S-transform provides better localization then the DWT. However, the S-transform suffers from computational burden [36]. The S-transform also requires more time and memory than the WT. As the power system operation based on quick action, hence S-transform based detection

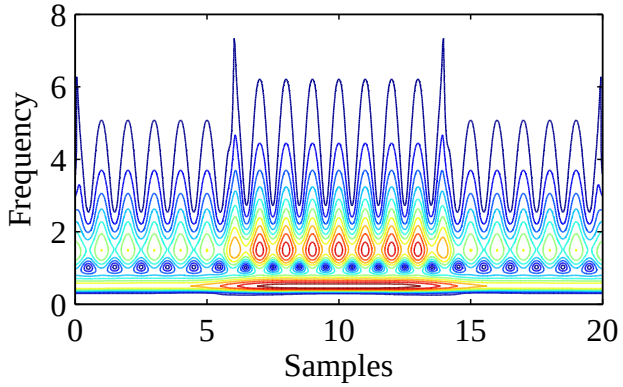

Figure 3.19: Localization of harmonic and swell in pure sine wave

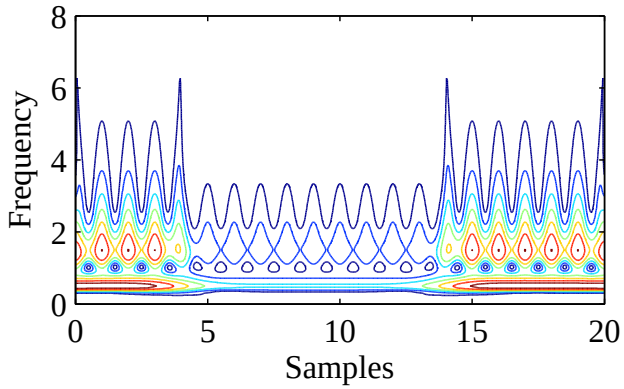

Figure 3.20: Localization of harmonic and sag in pure sine wave

and localization has its limitations.

3.7 Maximal Overlap Discrete Wavelet Transform (MODWT)

The MODWT is the modified version of the DWT. The sensitivity to the choice of the initial point of DWT is over come in MODWT by eliminating the down sampling of the outputs from the wavelet and the scaling filters at each stage [91]. This down sampling is eliminated in MODWT in order to obtain the insensitivity of the starting point. The MODWT coefficients are generated by merging two sets of the DWT coefficients which are developed by the separate application of the DWT calculation to X and to ζX.

In this operation the DWT calculation is applied to the circularly shifted vector ζX instead of X where ζ is a circular shifted matrix of dimension $N \times N$. If $X = \begin{bmatrix} X_0 \\ X_1 \\ \dots \\ X_{N-2} \\ X_{N-1} \end{bmatrix}$ is an $N \times 1$ column vector, then, $\zeta X = \begin{bmatrix} X_{N-1} \\ X_0 \\ X_1 \\ \dots \\ X_{N-2} \end{bmatrix}$ and $\zeta^{-1} X = \begin{bmatrix} X_1 \\ X_2 \\ \dots \\ X_{N-2} \\ X_{N-1} \\ X_0 \end{bmatrix}$.

The enhanced DWT i.e. MODWT has the ability to take any sample size N where as the DWT of the level J restricts the sample size to an integer multiple of 2^J. The MODWT is insensitive to the choice of starting point of a time series signal. The sensitive of the DWT's to the choice of initial point is eliminated in MODWT by eliminating the down sampling [38].

3.7.1 MODWT Approach in Power Quality Environment

The motivation for using of MODWT over the traditional DWT is due to the flexibility in choosing the signal irrespective of the length size. The last subsection the computational burden of the S-transform has been presented. Hence, MODWT is a suitable alternative for the localization of PQ disturbance. As the down sampling is eliminated in MODWT, the PQ disturbances are detected faster than the DWT and the S-transform. Moreover, the circular shifting based MODWT has one step ahead prediction which is suitable for the power system relaying operation. Similar to the DWT, the low-pass and high-pass filter are also employed in MODWT along with the mother wavelet. The block diagram representation of the MODWT is given in Figure 3.21.

The MODWT scaling filter $\widetilde{g}_l$ and $\widetilde{h}_l$ the wavelet filters are related to the DWT filters through (3.13) and (3.14)

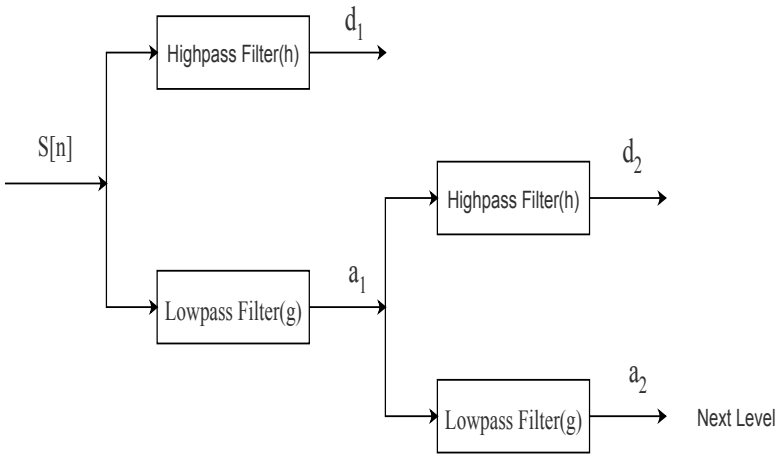

Figure 3.21: Block diagram representation of MODWT decomposition

$$\widetilde{g}_l = \frac{g_l}{\sqrt{2}} \tag{3.13}$$

$$\widetilde{h}_l = \frac{h_l}{\sqrt{2}} \tag{3.14}$$

The quadrature mirror principle of DWT is also applied for the MODWT filter as

$$\widetilde{g}_l = (-1)^{l+1} h_{L-1-l} \tag{3.15}$$

$$\widetilde{h}_l = (-1)^{l+1} g_{L-1-l} \tag{3.16}$$

where $l = 0, 1, 2, \ldots L-1$ and the L is the filter length.

The n^{th} element of the first stage scaling and the wavelet coefficients of the MODWT with the input time series signal $X(n)$ have been expressed in (3.17) and (3.18) as

$$\widetilde{V}_{1,n} = \sum_{l=0}^{L_1-1} \widetilde{g}_l X_{n-l mod N} \tag{3.17}$$

$$\widetilde{W}_{1,n} = \sum_{l=0}^{L_1-1} \widetilde{h}_l X_{n-l mod N} \tag{3.18}$$

where $n = 1, 2, 3, \ldots, N$ and the N represents signal length in sample.

The first stage detail and the approximation coefficient is calculated by expression

(3.19) and (3.20)

$$\widetilde{D}_{1,n} = \sum_{l=0}^{L_1-1} \widetilde{g}_l \widetilde{W}_{1,n+lmodN} \tag{3.19}$$

$$\widetilde{A}_{1,n} = \sum_{l=0}^{L_1-1} \widetilde{g}_l \widetilde{V}_{1,n+lmodN} \tag{3.20}$$

The MODWT scaling coefficients $\widetilde{V}_j$ and wavelet coefficients $\widetilde{W}_j$ at the n^{th} element of the j^{th} stage are given by the equations (3.21) and (3.22)

$$\widetilde{V}_{j,n} = \sum_{l=0}^{L_j-1} \widetilde{g}_{j,1} \widetilde{X}_{n-lmodN} \tag{3.21}$$

$$\widetilde{W}_{j,n} = \sum_{l=0}^{L_j-1} \widetilde{h}_{j,1} \widetilde{X}_{n-lmodN} \tag{3.22}$$

Similarly, the approximation coefficients $\widetilde{A}_j$ and the detail coefficients $\widetilde{D}_j$ of the n^{th} element of the j^{th} stage MODWT have been given by the (3.23) and (3.24).

$$\widetilde{A}_{j,n} = \sum_{l=0}^{L_j-1} \widetilde{g}^0_{j,l} \widetilde{V}_{1,n+lmodN} \tag{3.23}$$

$$\widetilde{D}_{j,n} = \sum_{l=0}^{L_j-1} \widetilde{h}^0_{j,l} \widetilde{W}_{1,n+lmodN} \tag{3.24}$$

where $\widetilde{g}^0_l$ is periodized $\widetilde{g}$ to length N and also the $\widetilde{h}^0_l$ is periodized $\widetilde{h}$ to length N. Hence, the original time series signal is stated in terms of the approximations and the detail coefficients and is given by equation (3.25) [42]

$$X(n) = \sum_{l=0}^{j} \widetilde{D}_j + \widetilde{A}_j \tag{3.25}$$

$\widetilde{D}$ is obtained by the circular filtering of $X(n)$ with h_j.

At each stage of the MRA of the MODWT, the detail coefficients contain high-frequency content and the approximation coefficients contain the low frequency content. The deviation in the voltage waveform due to the distortion has high frequency

content which appears more in details coefficients than the approximation coefficients. In this Chapter the detailed coefficients are analyzed.

3.7.1.1 Wavelet Filter Selection

The suitable wavelet selection plays a crucial rule in the signal analysis. The suitability of the wavelet for specific areas of application depends on basic property of the wavelet. The width of the wavelet filter is influences the result. Although the larger width wavelet has better matching with characteristics feature of the time series, their application is limited due to the following drawbacks

- Large width wavelet filter application decreases the degree of the localization of the discrete wavelet coefficients
- Also increases the computational burden.

On the other hand the short width wavelet provides reasonable result. The db8 wavelet is employed for the PQ disturbance analysis using MODWT.

3.7.1.2 Selection of Maximum Decomposition Level for MODWT

In MODWT, the selection of the number decomposition level J also plays a crucial rule like the DWT decomposition. The expression for the maximum level of decomposition is as $J_{max} \leq log_2(N)$, where $N \geq 0$.

3.7.2 MODWT Implementation in PQ Disturbance Localization

The equation$-$(3.13) to equation$-$(3.25) have been implemented to detect ten types of PQ disturbances. The down sampling free MODWT is chosen as a suitable alternative for the detection of the PQ disturbances. The PQ disturbance signals are fed to the MODWT in order to detect and localize the disturbance. The signals are analyzed up to the fourth level. The vertical axis presents the amplitude of the voltage signal volt V p.u. (per unit) and the horizontal axis presents the time (in second) in terms of samples.

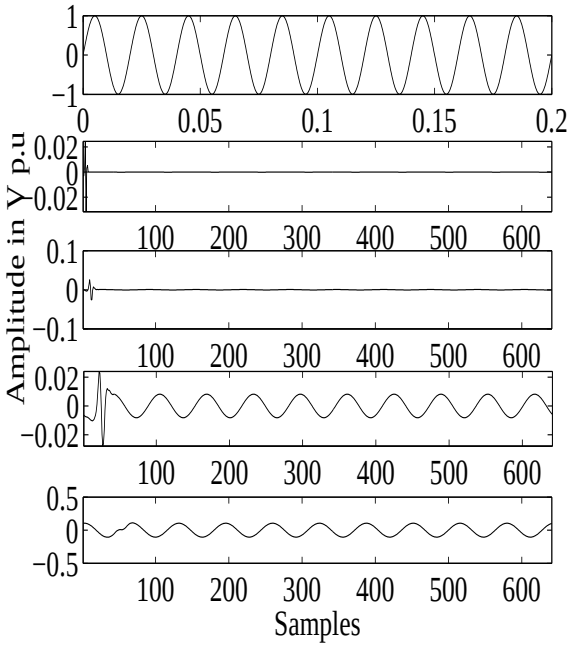

Figure 3.22: Localization of pure sine wave in MODWT decomposition

First of all the normal sine wave voltage signal is considered for analysis. The four finer decomposition level along with the original signal wave form is shown in Figure 3.22.

From Figure 3.22, it can be observed that, the first level is at the same alignment along with the original waveform and the origin of the signal is shifted to the right due to circular shifting. There is no deviation in wave form except the initial point as the original signal is disturbance free.

A pure sinusoidal voltage signal with sag is considered for analysis after the pure sinusoidal signal. The four finer decomposition level along with the original signal wave form is shown. From the Figure 3.23 it is observed that the first decomposition level has provided the exact time of the occurrence of the sag. The inception point of the sag is shifted along with the initial point of the signal towards right due to the circular shifting which assists the prediction in future inception.

Similarly, swell in pure sinusoidal voltage signal has been detected and localized in the finer levels of MODWT decomposition presented in Figure 3.24. The point of occurrence of the swell and the duration of disturbance is clearly detected at first

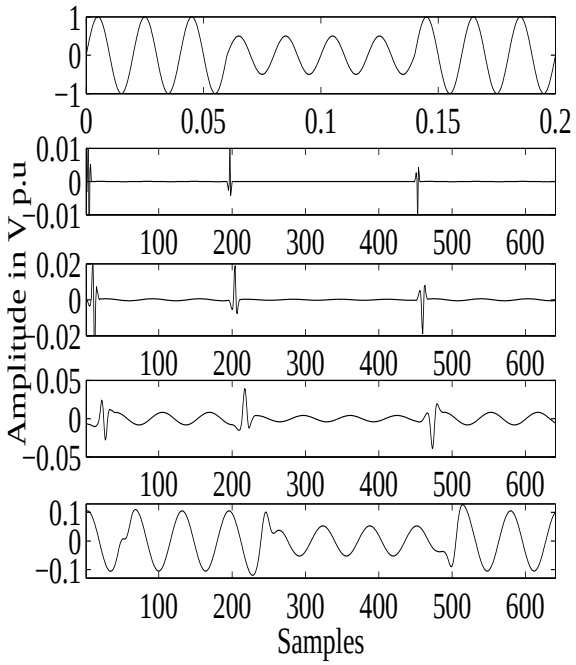

Figure 3.23: Localization of sag in pure sine wave using

decomposition level. The shifting property of the MODWT has helped in predicting of swell in the subsequent decomposition levels. Moreover, the MODWT provides a estimation of the disturbance location which helps in power system relaying.

The interruption in pure sinusoidal voltage signal is localized and detected at the decomposition level of the MODWT and the results are presented in Figure 3.25. The inception point of the interruption are located at the first decomposition level as the original signal and the first decomposition level are at the same alignment. Due to the circular shifting, the point of the interruption and the initial point of the signal are shifted. The one-step-ahead prediction of the MODWT helps in locating the onset timing of the further interruption in signal.

The pure sine wave with notches are precisely localized at the decomposition levels and waveforms are shown in Figure 3.26. The distortion due to the notch is clearly identified by the decomposition levels. The distortion in voltage signal due to the spike in each cycle are detected properly at the decomposition levels of the MODWT and shown in Figure 3.27 .

The harmonics with the fundamental voltage signal is considered for analysis in

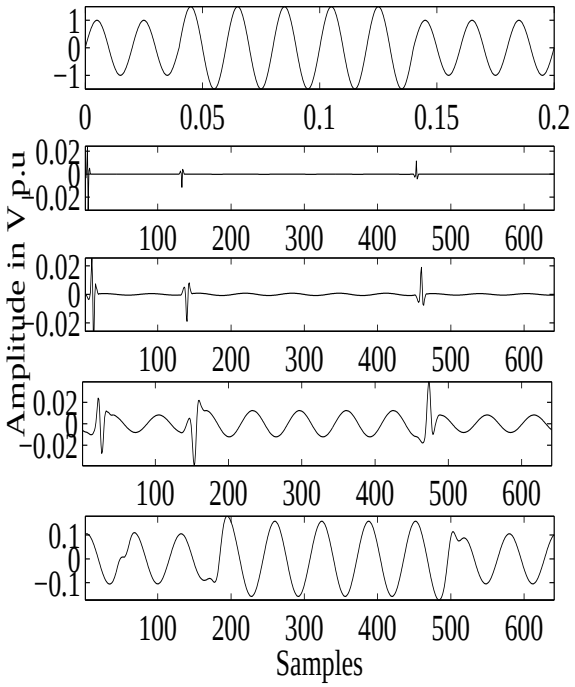

Figure 3.24: Localization of swell in pure sine wave

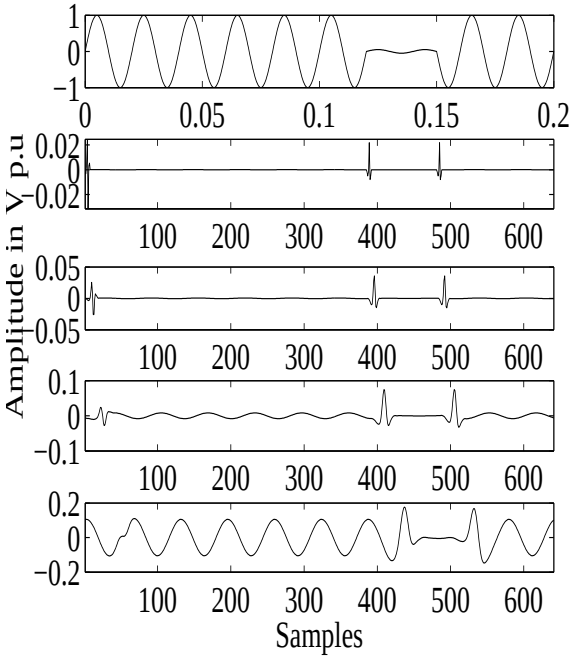

Figure 3.25: Localization of interruption in pure sine wave

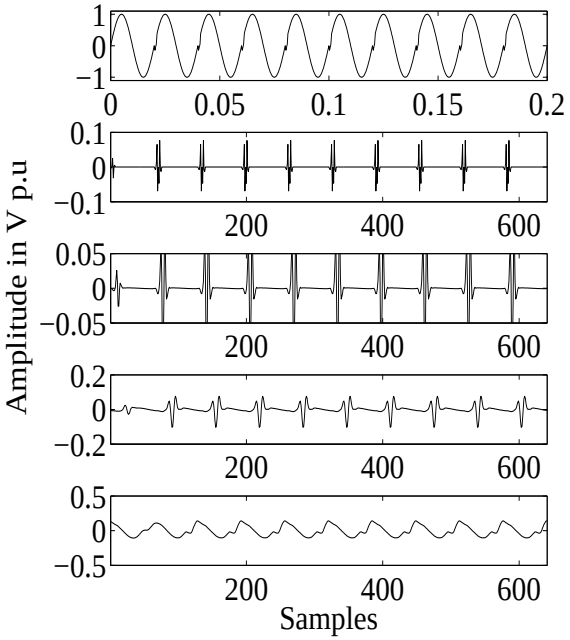

Figure 3.26: Localization of notch in pure sine wave

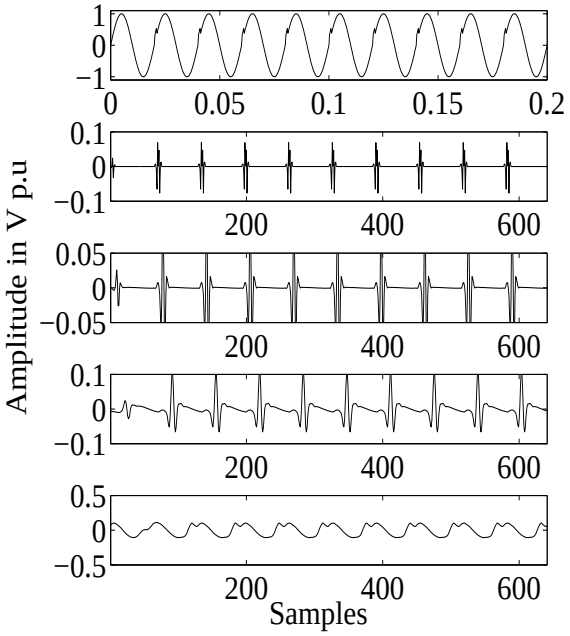

Figure 3.27: Localization of spike in pure sine wave

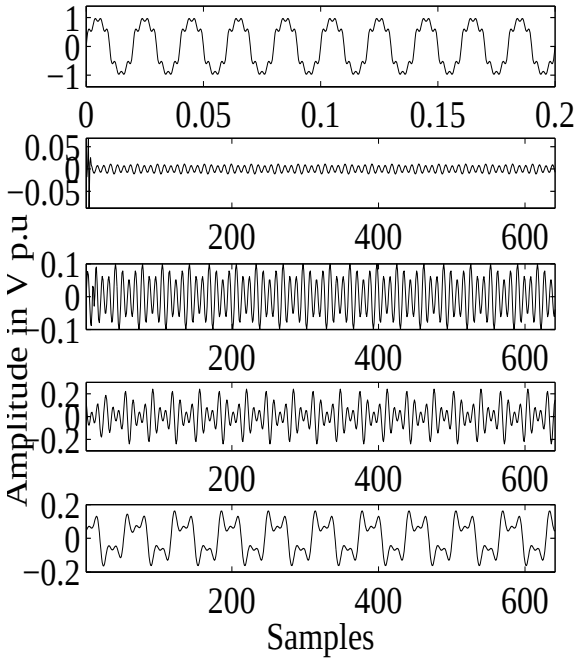

Figure 3.28: Localization of interruption in pure sine wave

.

Figure 3.28. From the Figures. 3.28 and 3.22, it can be observed that for the sinusoidal signal the magnitude of 1^{st} two levels are almost zero where as for the sine wave with harmonic signal, the 1^{st} two levels have some magnitude using MODWT similar to the DWT.

The distortions of a pure sine wave due the the sag and harmonic have been localized in the decomposition levels of MODWT as shown in Figure 3.29. Similarly the harmonic contained swell signal is decomposed in Figure 3.30.

From these Figures, we can recognize that the shift of the starting point does not affected either the amplitude or the shape of PQ disturbance determined by MRA of MODWT. The down sampling free MODWT has been detected the PQ disturbance properly. The one step ahead prediction due to the shifting makes MODWT as good predictor for the power system relaying. The twice DWT calculation in the MODWT also makes the operation slow. The modern power system operation prefers quick action, hence a faster detection technique like lifting based wavelet transform i.e the second generation wavelet transform can be suitable tool for the detection and the

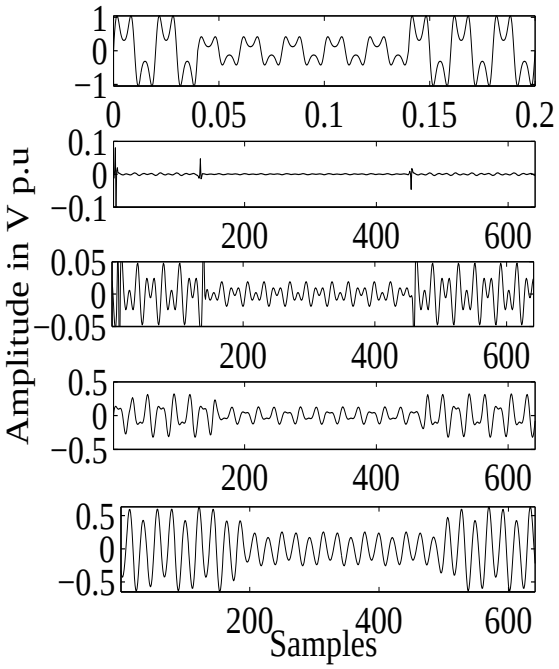

Figure 3.29: Localization of sine wave with sag and harmonics

.

localization. The detection and the localization using SGWT has been taken up in the next section.

The convolution based DWT is suffered inflexible choice of signal length. Similarly the ST is suffered from computational complexity. The modified DWT called as MODWT is also suffered from time of operation. Moreover, DWT is a frequency domain construction of wavelets which requires high computation time [56]. The time domain analysis based Second Generation Wavelet Transform over comes the drawback of conventional DWT and MODWT.

In this Chapter, the lifting based second generation wavelet transform is implemented in order to detect the and localize the aforementioned PQ disturbance signals.

3.8 Second Generation Wavelet Transform (SGWT)

DWT has been traditionally implemented by convolution or FIR filter bank structure. Such implementation require both large number of arithmetic computations and a large

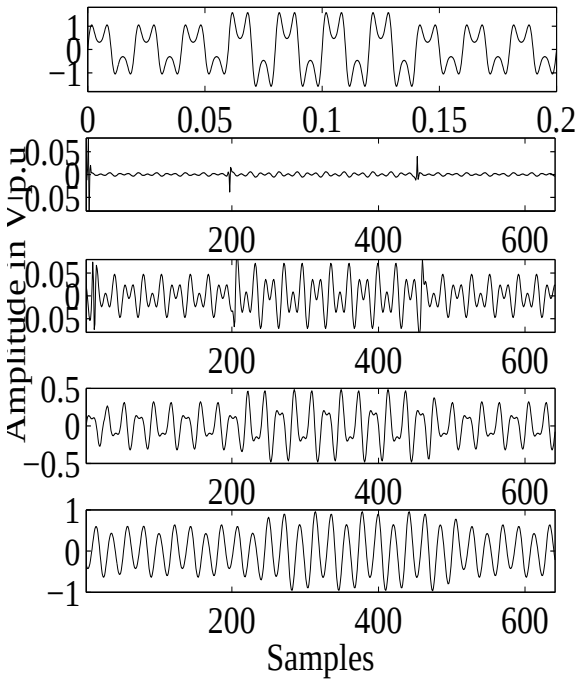

Figure 3.30: Localization of sine wave with swell and harmonics

.

storage features that are not desirable for either high speed or low power signal processing application. So, Sweldens has introduced a wavelet based on spatial construction of wavelets known as second generation wavelet transform (SGWT). The SGWT is a time domain analysis equivalent of traditional DWT. The first generation wavelet transforms, dilation and translation of one of few shapes are occurred. In this case, Fourier transform is often plays crucial role in wavelet construction. Moreover, the non-translation/dilation invariant lifting based spatial (time) transform where Fourier transform are no longer available [48]. The SGWT allows in-place implementation of the traditional DWT due to which SGWT requires no extra memory. The SGWT decreases the hardware requirement while improving the speed of calculation [49]. The main feature of the lifting based DWT scheme as to break up the high-pass and low pass wavelet filters in to sequence of upper and lower triangular matrix and convert the filter implementation into banded matrix (sparse matrix) multiplications.

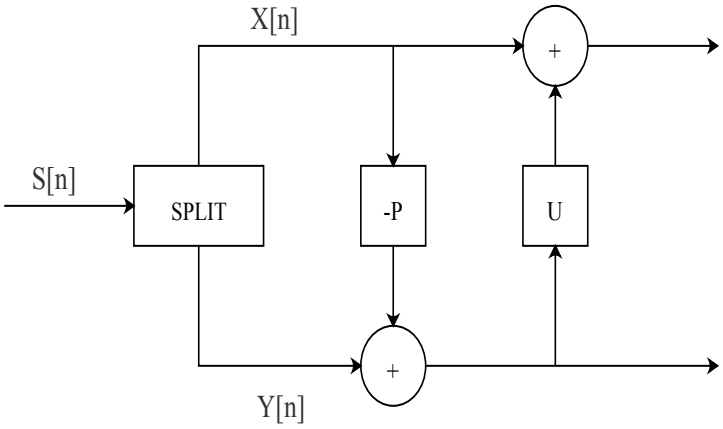

Figure 3.31: Block diagram representation of SGWT decomposition

3.8.1 SGWT Approach in Power Quality Environment

The SGWT is a spatial (or time) domain construction of biorthogonal wavelet based on the process known as the lifting scheme (LS) rather than on convolution used in traditional DWT. The SGWT was originally developed to adjust wavelet transforms to complex geometries and irregular sampling. The LS based SGWT share the same scaling function [47]. The flexible design of SGWT consists of iteration of three operations such as split, predict and update [48] is shown in Figure 3.31.

1. **Split**: In SGWT analysis, the original signal $S[n]$ is first divided into two disjoint subsets as the even index points $X[n]_{\text{even}}$ and the odd index points $Y[n]_{\text{odd}}$, which are correlated. The local correlation property has the possibility to predict and update as presented below.

$$S[n] = X[n]_{\text{even}} + Y[n]_{\text{odd}} \tag{3.26}$$

2. **Predict** : The details of the original signal $S[n]$ are determined in this step using the wavelet decomposition as given in (3.27). Using the predictor operator P, $Y[n]$ is predicted from $X[n]$.

$$d[n] = Y[n]_{\text{odd}} - P(X[n]_{\text{even}}) \tag{3.27}$$

3. **Update** : The approximation coefficients of the original signal $S[n]$ are deter-

mined by using (3.28). The update operator U is applied to the details and the result is added with $X[n]_{\text{even}}$ in this step.

$$C[n] = X[n]_{\text{even}} + U(d[n]) \tag{3.28}$$

The process is further iterate with the approximation generated at the first level.

Moreover, SGWT requires half number of computation as compared to convolution based traditional DWT and it allows a fully in-place computation feature of lifting. So SGWT is implemented ordered to reduce auxiliary memory consumption and to obtain quick result than the other traditional methods [92].

3.8.2 Selection of Mother Wavelet

The Second generation wavelet transform based power quality disturbance signal analysis initiate with selection of a appropriate mother wavelet. For SGWT implementation in PQ environment, db4 has been chosen as suitable mother wavelet for detection of both the slow and fast transient disturbances similar to the DWT.

3.8.3 SGWT Implementation in PQ Disturbance Localization

Ten type of power quality disturbances along with the pure sinusoidal waveform are processed through Figure 3.31. The signals are decomposed up to four decomposition levels. The horizontal axis represents the time in terms of samples and the vertical axis represents the magnitude i.e., amplitude in volt p.u.

A sinusoidal voltage signal has been fed for SGWT decomposition shown in Figure 3.31. The signal has been decomposed up to fourth decomposition level is presented in Figure 3.32 along with the original signal. As it is distortion free signal, so there is no deviation in the decomposition level.

The pure sine wave with sag has been considered for analysis in Figure 3.33. The original wave form and the four finer decomposition levels has been presented in Figure 3.4. The decomposition levels has been pin down the exact disturbance occurrence instant. The initial and end points of the disturbance has been clearly identified properly.

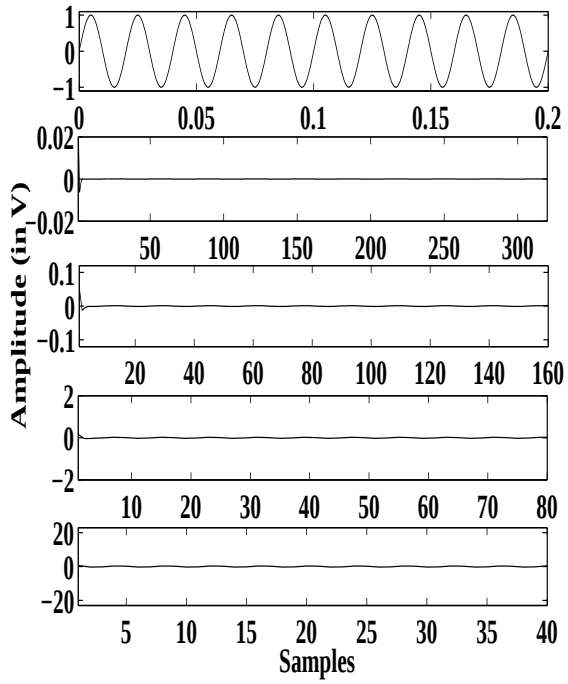

Figure 3.32: Localization of pure sine wave in SGWT decomposition

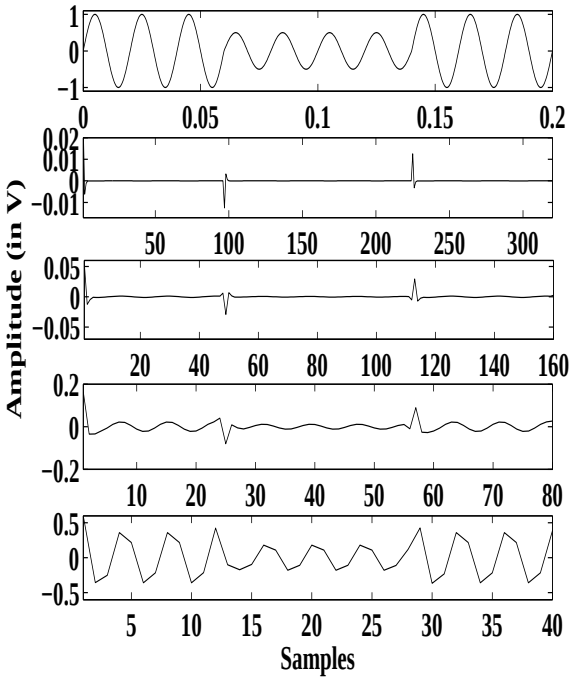

Figure 3.33: Localization of sag in pure sine wave

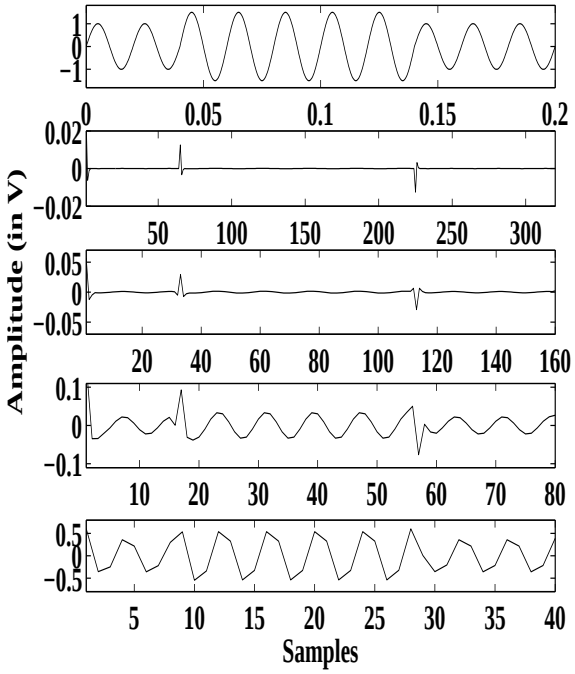

Figure 3.34: Localization of swell in pure sine wave

The swell in pure sine wave has been detected and localized in the finer decomposition levels of SGWT decomposition Figure 3.34. The point of occurrence and duration of swell has been clearly identified at all decomposition levels like DWT decomposition.

Pure sine wave signal with interruption is decomposed into finer levels with SGWT like others. The point of initiation of interruption has been clearly detected at the finer levels in Figure 3.35 The point of deviation due to interruption and duration of disturbance has been easily identified by the finer decomposition levels of SGWT.

A pure sine wave with notch at each cycle has been considered for analysis. The notches at each cycle of the wave form has been clearly detected and localized in the finer levels of SGWT decomposition in Figure 3.36.

The oscillatory transient signal has been considered for analysis. The signal has been decomposed upto four finer levels presented in Figure 3.37.

The sinusoidal voltage signal with flicker has been considered in Figure 3.38. The detection and localization of flicker have been carried out at the finer level of SGWT decomposition.

The spike at each cycle of voltage signal has been considered for analysis. The

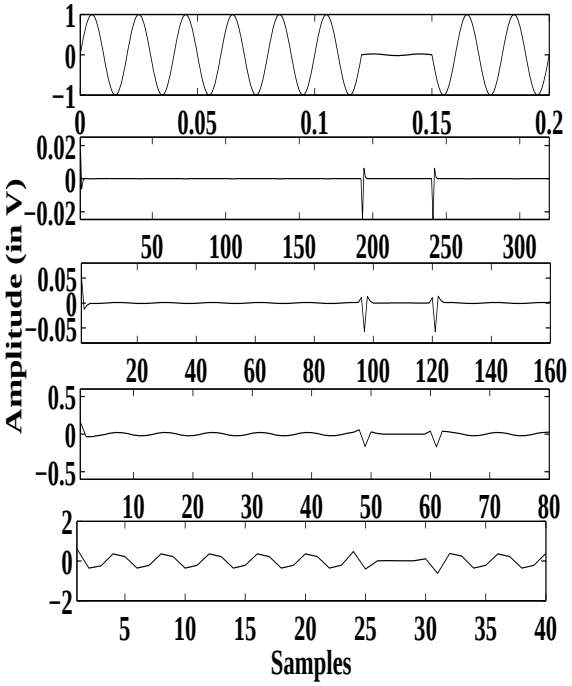

Figure 3.35: Localization of swell in pure sine wave

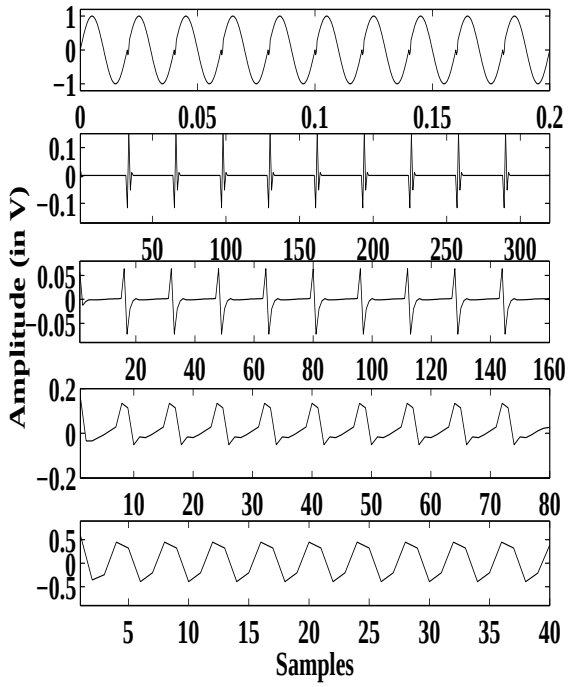

Figure 3.36: Localization of sine wave with notch

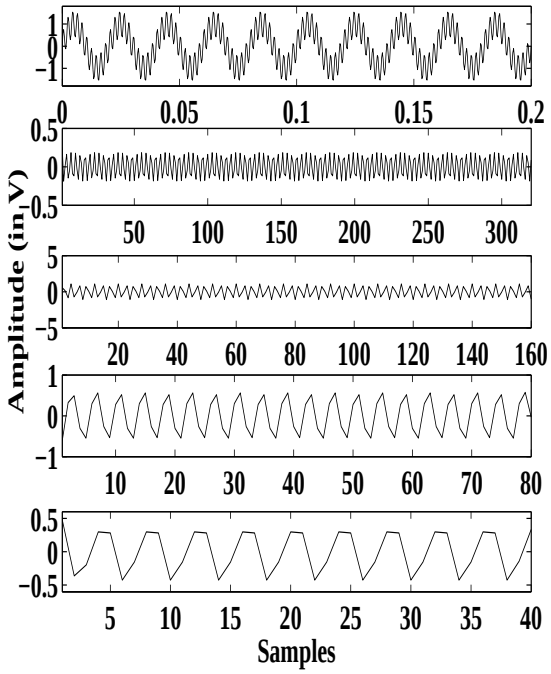

Figure 3.37: Localization of sine wave with oscillatory transient

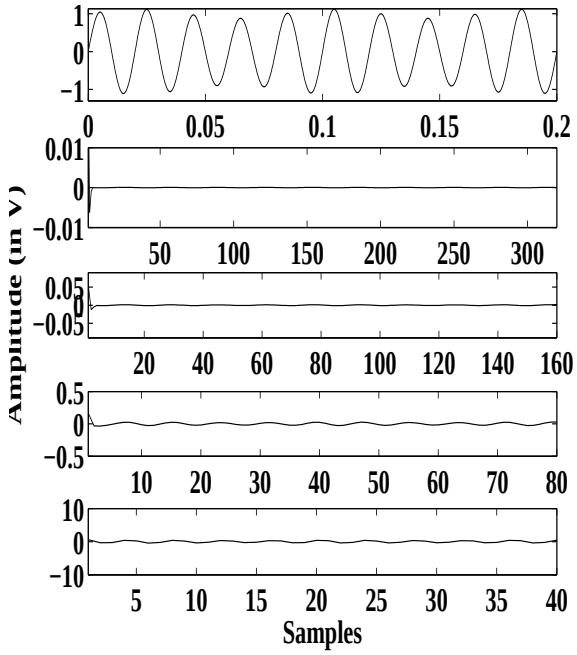

Figure 3.38: Localization of sine wave with flicker

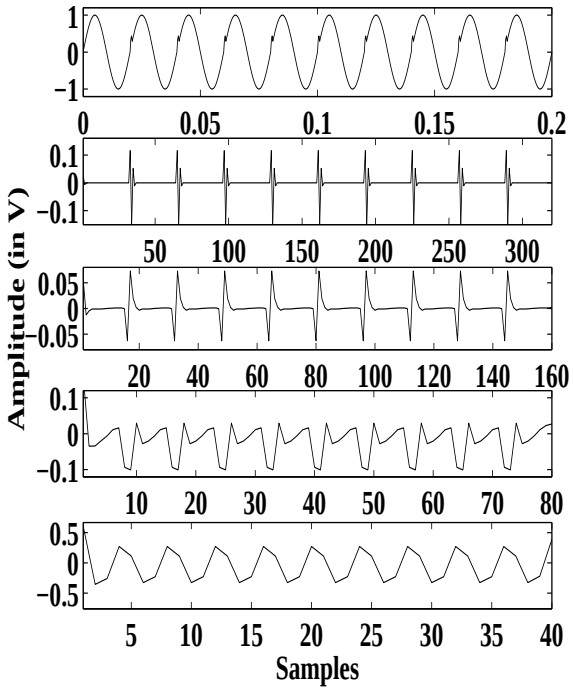

Figure 3.39: Localization of sine wave with spike

spike has been detected and localized even at the finer decomposition level of SGWT in 3.39.

The harmonic with fundamental has considered for analysis in Figure 3.40. By comparing Figure 3.32 and Figure 3.40, it has been observed that the magnitude of harmonic content signal is more than the pure sine wave at their respective level.

The sag with harmonic signal has analyzed in SGWT in Figure 3.41. The distortion has been detected and localized at the finer level of SGWT like DWT and MODWT.

Swell with harmonic in voltage signal has considered for analysis in Figure 3.42. The distortions has been also detected and localized at the finer decomposition levels.

3.9 Comparative Analysis of the PQ Disturbance Detection Techniques

The aforementioned PQ disturbance signals are analyzed with four decomposition methods like DWT, ST, MODWT and SGWT. Pure sine wave voltage signal has been

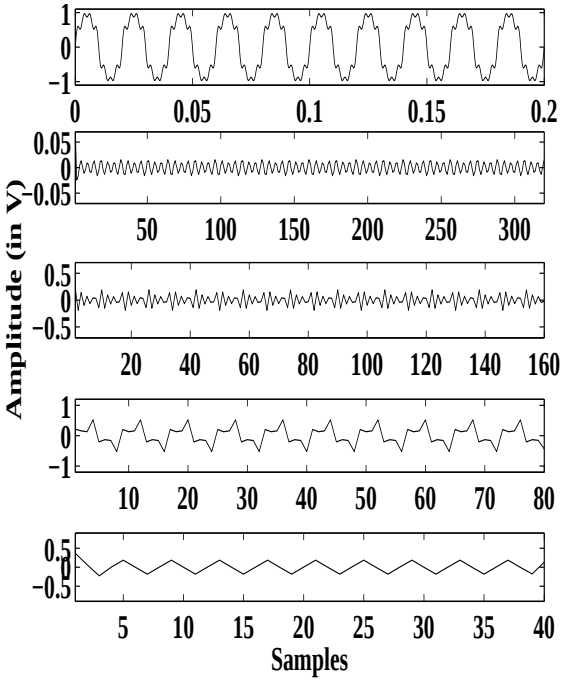

Figure 3.40: Localization of sine wave with harmonics

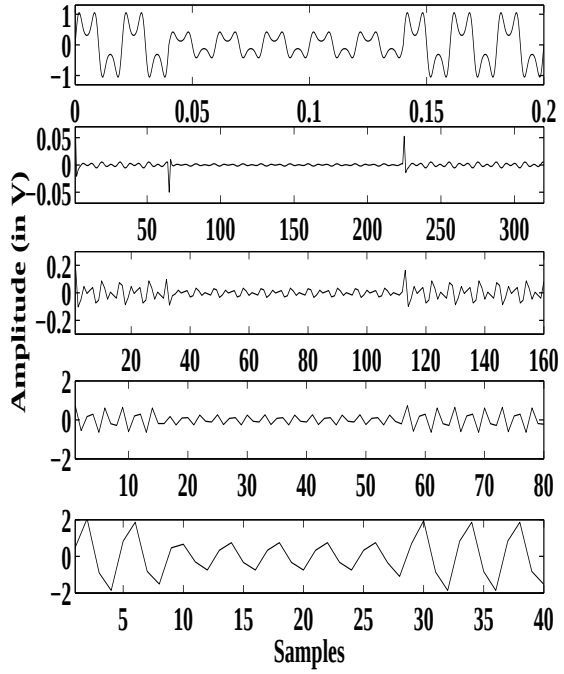

Figure 3.41: Localization of sine wave with harmonics

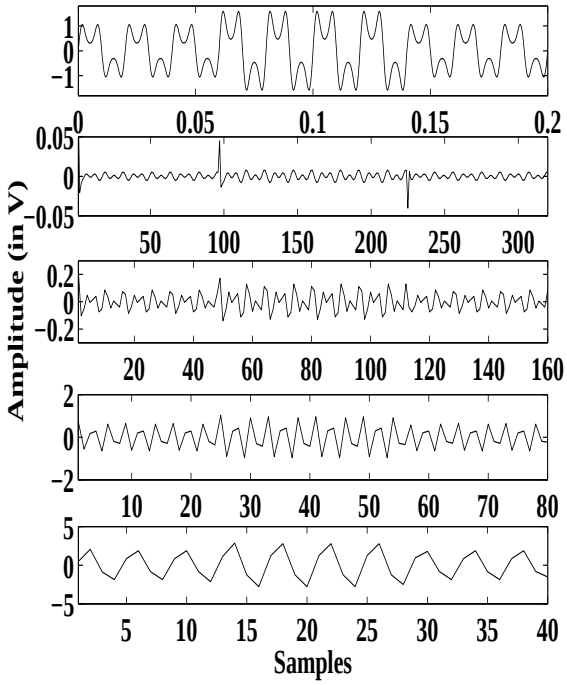

Figure 3.42: Localization of sine wave with harmonics

considered for analysis with aforementioned methods shown in Figure 3.43. As the pure sine wave is the distortion free, so there are no deviation in the output waveform in other methods except MODWT. In MODWT, the initial point has been shifted to right due to the circular shifting.

Pure sine wave with sag has considered for analysis with these aforementioned techniques in Figure 3.44. Sag has been localized by all the detection methods. The inception and end point of sag has been localized in all the cases properly. Though in ST, sag has been identified properly, but it requires more time and memory. The MODWT has provided the inception point of sag with same alignment of the original signal at the first level like DWT and SGWT whereas in other level the inception point is shifted due to circular shifting.

Similarly, swell with harmonic signal has considered for analysis with all the aforementioned techniques in Figure 3.45. The distortion has been localized properly by all the techniques like the sag signal. Similarly, notch at each cycle of pure sine wave has been considered in Figure 3.46. The distortion due to notch has clearly identified by the methods. Similarly other signals can be analyzed. Though all the aforementioned

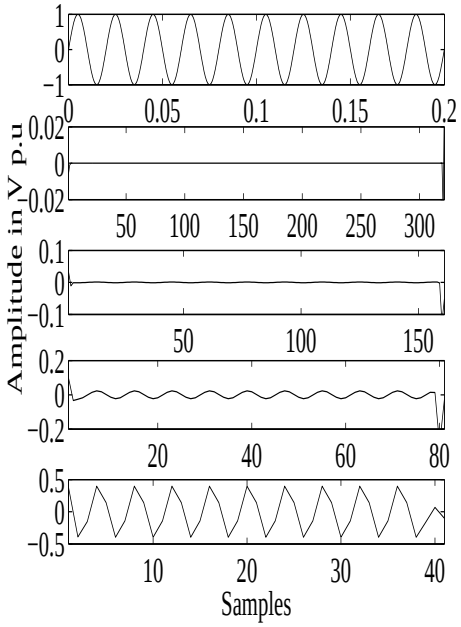

(a) DWT analysis

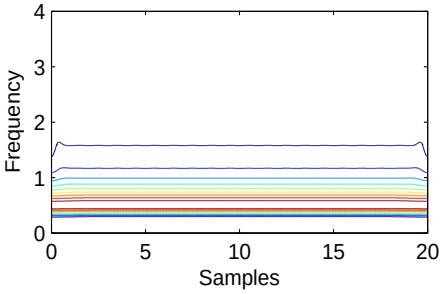

(b) ST analysis

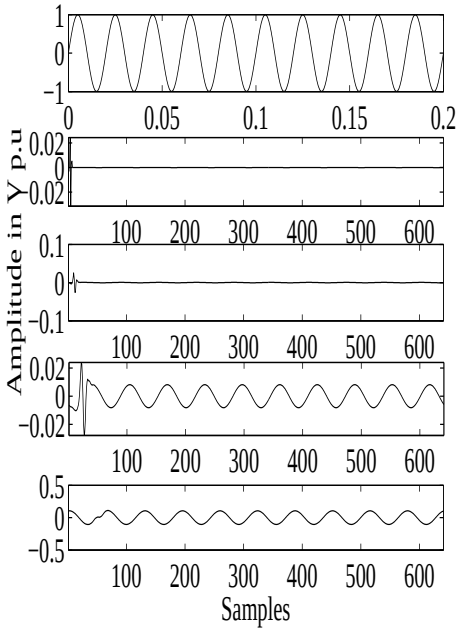

(c) MODWT analysis

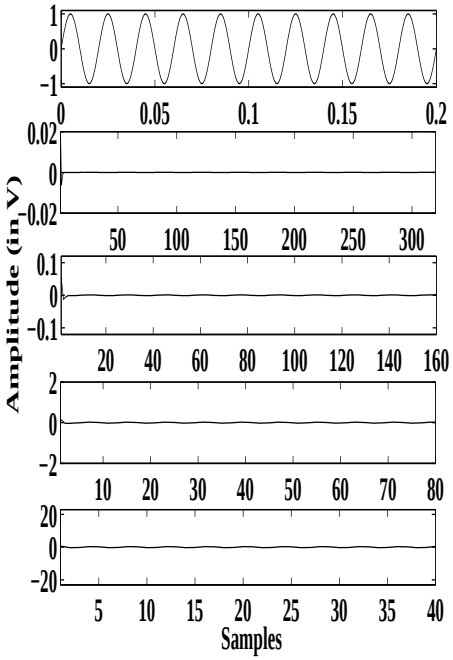

(d) SGWT analysis

Figure 3.43: Localization of pure sinusoidal voltage signal

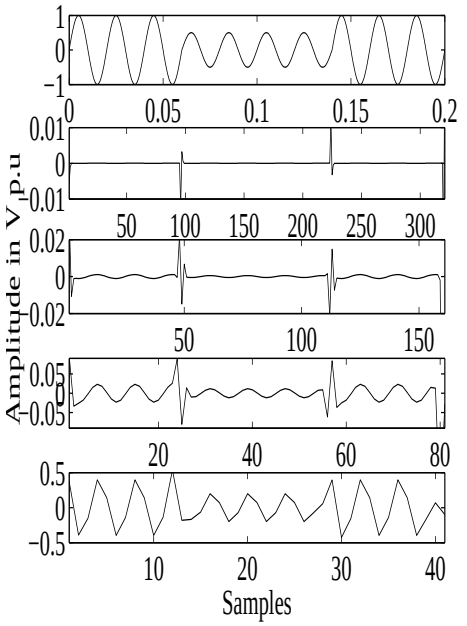

(a) DWT analysis

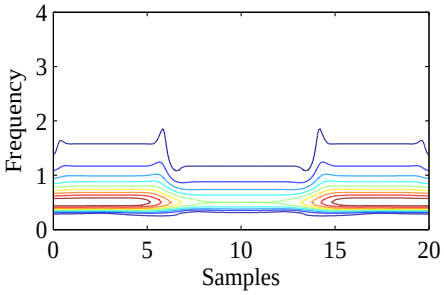

(b) ST analysis

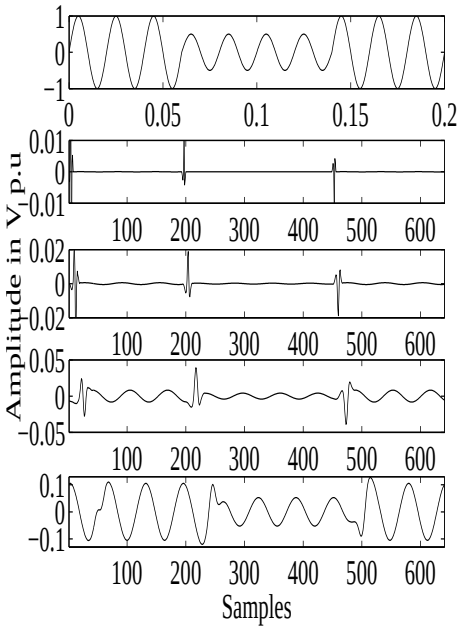

(c) MODWT analysis

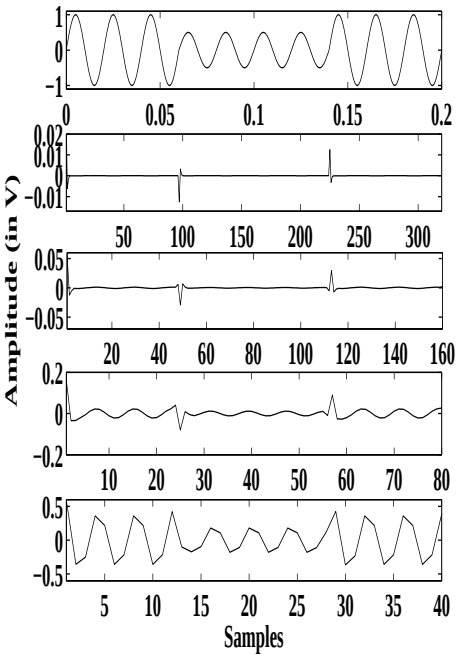

(d) SGWT analysis

Figure 3.44: Localization of sag in pure sinusoidal voltage signal

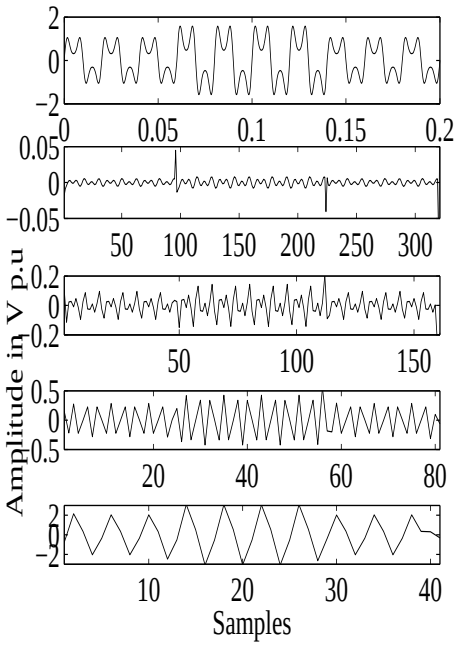

(a) DWT analysis

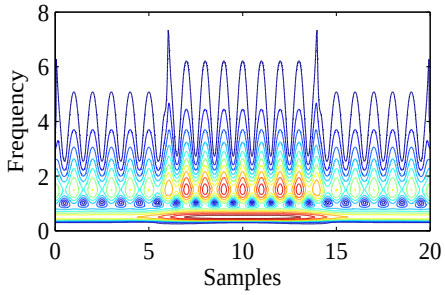

(b) ST analysis

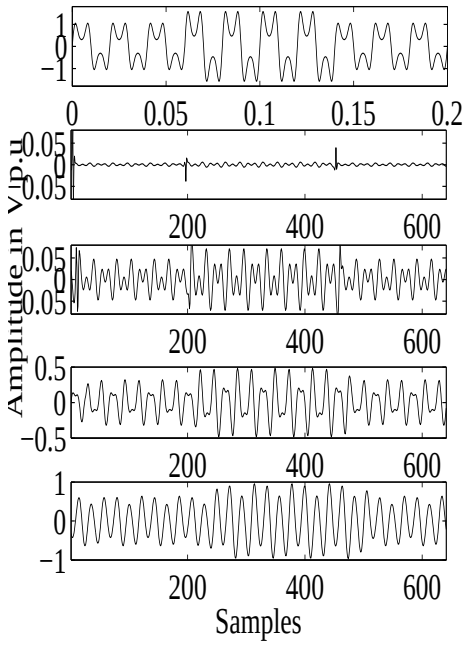

(c) MODWT analysis

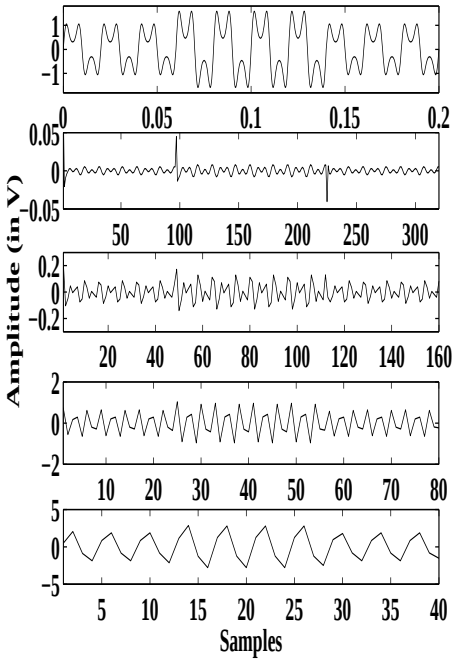

(d) SGWT analysis

Figure 3.45: Localization of swell and harmonic in pure sinusoidal voltage signal

Table 3.2: Detection time using DWT and SGWT

Signal Name	Case-I	Case-II	Case-III	Case-IV	Case-V	Case-VI	Case-VII	Case-VIII
Normal voltage	0.427848	0.388834	0.403922	0.383851	0.405932	0.383124	0.411128	0.379815
Sag	0.354972	0.391306	0.405250	0.351647	0.379606	0.348972	0.384160	0.353076
Swell	0.3990793	0.360704	0.395563	0.358637	0.379376	0.345644	0.389896	0.359110
Notch	0.392118	0.358708	0.391223	0.349225	0.399078	0.355296	0.387627	0.354749
Spike	0.405006	0.357652	0.400942	0.361598	0.383911	0.350353	0.384353	0.346988
Interruption	0.392788	0.351088	0.402356	0.356198	0.400476	0.360466	0.386810	0.348666
Flicker	0.422033	0.390208	0.659233	0.571185	0.420994	0.382794	0.416659	0.388962
Harmonics	0.434865	0.387819	0.410627	0.383050	0.428155	0.388043	0.406228	0.379664
Swell + harmonic	0.397851	0.358214	0.404568	0.354992	0.380966	0.358092	0.379928	0.344774
Sag+harmonic	0.391306	0.358214	0.398544	0.364737	0.380000	0.351252	0.388362	0.352663

detection methods provide good result but the SGWT is faster than the others which is discussed in subsequent subsection.

3.9.1 Processing Time Comparison of PQ Disturbance Detection

The aforementioned ten type of PQ disturbances signals along with pure sinusoidal signal are simulated with $i5$ CPU with 4.00 GB RAM, 32 bit operating system. The processing time for decomposition at four different instants in both DWT and SGWT are shown in Table 3.2. In the Table 3.2, Case−I,III,V,VI are the processing time(in second) of DWT decomposition at four different instants. Similarly Case−II, IV, VI and VIII are representing SGWT decomposition time at the same instants. From the Table, it can be observed that in each case, the SGWT is faster than the traditional DWT.

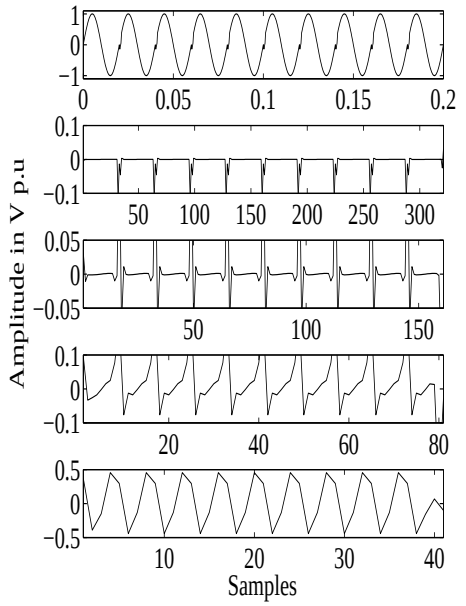

(a) DWT analysis

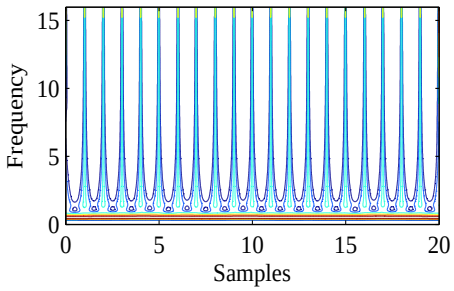

(b) ST analysis

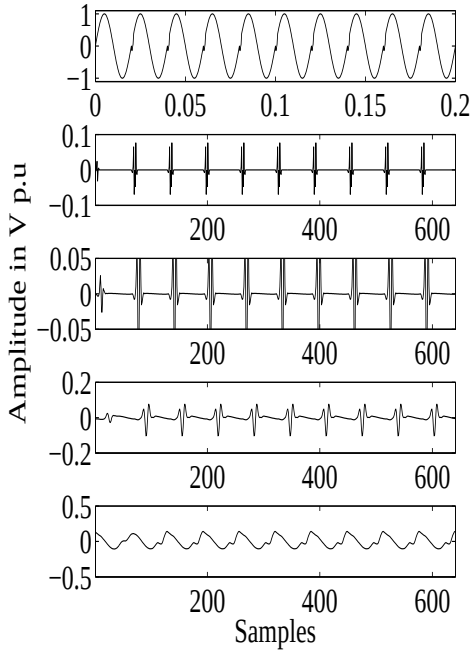

(c) MODWT analysis

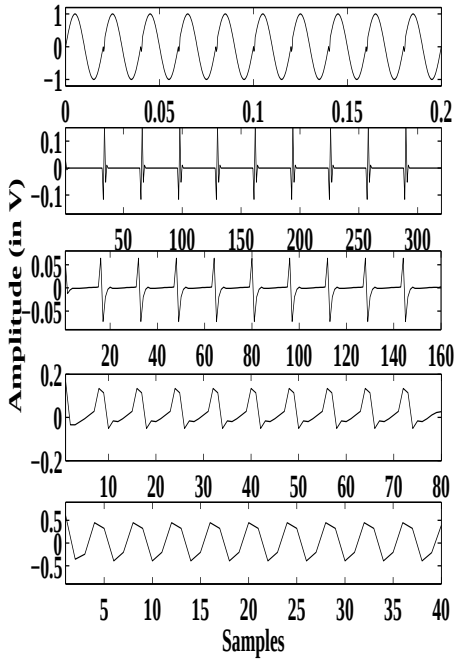

(d) SGWT analysis

Figure 3.46: Localization of notch in pure sinusoidal voltage signal

Table 3.3: Detection time using DWT,ST,MODWT and SGWT

Signal Name	DWT(S)	ST(S)	MODWT(S)	SGWT(S)
Sag	1.235055	1.714281	0.674638	0.615430
Swell	0.639154	0.787957	0.579269	0.470810
Notch	1.257431	2.252060	0.931468	0.476123
Spike	0.587702	0.889862	0.579528	0.464816
Interruption	0.640705	1.294703	0.641956	0.503307
Flicker	0.985968	1.824405	0.828924	0.716523
Harmonics	1.326254	1.957118	0.968240	0.585656
Swell+harmonic	0.589112	0.975711	0.562793	0.425167
Sag+harmonic	0.613254	0.853998	0.578844	0.483502

Similarly, the processing time of DWT, ST, MODWT and SGWT for detection of PQ disturbances measured from Core $i5$ CPU with 6.00 GB RAM, 64 bit operating system is presented in Table 3.3. The possessing time of one signal from each event has been presented in this Table. The signals has been decomposed four finer levels with the variants of WT. From the Table, it has been observed that the ST requires more than the other methods, whereas the SGWT requires less time. As the power system operation based on quick action, so SGWT is suitable for faster localization of PQ disturbances.

From Table 3.3, it can be observed that SGWT is the faster technique than the down sampling free MODWT. Whereas the DWT is faster than the ST. As, the signals have been decomposed up to finer levels, down sampling free MODWT required less time than the traditional DWT for analysis.

3.10 Chapter Summary

In this Chapter, the PQ detection and the localization has been carried out using ST and three types of WT, namely the DWT, MODWT and the SGWT. The ST performs

better localization than the DWT. But ST is computationally intensive. The MODWT is down sampling free and in this process, it provides proper localization of the PQDs along with the shifting. The down sampling free MODWT is insensitive in the choice of the signal length. Moreover, compared to ST, it is not computationally intensive. Hence, the MODWT is more effective than the DWT and ST in the detection and localization of PQ disturbances. The insensitivity to the choice of starting point of time series turns MODWT as a suitable tool in real time environment. However, the lifting based SGWT is faster than the MODWT as well as the DWT. SGWT requires half number of computation as compared to convolution based DWT and MODWT. The SGWT also reduces auxiliary memory consumption.

Chapter 4

Feature Extraction and Different Approaches for Classification of Power Quality Disturbances

4.1 Introduction

In the previous Chapter-3, ten different types of voltage signals along with the normal voltage signal have been analyzed. The inception and the end points of the disturbances have been properly identified by the variants of WT. A healthy power system operation requires proper and quick mitigation of the disturbances. The mitigation of the PQ disturbances requires proper detection and identification of the source of the disturbance.

The automatic and the fast characterization of the different power quality disturbance signals has become an emerging issue for the power system researchers. Some common automated classification models are based on the Artificial Neural Network (ANN) [57], [58], fuzzy and neuro-fuzzy systems [62], [63], [30]. But the ANN suffers from more number of training cycles which results in a huge computational burden. However, the main disadvantage of the traditional ANN based classifier is the requirement of retraining when a new phenomenon is added. Similarly, the Hidden Markov Model (HMMs) classifier fails to classify the slow phenomena like interruption, sag etc properly [93], [64].

The automatic and fast characterization of different power quality disturbance signals have been become an emerging issue for for power system researchers. Some common automated classification models are based on the Artificial Neural Network (ANN) [56], [57], fuzzy and neuro-fuzzy systems [62], [94], [30]. But the ANN suffers from the more number of training cycles which makes a huge computational burden. However, the main disadvantage of the traditional ANN based classifier is the requirement of retraining when a new phenomenon is added. Similarly, the Hidden Markov Model (HMMs) classifier is fails to classify the slow phenomena like interruption, sag etc properly [93], [64].

In this Chapter, two automatic classifiers such as the decision tree (DT) and the ensemble decision tree i.e random forest (RF) have been proposed for the classification of different PQ disturbance signals. For the classification of a signal type, the first step is retrieval of the input patterns from the signals in the absence and the presence of Additive White Gaussian Noise (AWGN). Also the results of the MLP and the HMMs classifiers have been discussed. The suitable features have been extracted from the output of the four different transforms implemented in Chapter-3. In order to reduce memory consumption, the extracted features are provided as outputs to the classifiers in stead of providing the raw data. Four features have been extracted for each decomposition level.

After the feature extraction, the entire data set is split into the training set and the testing set. The classification accuracy (%CA) has been calculated with the testing data in order to recognise the disturbances. The (%CA) has been calculated with the data set both in noisy and noiseless environment with four different classifiers.

4.2 Important Steps carried out in this Chapter

- To synthesize large number of signals for each class by varying the magnitude and the duration of the disturbance in the absence and presence of noise.
- To extract suitable features from the output of the signal transformation in ordered to provide input to the classifiers.
- To characterize different types of signals in terms of classification by the proposed

classifiers.

4.3 Organisation of the Chapter

In order to realize the desired objective, the data preparation, feature extraction and the classification approach have been carried out.

This Chapter is organized as follows: the synthesis of data has presented in Section-4.4. Section-4.5 presents idea about extraction of selected features. Similarly, brief description about data mining classifiers has presented in Section-4.6. Section-4.7 provides classification of different types of synthesized data. The concluding remarks are provided in Section-4.8.

4.4 Data Preparation

The data sets used in this Chapter have been synthesized in MATLAB simulation environment using the disturbance model presented in Table 3.1 in Chapter-3. The unit step function $u(t)$ in the whole Table 3.1 provides the duration of disturbances present in the pure sine waveform. During the synthesis of the disturbance signal from the parametric model, the position of $u(t)$ and value of α have been varied substantially. Hence large number of signals has been obtained by varying magnitude (by varying α) on different points on the wave (by changing the parameters t_1 and t_2) and the duration of the disturbance $(t_2 - t_1)$. The point on the waveform is the instant on the sinusoid when a disturbance begins and is controlled by the position of the unit step function $u(t)$. In the real world, the PQD signals may have any point on the waveform which is beyond the control, so a variety of disturbances have been generated with different points on the wave duration of disturbance and magnitudes. The flicker signal has generated by changing the flicker frequency β and the its amplitude α. The transient signals are synthesized by varying its frequency f_n, amplitude α, and the inverse of the time constant of decay τ. However the harmonic signal consists of a combination of third, fifth and seventh harmonic. The momentary interruption signals are generated with the variation of amplitude during interruption. Finally, the spike and notch are the short duration disturbance as compared to the sag and swell. The

hundred number of cycles of voltage signals are considered with sampling frequency 3.2 kHz. By varying the parameters, total 34090 signals are synthesized. Moreover, the white Gaussian noise with different noise to signal ratio (SNR) has been added to the pure PQ signal in order to get a noisy environment. Each signal has been fed to the variants of the WT described in Chapter-3. The signals are decomposed up to seven levels. Four selected features have been extracted at each decomposition level. Hence, for each signal 28 features are extracted in total. The feature extraction has been described in next subsection.

4.5 Feature Extraction

The input to the classifiers are extracted features from the output of the signal decomposition instead of directly using the raw data in ordered to reduce the computational burden. The quantitative analysis in terms of features like the energy content, the standard deviation (STD), the cumulative sum (CUSUM) and the entropy of the transformed signal is performed in order to reduce the classification error. The basis of choosing the features is explained below along with the proper expressions [53].

- **Energy** : According to Parseval's theorem the energy of the distorted signal will be partitioned at different resolution levels in different ways depending on the power quality disturbances signals. So, it has been established that energy distribution pattern changes when the amplitude and frequency of the signal changes [51] and [26].

$$\text{Energy} \quad ED_i = \frac{1}{N}\sum_{j=1}^{N} |D_{ij}|^2 \tag{4.1}$$

  where $i = 1, 2, 3, \ldots, l$ (level of decomposition) and N is the number of samples in each decomposed data. D stands for detail coefficient.

- **Entropy** : The spectral entropy of the non-stationary power signal disturbances is an effective parameter for the classification of the signal. The entropy value for low frequency disturbances like the voltage swell, the voltage sag, the momentary interruption and the pure undistorted sinusoidal signal is minimum.

The harmonics contained in the signals such as sag with harmonics, swell with harmonics have a comparatively high entropy value. For flicker type signals the entropy value is minimum. Similarly in case of the short duration non-stationary power signal disturbances such as the notches and the spikes have very low entropy values. While transients have relatively higher entropy value [52].

$$\text{Entropy} \quad ENT_i = -\sum_{j=1}^{N} D_{ij}^2 \log(D_{ij}^2) \tag{4.2}$$

- **Standard deviation** : Assuming a zero mean, the standard deviation can be considered as a measure of the energy of the considered signal. Standard deviation is used to differentiate the low frequency and the high frequency signals [26].

$$\text{Standard deviation} \quad \sigma_i = \left(\frac{1}{N} \sum_{j=1}^{N} (D_{ij} - \mu_i)^2 \right)^{\frac{1}{2}} \tag{4.3}$$

- **CUSUM** : The cumulative sum method uses the samples for the localization of the distortion in the signal. The CUSUM is computed by the sum of the consecutive samples of the power quality signal after being passed through the aforementioned transforms [95].

$$\text{CUSUM} \quad CM_i = \sum_{j=1}^{N} (D_{ij} - \mu_i)^2 \tag{4.4}$$

where $Mean \quad \mu_i = \frac{1}{N} \sum_{j=1}^{N} D_{ij}$

These four features have been extracted from the output of the transformation. At each level four features are extracted, so for each signal in WT $4 * 7$ feature vector have been formed. After calculating the features for the complete data sets, the feature vectors are normalised between $[0, 1]$ by considering the maximum value of the corresponding feature vectors as the base. However, the normalisation is one of the important steps of pre processing of the data before classification. This vector normalisation has been carried out in order to avoid the influence of high range feature vectors over low range ones. The extracted features have been fed as put to the

proposed data mining classifiers like the decision tree (DT) and random forest (RF).

4.6 Data Mining based Classification Approach

Data mining is an inter disciplinary field which performs the extraction of the useful features and the useful patterns from the stored historical data for decision making or classification. In other words, the data mining tool is an suitable analytical tool which discovers hidden valuable knowledge by analysing large amount of data. The data mining operation can be divided in to three phases like the training, the testing and the data validation. In training phase, the random sampled data are used to develop a data mining model. The developed model is tested for the conformity as well as the accuracy by implementing the validation data. In validation phase, the miner has the ability to adjust the model by minimising an error criterion. The validation data are also implemented to estimate the error in ordered to inquiry the performance of the models in normal operating conditions. For the classification, the supervised models are used which employs labeled training data and may require additional user input during the training phase. The class to which a training datum belongs is known *apriori*. These labeled data are employed to build a data mining model. The unlabeled test data can be classified using this model [96], [97].

4.6.1 Steps in Data Mining Operation

The operation of data mining approach consists of different steps which are presented below.

- **Data gathering and filtering** : The data gathering step gathers the data by creating a warehouse. The data filtering extracts essential and require attributes from the operational data.
- **Data standardisation** : All the categorial variables like the date, the time are standardised to the lowest denomination by collapsing unwanted categories.
- **Data cleaning** : In cleaning operation, all the data that violate the rules are either discarded or transformed.

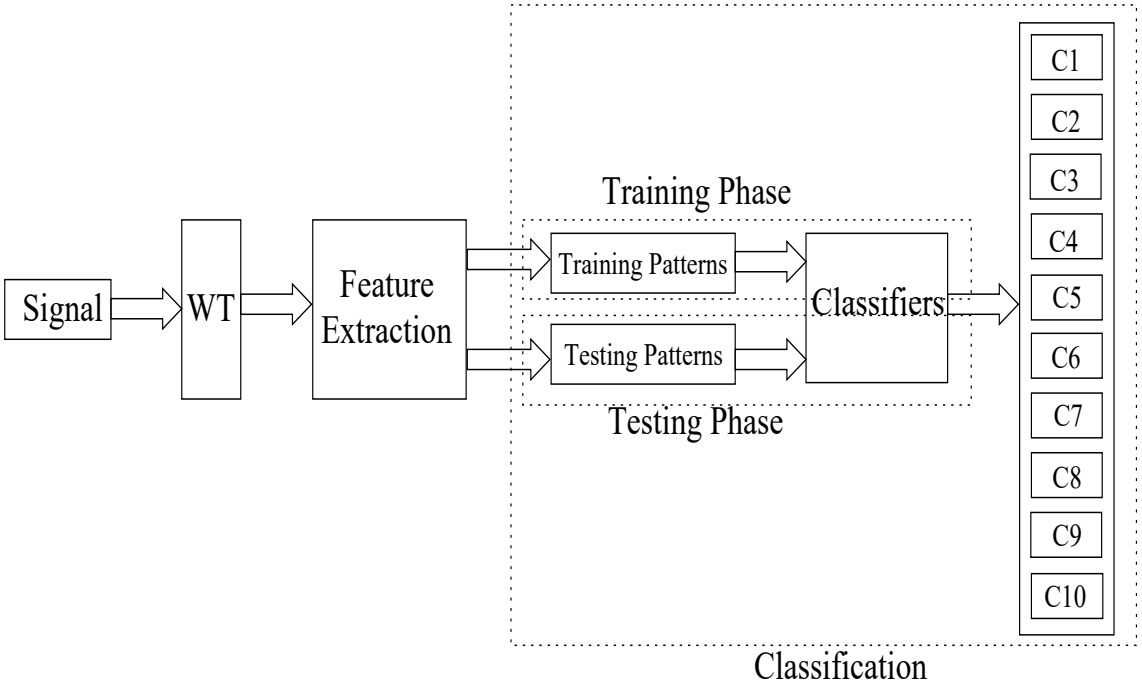

Figure 4.1: Block diagram of classification process

- **Loading of filtered transaction data into the data warehouse** : All formatting characters are standardised and all types of errors present in the data are corrected in this step.

- **Summarising Data** : Extract-Transform-Load (ETL) utilities are implemented to load the data into the warehouse. Data warehouse contains highly summarised data. Data are pre-summarised and collapsed in order to analyze, categorise and store in the OLAP structure.

- **Security and user management** : The scrutiny treats like jamming, session hijacking, processor overloading etc are done. The user management are also carried out using authentication and authorisation.

- **Data analysis and visualisation** : The data mining tools come bundled with data analysis and proprietary visualisation.

4.6.2 Data Mining Approaches

Depending upon the type of data and the objectives, data mining employs different approaches. These approaches are presented below

- **Association rules** : Association rules are built from the related activities
- **Clustering** : A large heterogeneous population breaks into smaller number of homogeneous group.
- **Classification** : Organisation of labeled data into distinct categories or classes.
- **Regression** : Modelling of a single variable from one or more independent predictor variables.
- **Optimisation** : Solving of complex problems.

Among all these above approaches, the classification has been played vital rule in the financial data analysis, retail industry, the telecommunication industry, the biological data analysis and in scientific applications etc. The classification approach includes the decision tree, neural network, support vector machine (SVM) and random forest etc. The decision tree and the random forest have been proposed for analysis of single and combined signals of large number of data set.

4.6.3 Decision Tree (DT)

Decision tree is a supervised learning method in which the learning occurs from the class-labeled training tuples. A decision tree is a flowchart like tree structure which can be designed from top to down, bottom to up and other special approaches. However, top to down approach is commonly accepted and generally are drawn from left to right. Generally the tree is constructed in a top-down recursive divide and conquer manner. A tree consists of three parts as the root node, the internal node and the leaf node. A node maps a certain characteristic and the branches carry a range of values [98]. The basic block diagram of a DT is presented in Figure 4.2

- **Root node** : In this node, the operation of DT starts with the entire data samples.

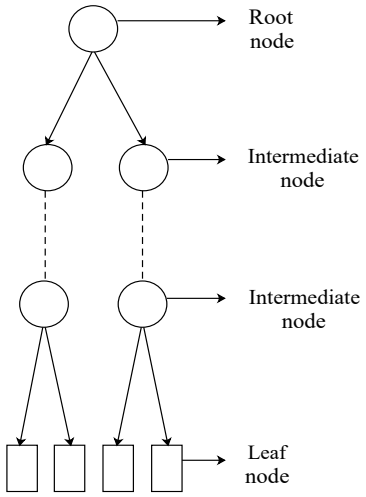

Figure 4.2: Structure of DT

- **Internal node** : The next step is the division of the records according to their features. The assigned node is called the *internal node*.
- **Leaf node** : Similarly, the next step is assignment of a class label to the nodes. The class label assigned nodes are called as *leaf node*.

The most widely used top-down algorithm of DT have been presented.

4.6.3.1 The Algorithm of a decision tree

The Generation of a decision tree with the training tuples of data partition P [99].

4.6.3.2 *Input*

- **Data partition** : The data partition, P consists of the training tuples and their associated class labels.
- **Attribute list** : The attribute list is the set of candidate attributes.
- **Attribute selection methods** : The procedure of determination of splitting criteria which gives the *best* partition of the data tuple into individual classes. This criterion consists of a *splitting attribute* and which is a *split point* or *splitting subset*.

4.6.3.3 *Output*

- **Decision tree** : The output of the algorithm is a decision tree.

4.6.3.4 *Method*

- **Root node creation** : Creation of a root node N.
- **Class labeling** : If tuples in P are all of the same class, C than return N as a terminal or leaf node labeled with the class C.
- **Majority voting** : If attribute list is empty then return N as a leaf node labeled with the majority class in P.
- **Splitting** : Application of attribute selection method (P, attribute list) in order to find the *best* splitting criterion;
- Labeling node N with splitting criterion;
- **Splitting attribute removing** : If splitting attribute is discrete-valued and multiway splits allowed where they are not restricted to binary trees.
- **Partitioning**: For each outcome j of splitting criterion // partitioning the tuples and grow subtrees for each partition

  Let P_j be the set of data tuples in P satisfying outcome j;

  If P_j is empty then
  attach a leaf labeled with the majority class in P to node N;
  else attach the node returned by Generate decision tree (P_j, attribute list) to node N;

- Returning N;

The splitting criterion that *best* separate the data partition P of class labeled training tuples into individual class is based on *attribute selection measures*. The $information\ gain$ has been used as attribute selection measures.

The expected information needed to classify a tuple in P is expressed as

$$Info(P) = -\sum_{i=1}^{m} g_i log_2(g_i) \tag{4.5}$$

where (g_i) is the probability of an arbitrary tuple in P belong to class C_i. The $Info(P)$ is also termed as the entropy of the data partition P.

In DT extension of information gain called as gain ration has been implemented to reduce the bias. The gain ratio is the normalization to information gain with a *split information* value and the *split information* is defined as

$$SplitInfo(P) = -\sum_{j=1}^{v} \frac{P_j}{P} log_2(\frac{P_j}{P}) \tag{4.6}$$

where training data set P partitioned in to A and A is test attribute. The gain ratio is expressed as

$$GainRatio(A) = \frac{GainA}{SplitInfoA} \tag{4.7}$$

The attribute with maximum gain ratio is selected as the splitting attribute.

4.6.3.5 Limitation of the Decision Tree

1. **Instability** : DT is extremely sensitive to small perturbations in the data set considered for analysis.

2. **Data Fragmentation** : The DT model created at the split introduces bias as each split leads to a reduced data set that are under consideration.

3. **Limited Implementation** : When there are lot of un-correlated variables, the efficiency of DT decreases.

4. **Over Fitting** : Some times DT suffers from over fitting in order to classify large number of classes simultaneously.

The DT, has been used widely in power quality analysis. Although the DT has become a good classifier than the neural network and the fuzzy logic, the ensemble

DT called as RF has the capability to classify large number of classes simultaneously. The RF remove the over fitting problem of the DT successfully.

4.6.4 Random Forest (RF)

Random forest is developed by Leo Breiman [71]. The RF fits many classification trees to a data set and then combines the prediction from all correlated trees. Each tree depends on the value of a separately sampled random vector. The instability of individual trees in DT overcomes by RF since they gain relatively low bias when grown adequately [72].

4.6.4.1 Some more Advantages of Random Forests

1. The RF is a very "fast tool" for the classification, the clustering and the regression.
2. It has good generalization ability through the "randomized" training.
3. The RF has the ability of multi−class automatic feature sharing.
4. Finally, the training and testing algorithms of RF is simple.

Some more features of Random Forests are presented below.

4.6.4.2 Features of Random Forests

1. Excelled in accuracy among current algorithms.
2. Efficiently run on large data bases.
3. RF handle large number of input variables without variable deletion.
4. It provides proper estimation of variables which are important in the classification.
5. It generates an internal unbiased estimate of the generalization error as the forest building progresses.

6. It is an effective method for estimation of the missing data and also maintains accuracy even when a large proportion of data is missing.

7. It balances error in unbalanced data sets.

8. Generated forest model can be preserved for future implementation on other data.

9. It offers an experimental method for detecting variable interactions.

The basic block diagram of a RF with n number of trees is presented in Figure 4.4. The basic construction of RF starts for k^{th} tree of n^{th} number of trees in the RF with the generation of a random vector ψ_k which is independent of past random vectors $\psi_k \ldots \psi_{k-1}$ with the same distribution. A single tree is grown with the training set $\mathbb{I}$ and the set of attributes present in ψ_k, resulting in a classifier $C_k(p, \psi_k)$ with an input vector p. Moreover in random split selection, ψ consists of a number of random integers n_{try}. Each tree in the RF classification caste a vote for most popular class at input p. The algorithm of the RF is carried out using the following steps.

1. For $k = 1$ to n_{tree} .

   (a) Draw n_{tree} bootstrap samples from the training set $\mathbb{I}$.

   (b) Grow an RF tree $C_k(p, \psi_k)$ to the bootstrapped data, by recursively iterating the steps for each terminal node of the tree until there is no possibility of further split. (Unpruned tree of maximal depth)

      i. Select n_{try} variables from the features.

      ii. Pick the best variable/split point among the n_{try}.

      iii. Split the node into two daughter nodes.

2. Output the ensemble of trees. $\{C_k(p, \psi_k), k = 1, \ldots, n_{tree}\}$

Similarly, it predict new data by aggregating the predictions of the n_{try} trees (majority votes for classification, average for regression).

For the classification, the class that most trees vote for is returned as the prediction of the ensemble as

$$\mathbb{I}_{RF}^{n_{tree}} = \text{majority vote} \left\{ \hat{\mathbb{I}}_k(p) \, k = 1, \ldots, n_{tree} \right\} \tag{4.8}$$

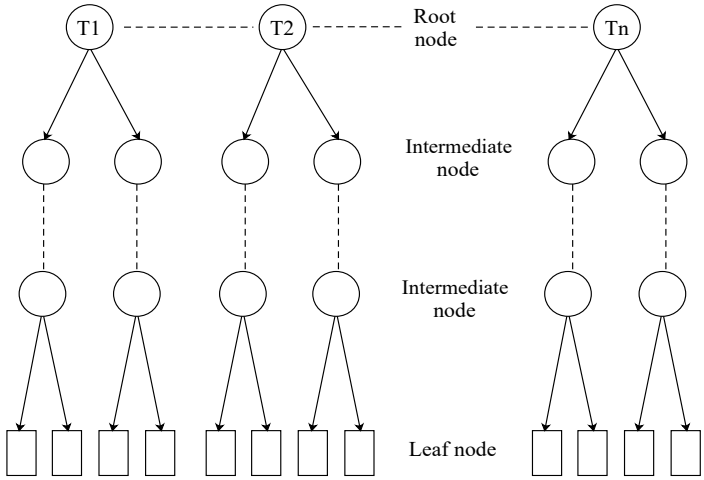

Figure 4.3: Structure of RF

where C_k is the class prediction of the k^{th} RF tree steps.

4.6.4.3 Gini Diversity Index

The Gini Diversity Index optimization is chosen to minimise the node impurity and evaluated as

$$\sum_{m=1}^{C} \widetilde{T}_{mp}(1 - \widetilde{T}_{mp}) \tag{4.9}$$

where C is the number of classes, $\widetilde{T}_{mp}$ is the proportion of patterns belonging to class m in node p.

The inputs for the RF operation are the input data (predictor and response), the number of trees used and number of variables at each split. The input data set are classified at each split by variables. For RF classifier approach, number of trees required need to be determined and for this purpose OOB (out of bag) error is considered. The OOB error rate is an indication of how well a forest classifier performs on the data set. In Random Forest, two third of the samples are used to built up the training model. The remaining one-third of the samples (OOB) is used to compute the OOB error, which is an unbiased estimation of the training error [100]. The OOB error rate of a

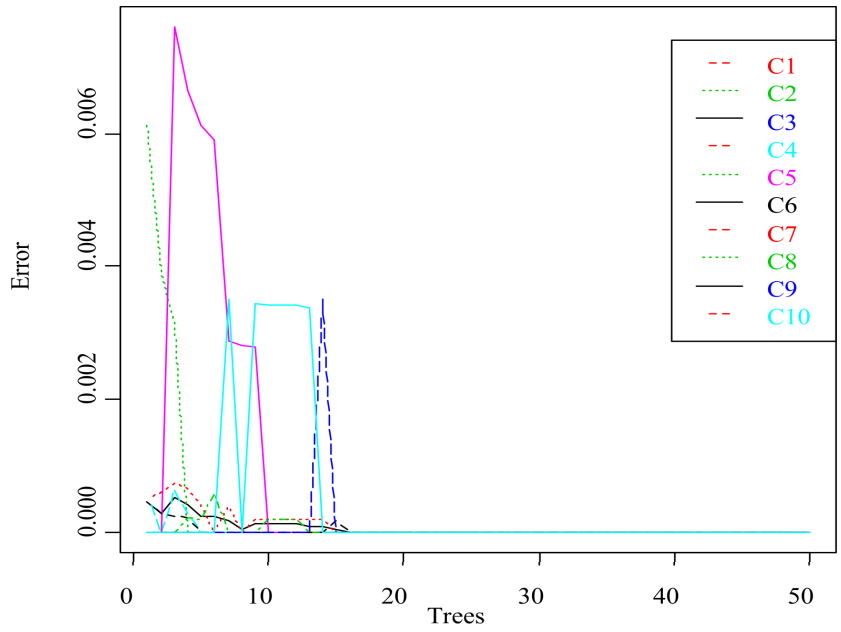

Figure 4.4: Error of RF with pure data

forest is defined by (4.10)

$$OOB_{error} = \left(\frac{1}{n_{tree}}\right) \sum_{i=1}^{n_{tree}} \left[y_i - gOOB\left(X_i\right)\right]^2 \tag{4.10}$$

where y_i is the ith element of the training dataset (X), $gOOB$ is the aggregated prediction and X_i is the bootstrap sample.

The graph of OOB error vs number of trees for ten disturbances is plotted in Fig. 4.4 with pure signal (i.e., without noise). A plot of error Vs number of trees with noisy data (20dB) is plotted in Fig. 4.5. From those figures it can be observed that for pure data the error start to stabilise around twenty trees. However, in case of noisy data, the error start to stabilize for relatively more number of trees (approximately 50). Therefore, in this case 50 number of trees are considered for testing purpose. In Fig. 4.4 and Fig. 4.5, each graph is nothing but each class.

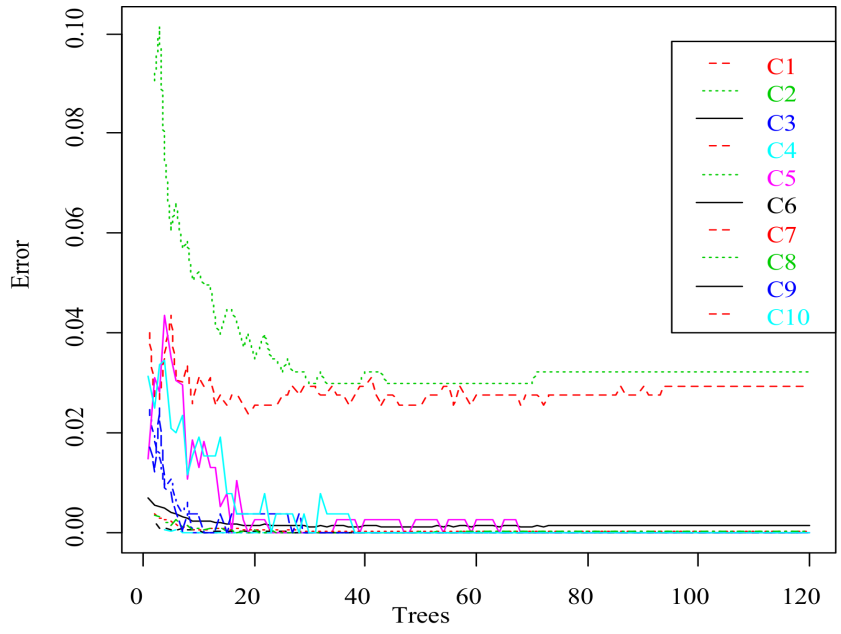

Figure 4.5: Error of RF with noisy data

4.7 Classification of Synthesized PQ Disturbance Signals

In the previous subsections the data preparation, feature extraction and mining based classification approach have been described. The classifiers such as Multilayer perceptron (MLP), Hidden Markov models (HMMs), DT and RF has been tested with various PQ disturbances (without noise) and classification accuracy (CA%) is shown in Table 4.1. The input to the classifiers are the features extracted from the DWT, MODWT and SGWT decomposition.

The equations (4.11) to (4.12) have implemented to compute the classification accuracy ($CA\%$) in the absence of noise in Table 4.1 for these data mining classifiers. The classification accuracy is a measure of the performance index of PQ is defined [69], [101] as

$$\text{Classification Accuracy}(\%) =$$

Table 4.1: CA (%) of Pure Signals

CLASS	DWT				MODWT				SGWT			
	MLP	HMMs	DT	RF	MPL	HMMs	DT	RF	MLP	HMMs	DT	RF
C1	86.56	76.21	95.08	97.05	87.57	77.09	96.98	98.78	88.99	78.43	97.78	100
C2	86.96	98.32	98.17	98.78	87.12	98.34	98.36	98.79	88.21	98.97	98.78	100
C3	90.01	0	97.56	100	90.78	0	98.72	100	90.98	0	100	100
C4	89.94	98.01	100	100	90.03	98.45	100	100	91.12	99.18	100	100
C5	87.79	92.01	97.01	100	87.98	93.12	98.75	100	88.02	94.67	99.03	100
C6	91.11	47.61	98.12	99.65	92.13	48.63	98.14	99.78	92.67	49.56	99.27	100
C7	87.34	43.32	99.16	100	88.09	44.78	100	100	89.36	45.36	100	100
C8	88.47	73.60	95.74	99.65	89.91	74.37	97.74	99.76	90.67	75.65	98.76	100
C9	90.34	100	97.47	98.57	90.78	100	97.45	99.56	91.02	100	98.78	100
C10	89.07	98.02	97.32	100	90.65	98.45	97.67	100	91.13	99.73	98.45	100
TOTAL %CA	89.82	71.02	97.87	99.73	90.50	72.32	98.87	99.71	90.89	75.92	99.03	100

Table 4.2: CA (%) of Signals with 20dB

CLASS	DWT				MODWT				SGWT			
	MLP	HMMs	DT	RF	MPL	HMMs	DT	RF	MLP	HMMs	DT	RF
C1	80.26	93.56	90.37	93.25	80.93	93.78	91.13	93.42	81.09	94.25	91.89	94.04
C2	80.17	91.08	95.36	94.24	81.15	91.76	95.98	94.89	81.24	92.13	96.21	95.15
C3	84.13	0	94.51	96.90	84.82	0	94.89	97.06	85.18	0	95.35	97.01
C4	83.22	100	95.13	96.46	84.03	100	95.17	96.90	85.11	100	96.19	97.22
C5	81.23	80.34	94.43	96.47	83.14	88.78	95.98	96.86	84.24	81.08	97.08	96.98
C6	84.12	1.56	95.15	95.63	84.96	2.67	95.76	95.79	86.68	10.67	96.26	97.23
C7	82.02	34.76	94.01	96.04	83.12	35.56	95	96.62	84.60	37.82	95.98	97.12
C8	82.16	55.95	91.19	94.06	82.89	56.23	91.71	94.86	83.79	57.56	92.02	95.46
C9	84.05	92.56	93.06	93.53	84.72	93.69	92.64	94.54	85.31	93.24	94.75	95.23
C10	83.26	91.38	92.82	94.90	83.98	91.87	92.87	95.10	86.23	92.56	93.47	96.13
TOTAL %CA	82.65	62.34	93.83	95.74	83.46	65.56	94.27	96.31	85.89	68.93	95.46	96.95

Table 4.3: CA (%) of Signals with 25dB

CLASS	DWT				MODWT				SGWT			
	MLP	HMMs	DT	RF	MPL	HMMs	DT	RF	MLP	HMMs	DT	RF
C1	80.56	89.45	90.73	93.52	81.03	89.87	91.31	93.63	81.90	91.02	91.98	94.40
C2	80.54	92.34	95.63	94.42	81.51	92.67	96.09	94.98	81.42	92.97	96.61	95.51
C3	84.31	0	94.15	96.98	85.12	0	94.92	97.60	85.81	0	95.53	97.47
C4	83.42	100	95.31	96.64	84.13	100	95.71	97.29	85.71	100	96.91	97.78
C5	81.32	81.45	94.53	96.74	83.41	81.56	96.28	97.16	84.42	82.04	97.80	97.50
C6	84.21	4.90	95.51	95.83	85.20	5.76	95.86	96.07	86.86	8.20	96.62	97.93
C7	82.20	36.89	94.11	96.54	83.21	37.57	95.43	96.92	84.82	38.94	96.48	97.69
C8	82.61	56.92	91.67	94.73	83.19	56.98	91.91	95.04	83.95	57.23	92.29	96.46
C9	84.50	93.24	93.43	93.64	84.74	93.75	94.14	94.84	85.71	93.94	95.15	95.32
C10	83.62	92.23	92.98	95.09	84.08	92.67	93.07	95.91	86.33	92.93	93.74	96.52
TOTAL %CA	83.09	63.05	94.28	96.15	84.14	64.02	95.12	97.32	86.38	66.34	96.16	97.09

$$\frac{\text{Number of samples correctly classified}}{\text{Total number of samples in the class}} \times 100 \tag{4.11}$$

$$\text{Total Classification Accuracy of a data set}(\%) = \frac{\text{Total number of samples correctly classified in the data set}}{\text{Total number of samples in the data set}} \times 100 \tag{4.12}$$

In the Table 4.1, the ($CA\%$) of MLP and HMMs classifiers also have been presented in order to observe the efficacy of the proposed data mining classifiers. From, Table 4.1, it has been observed that for each data set the overall ($CA\%$) of MLP is better than the HHMs as it fails to classify interruption, harmonic like slow disturbances. RF has better recognition rate on all the data sets i.e DWT, MODWT, SGWT decomposed data set. Moreover, the RF has recognised all the disturbances of SGWT based data perfectly.

In actual practice, the measured signal is corrupted with noise. Generally the

Table 4.4: CA (%) of Signals with 30dB

CLASS	DWT				MODWT				SGWT			
	MLP	HMMs	DT	RF	MPL	HMMs	DT	RF	MLP	HMMs	DT	RF
C1	81.05	94.18	91.23	94.02	81.93	94.72	91.84	91.10	82.14	94.72	92.13	95.03
C2	82.04	84.45	96.13	94.82	82.01	84.67	96.89	95.18	82.13	85.23	96.91	95.95
C3	84.42	0	94.72	97.41	85.72	0	95.32	97.95	86.01	0	95.83	97.74
C4	84.12	100	96.01	97.16	84.63	100	96.17	97.92	86.12	100	97.04	98.38
C5	81.72	81.78	94.83	97.07	83.87	81.96	96.48	97.65	84.72	82.04	98.30	97.89
C6	84.81	4.97	95.91	96.03	85.70	5.89	96.16	96.70	86.96	8.87	96.92	98.03
C7	82.40	47.34	94.81	96.84	84.01	48.89	95.93	97.02	85.92	49.93	96.88	97.89
C8	83.01	56.95	92.37	95.03	83.91	57.03	92.04	95.54	84.05	57.56	92.89	96.84
C9	84.92	96.12	93.53	94.01	85.04	96.35	94.79	95.24	85.91	96.78	95.86	95.76
C10	84.82	96.03	93.48	95.91	84.78	96.26	93.89	96.21	86.83	96.45	94.24	97.93
TOTAL %CA	84.62	63.67	95.06	97.34	85.25	65.45	96.15	98.02	87.24	68.87	97.06	98.35

Table 4.5: CA (%) of Signals with 35dB

CLASS	DWT				MODWT				SGWT			
	MLP	HMMs	DT	RF	MPL	HMMs	DT	RF	MLP	HMMs	DT	RF
C1	81.91	95.13	91.63	94.86	82.12	95.45	92.02	91.62	82.41	92.45	92.13	95.03
C2	82.89	85.32	96.85	95.12	82.83	85.76	97.09	95.81	82.33	86.13	96.91	95.95
C3	85.02	0	95.42	97.73	85.92	0	95.52	98.15	86.91	0	95.83	97.74
C4	84.82	100	96.87	97.82	84.93	100	96.71	98.02	86.72	100	97.04	98.38
C5	81.82	82.13	95.60	97.92	84.27	82.43	96.84	97.85	85.32	83.32	98.30	97.89
C6	84.92	5.78	96.21	96.85	85.90	6.35	96.61	97.03	87.16	9.78	96.92	98.03
C7	82.85	48.34	95.31	97.82	84.81	49.45	96.03	97.82	86.02	49.97	96.88	97.89
C8	83.92	57.34	92.67	95.92	84.01	58.45	92.64	95.93	84.95	58.76	92.89	96.84
C9	85.12	97.15	93.93	94.92	85.54	97.34	94.97	95.93	86.07	97.56	95.86	95.76
C10	85.54	97.32	93.58	96.05	84.88	97.45	93.98	96.92	87.03	97.78	94.24	97.93
TOTAL %CA	85.27	65.62	96.23	98.12	86.15	66.32	97.05	98.46	88.12	69.75	97.06	98.75

Table 4.6: CA (%) of Signals with 40dB

CLASS	DWT				MODWT				SGWT			
	MLP	HMMs	DT	RF	MPL	HMMs	DT	RF	MLP	HMMs	DT	RF
C1	82.12	82.04	92.41	95.27	82.74	82.14	92.92	92.12	82.61	82.87	92.81	95.73
C2	83.48	86.32	97.28	95.92	83.43	86.43	97.89	96.01	82.72	86.73	97.21	96.45
C3	85.92	0	96.92	98.31	86.90	0	95.82	98.85	87.21	0	96.23	98.24
C4	85.32	100	97.27	98.52	85.92	100	97.01	98.92	87.22	100	97.34	98.78
C5	82.52	83.03	95.91	98.52	84.91	83.46	97.34	98.15	86.72	84.09	98.31	98.79
C6	85.32	7.08	96.82	97.45	86.92	8.34	97.01	97.73	87.76	10.03	97.22	98.93
C7	83.35	49.14	95.81	98.60	85.54	49.35	96.93	98.02	86.52	49.81	97.28	98.49
C8	84.32	58.24	92.72	96.53	84.91	58.29	92.94	96.23	85.05	58.57	93.19	97.24
C9	85.86	98.13	94.23	95.82	85.94	98.24	95.17	96.23	86.87	98.76	96.26	96.71
C10	85.82	98.30	94.43	96.92	85.48	98.67	94.18	97.02	87.89	98.92	94.84	98.43
TOTAL %CA	86.58	66.38	97.43	99.02	87.25	67.06	98.15	99.01	89.16	71.04	98.16	99.35

noise comes from the voltage and the current sensing devices. The noise is generally a white Gaussian noise and value of signal to noise (SNR) ratio lies between 20 dB to 40 dB [102], [30], [103], [104]. Therefore, the proposed methods are tested with noisy data and classification results for different SNR are shown in Table 4.2 to Table 4.6. All the feature extraction schemes are compared for the classification accuracy. The last row of each table provides the total (%CA) of the data set where as other rows provide the (%CA) of individual class of the data set.

In the, Table 4.2, the PQ signals with 20 dB noise has been classified. By comparing, Table 4.1 and Table 4.2 it is observed that the noisy data has lower recognition rate than the pure signal. All the methods have provided similar type of results like the pure PQ signals.

Similarly, the Table 4.3 has characterised PQ signals with noise 25 dB. The individual ($CA\%$) of signals using MLP classifier is more or less than the HMM classifiers but the overall ($CA\%$) of MLP is more as HMMs are suitable only for the fast signals. The RF has properly classified the SGWT based data set like the other cases. The

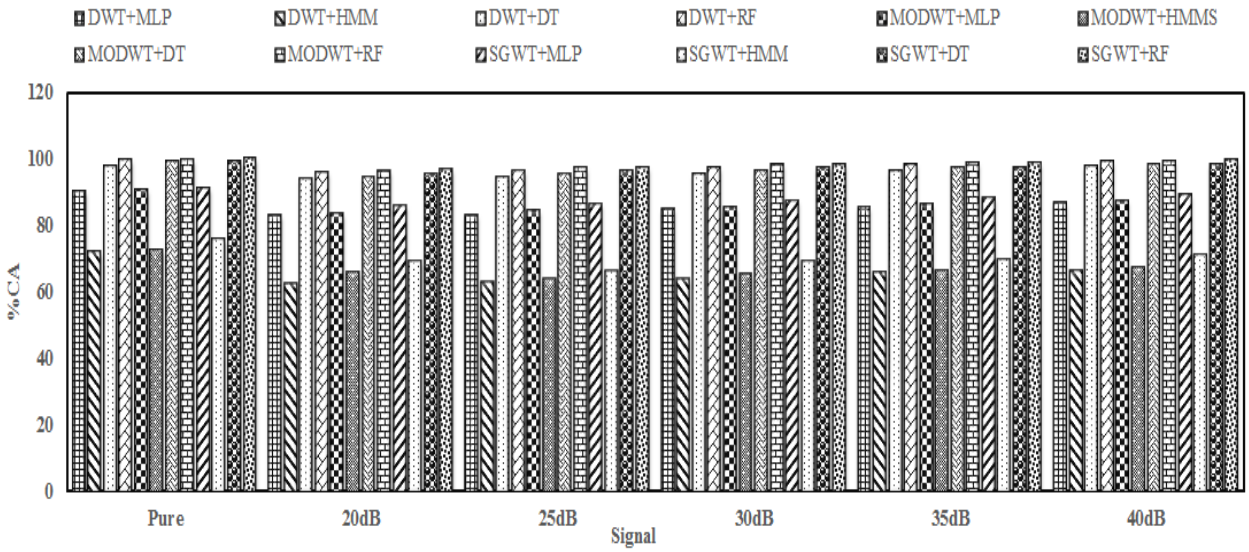

Figure 4.6: Classification accuracy of different set of signal

recognition rate of all the methods are lower than the pure signals and lower than the signal with noise 20 dB doped data set.

The Table 4.4 has given the ($CA\%$) of PQ signals with 30 dB. All three data set has similar results but the recognition rate Table 4.4 is higher than the signal with 25 dB and 20 dB noise.

The Table 4.5 and Table 4.6 have given the ($CA\%$) signal with 35 dB and 40 dB noise respectively. These Tables have yielded similar results like the previous cases. The overall recognition rate of MPL is higher than the HMMs and lower than the DT and RF. Though DT has good ($CA\%$) value for each data set but for large data set DT suffers from the data over fitting. The data over fitting free RF has good ($CA\%$) than the other methods for all the data set.

The total classification of each type of data set of all the classifiers have been laid out in Figure 4.6. From this Figure, it can be interpreted that, the classification rate of DT and RF is better than the traditional method for all type of data set. Among the four classifiers, the RF is the superior than the others as it has highest $\%CA$ value.

4.8 Chapter Summary

In this Chapter, different power quality disturbances are decomposed up to seven levels. The useful features of the ten types of PQ disturbances have been extracted using the DWT, MODWT and SGWT in the presence and absence of AWGN. For each signal at each decomposition level four features are extracted. These features are fed as input to the classifiers. The four different classifiers have been implemented in order to recognise the signals in noisy as well as noise free environments. It is observed that Neural Network based MLP gives comparatively less classification accuracy. Though the HHMs properly classifies the fast disturbances, but the over all classification accuracy is poor as it fails to classify the slow disturbances such as the interruption. The proposed data mining based decision tree recognises all types of disturbances, but it suffers from the over fitting problem. So, the ensemble decision tree solves over fitting problems, implemented to classify large class data set. The recognition rate and the performance of the RF classifier is appreciable for slow as well as the transients signals. Moreover, the RF classifier can classify single as well as multiple disturbances for large number of classes efficiently as compared to the other classifiers. Using the variants of the WT as the feature extractor and RF as classifier, a satisfactory classification accuracy of PQ disturbances is achieved. However, among all the classifiers, the RF has superior classification rate as compared the other classifiers in noisy as well as noise free environment. Though DWT, MODWT and SGWT based data set give approximately similar classification accuracy, the SGWT is the preferred candidate because it is fast and consumes less memory.

In Chapter-3 and in this current Chapter, the process of detection, feature extraction and classification has been carried out with the synthetic data. In the next Chapter the same process has been carried out with real time data.

Chapter 5

Detection and Classification of Real Time Power Quality Signals

5.1 Introduction

In the previous Chapter-4, different types of synthesized power quality disturbance signals are classified with the data mining based classifiers. It was inferred that the RF classifier is the best classifier out of all the classifiers for the classification of large number of classes.

In this Chapter, the aforementioned classification techniques are implemented for the real data classification in order to validate the efficiency of the classifiers. The input features are extracted from the ST and WT variants. These aforementioned techniques are implemented both on the single phase and three phase voltage signals. The signals are captures from the transmission line panels.

5.2 Important Steps carried out in this Chapter

- Collection of large number of data from the transmission panels.
- Processing of real time signal through the transformation in order to extract the suitable features.
- To characterise different type signals in terms of classification accuracy by the

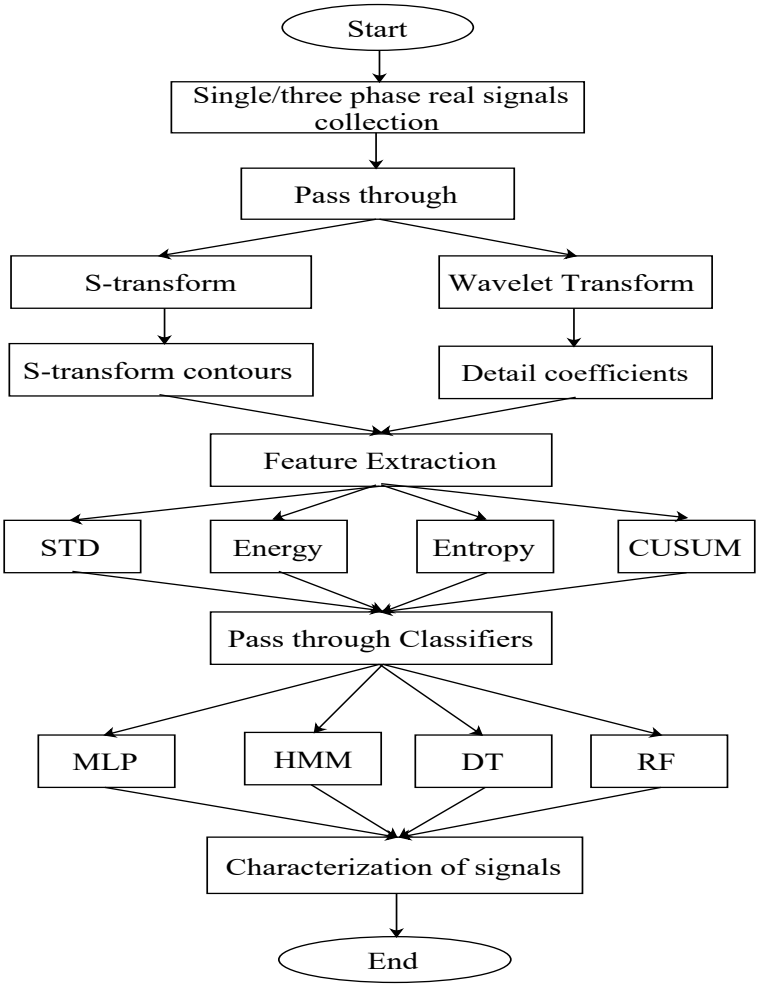

Figure 5.1: Flow chart presentation of the Chapter work

proposed classifiers.

5.3 Organisation of the Chapter

This Chapter is organized as follows: Section-5.4 has presented the collection and classification of single phase voltage signal. Similarly, collection as well as classification of three phase voltage signal has been presented in Section-5.5. Finally, the Section-5.6 provides the concluding remark of the chapter. All these procedures have been presented in the form of flow chart shown in Figure 5.1.

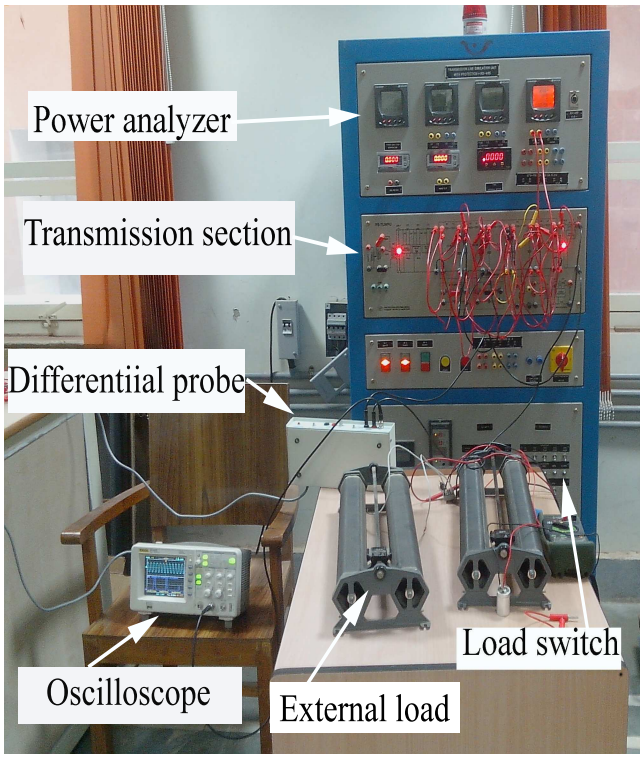

Figure 5.2: Experimental setup for single phase voltage signal collection

5.4 Single Phase Voltage Signal Collection Process

In order to get the real data, seven types of PQ signals have been generated by employing transmission line panel, the load and the storage oscilloscope. The transmission demo panel comprises a line model with the length 400 Km and voltage of 220 kV. The lumped parameter line model with five cascaded networks each of them has been designed for 80 km parameters. The fault simulating switch has been provided to create the fault condition. This transmission line panel also comprises digital DSP based power analyzers, voltmeters, ammeters, push buttons, indicating lamp and accessories. A digital timer is also present. The demo panel is also provided with protective devices i.e MCB'S to give protection from any abnormal condition occurring during the actual demonstration and experiments. The numerical impedance relay and the numerical over current relay are also associated to give trip signal to the circuit breaker. The current carrying capacity of the model is 5 Amp.

The seven types of signals are sag, swell, interruption, sag with swell, sag with

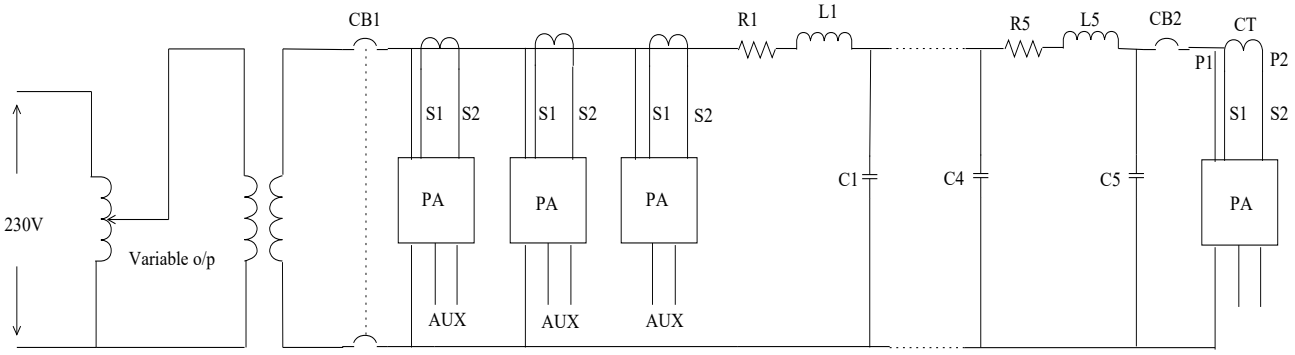

Figure 5.3: Circuit diagram of the single phase transmission panel connection

interruption, swell with interruption and sag and swell with interruption. A 220 V is applied to the transmission line panel and by changing the load and creating fault, the various disturbances are created. The disturbances are then stored in storage oscilloscope. Then data is extracted from the oscilloscope and fed to the MATLAB for feature extraction and subsequent classification. The details of experimental set up is given in Figure 5.2. Similarly, the circuit diagram of the transmission panel has been shown in Figure 5.3. The captured single phase voltage signals with sag, swell and interruption are presented in Figure 5.4.

5.4.1 Description and Operation of Main Part of Single phase transmission line simulation panel

The total panel is spitted into five main parts, which has been described below

5.4.1.1 Input and output terminals

The interconnection between protective CT and solid state impedance relay are carried out internally with the connection diagram on front panel. The flexible copper cable has used for input supply connections.

5.4.1.2 Panel Meters-Power Analyzer

Total four power quality analyzers are installed in this panel. The DSP based two digital panel meters are implemented to measure line current, line voltage, power factor,

active power (KW), reactive power (KVAR) etc with $RS485C$ port of transmission line at sending end receiving end. Another two analyzers are mounted for measurement of compensation and loading parameter. It can de implemented two purposes like RE to SE pf or vice versa. The maximum analyzer voltage is $0 - 300$ Vrms and maximum current $5A$. CT $10/5A$ can be used externally with $230V$ AC supply.

5.4.1.3 Panel Meters-Power Analyzer

The $0.0001 - 9999$ seconds, four digit, digital timer -Selectron make with 230 V AC supply is mounted in order to measure time delay required to clear the fault. The timer will start time counting on closing of any fault simulating switch and it will stop when protective relay operates and gives signal to open the circuit breakers.

5.4.1.4 ON/OFF Switches

To switch on/off the input supply, 10 A, DP MCB is used. One 32 Atwo pole, rotary switches are used fault simulating switch. The SW1 is used to simulate the phase to earth fault in transmission line at a distance 240 Km, 320 Km, 400 Km from sending end.

5.4.1.5 Transmission Line Model

Transmission line model is designed for 400 Km, 220 KV transmission line with five π sections cascaded each for 80 Km line length. The lumped parameters are as $R = 2.6E, C = 0.6, 0.8, 1.4uF, L = 35mH$. The current capacity of model is 5Amp.

The detail specifications of this single phase transmission panel has given in Appendix-A.

5.4.2 Classification of the Real Time Single Phase Voltage Signal

The aforementioned classifiers are implemented for the classification of real single phase voltage signals.

Four features are extracted from the contours of ST and fed to the classifiers like the other cases discussed before. The feature extraction time for the S-Transform

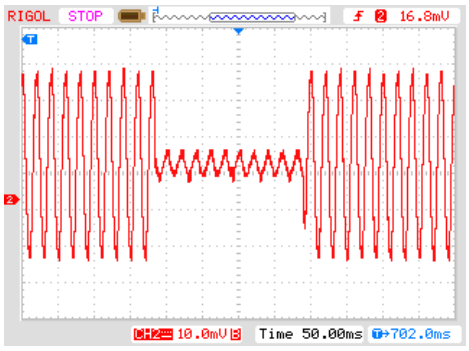

(a) Voltage with sag

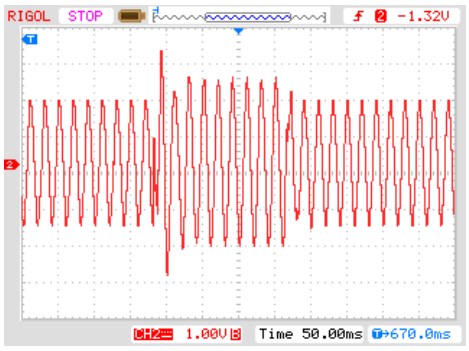

(b) Voltage with swell

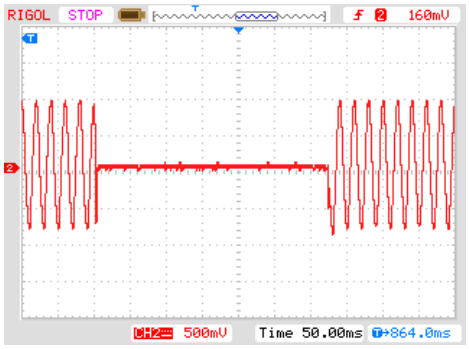

(c) Voltage with interruption

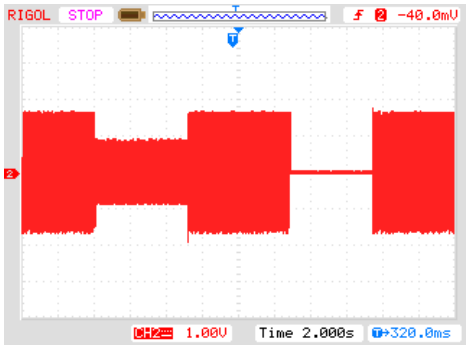

(d) Voltage with interruption and sag

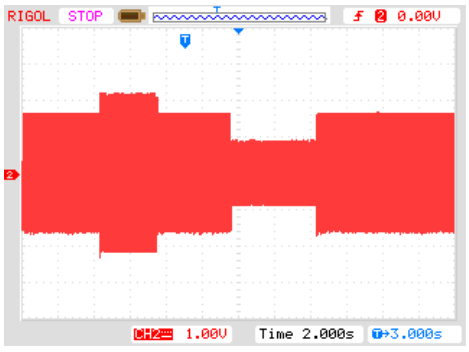

(e) Voltage with sag and swell

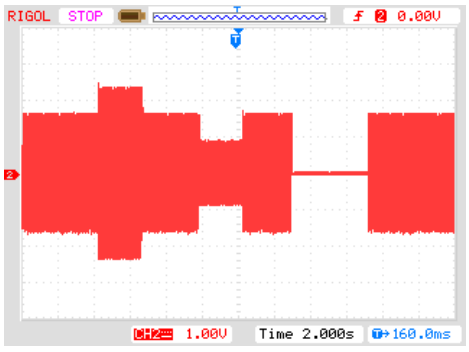

(f) Voltage with sag, swell and interruption

Figure 5.4: Single phase real voltage signals with disturbances

Table 5.1: Feature extraction time of S-transform and SGWT

Signal	Number	Feature extraction time in (sec)	
		SGWT(sec)	ST(sec)
Sag	1220	15.09	164.13
Swell	1070	13.50	160.87
Interruption	1520	18.23	195.67
Flicker	155	1.98	415.89
Harmonic	4335	75.54	605.78
Sag+harmonic	120	1.68	17.55
Swell+harmonic	120	1.70	18.91
Oscillation	215	2.90	35.40

and the SGWT are recorded in MATLAB environment and compared in Table 5.1. Moreover, time is calculated by running the SGWT and S-Transform algorithm on a core-i5, 2.40 GHz in MATLAB environment.

From Table 5.1, it can be observed that time required for the feature extraction of S-Transform is relatively more than SGWT for all the types of signals. As, S−Transform requires more time for the feature extraction, so it has not been applied to extract features of synthesized data sets. Moreover, the ST has been implemented for feature extraction of real PQ disturbance signals. The proposed MODWT, SGWT techniques are compared with S−Transform, DWT and results are enlisted in Table 5.2, it can be seen that classification accuracy is more or less same for S−Transform and SGWT schemes based data set. RF has better classification rate as compared to other classifiers for all types of data set.

The captured signals are single phase voltage signals. One of the tree in RF has been presented in Figure 5.5. The number of rules for all the trees in the forest may not be the same and the constant value of Gini diversity index gives the best split. The data set contains variable X ($X1$-standard deviation, $X2-$energy of details, $X3$-CUSUM, $X4-$entropy) and $L(L1, L2, \ldots, L7$ level of decomposition) which constitute 28 features. In RF the output patterns are trained till a constant value of Gini Diversity Index is obtained. This constant value provides fully grown tree with higher classification accuracy.

The lifting based SGWT is simple and requires less memory as compared to the

Table 5.2: CA (%) of real time Signals

CLASS	DWT				MODWT				SGWT				ST			
	MLP	HMMs	DT	RF	MPL	HMMs	DT	RF	MLP	HMMs	DT	RF	MPL	HMMs	DT	RF
C1	82.56	72.36	93.08	93.23	83.50	73.32	93.92	93.78	84.09	78.43	94.72	95.34	84.69	79.04	95.23	96.09
C2	83.36	92.47	94.17	95.08	84.21	92.67	94.76	95.10	84.87	98.97	95.21	96.45	84.87	99.02	97.03	98.20
C3	87.21	0	93.56	95.87	87.79	0	96.92	97.04	87.98	0	96.98	97.37	85.64	0	95.02	96.01
C1+C2	85.34	88.34	96	96.02	85.83	88.45	96.90	97.26	86.02	88.61	97.02	97.94	86.58	89.02	95.91	97.90
C1+C3	84.39	13.01	93.24	95.82	84.93	13.12	96.05	96.36	85.02	15.43	96.86	98.40	86.94	16.03	95.94	96.41
C2+C3	83.16	47.61	92.43	93.05	83.19	48.63	93.65	94.98	84.61	49.56	95.23	98.43	85.02	50.06	98.68	99.17
C1+C2 +C3	84.34	43.32	93.02	96.54	85.02	44.78	96.78	97.39	85.30	45.36	97.94	97.69	86.02	46.06	95.98	98.65
TOTAL %CA	84.21	60.34	94.83	95.36	85.75	61.62	95.07	96.14	86.81	62.92	97.33	98.66	86.98	63.46	96.68	98.29

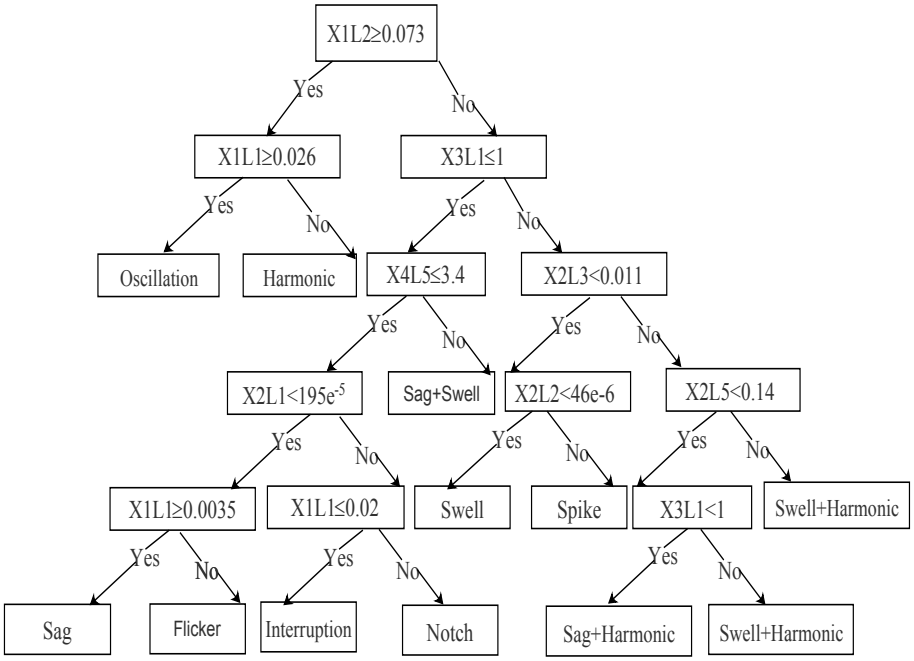

Figure 5.5: Tree structure of RF

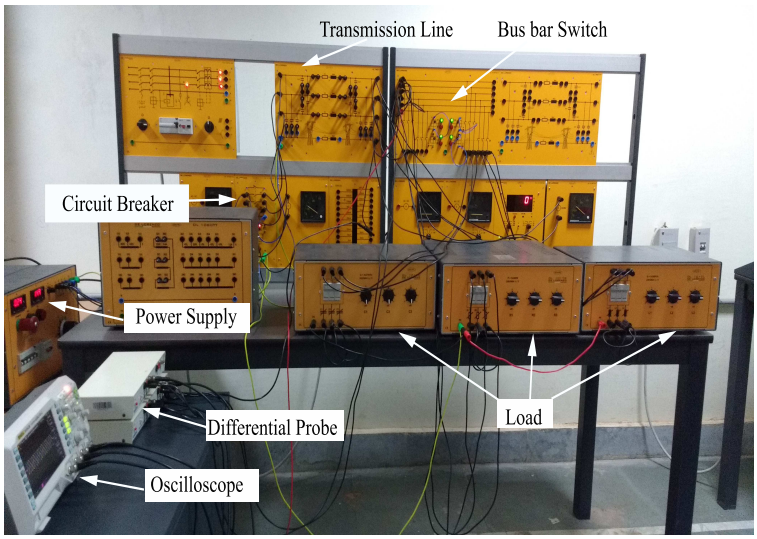

Figure 5.6: Experimental setup for three phase voltage signal collection

S-Transform and other WT variants. However, these proposed methods have been also implemented on three phase voltage signals captured from another transmission panel. They have been presented in subsequently.

5.5 Three Phase Voltage Signal Collection Process

Similar to the single phase voltage signals, three phase signals are captured from an overhead power transmission line of length 360 km. The transmission demo panel comprises a line model of voltage of 380 kV. The equivalent circuit of the line is π model with concentrated parameters. The demo panel comprises of natural load 600 MW. A 380 V is applied to transmission line panel and by changing the load and creating fault, the various disturbances are created like the single phase. These disturbances are then stored in a storage oscilloscope like the single phase signal and then data is extracted from oscilloscope and fed to the MATLAB. The details of the experimental set up is given in Figure 5.6. Similarly, the circuit diagram of the transmission panel has been shown in Figure 5.7. The specifications of the panel has given in Appendix-B. Some of three phase real signals have been presented in Figure 5.8. These three phase signals are fed to the aforementioned classifiers in the subsequent subsection.

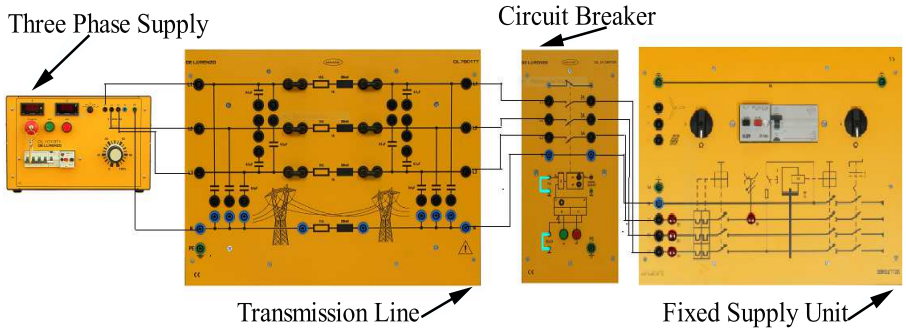

Figure 5.7: Circuit diagram of the three phase transmission panel connection

Table 5.3: Class label assignment

Signal Name	Class name
Sag	R1
Swell	R2
Interruption	R3
Transient	R4
Sag + swell	R5
Harmonic	R6
Harmonic+sag	R7
Harmonic+swell	R8
Spike	R9

5.5.1 Classification of Real Time Three Phase Voltage Signal

The proposed techniques have been tested with three phase PQ disturbance signals as in case of single phase. Total nine types of single and combined three phase voltage signals have been passed through the variants of the WT, the ST and extracted features are fed to aforementioned four classifiers. The $\%CA$ of the the data set has been calculated in Table 5.4.

The classification of three phase PQ disturbances have been presented in Table 5.4. From Table 5.4, it can be observed that $\%CA$ value of three phase signals are very close to the single phase $\%CA$ value. The RF classifier has provided satisfactory result compared to all other classifiers. Moreover $\%CA$ of SGWT based data set is very close to the ST based data set like that of the single phase signal case.

The performance of the classifiers of in terms of total classification accuracy each series of data has been in real environment has been represented in Figure 5.9. The RF

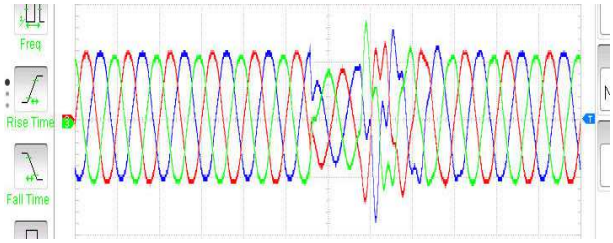

(a) Voltage with sag

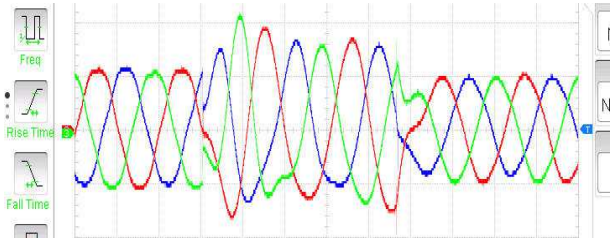

(b) Voltage with swell

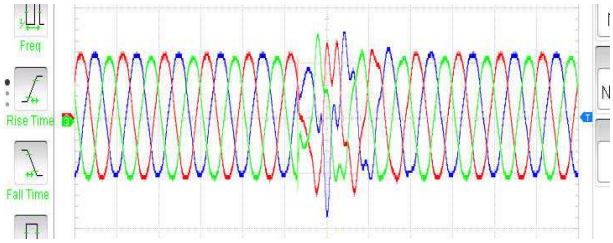

(c) Voltage with transient

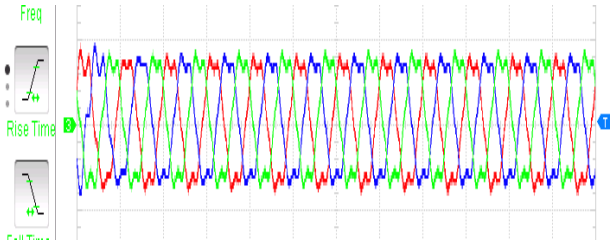

(d) Voltage with harmonics

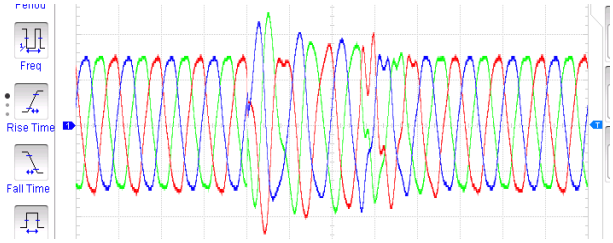

(e) Voltage with Swell and harmonics

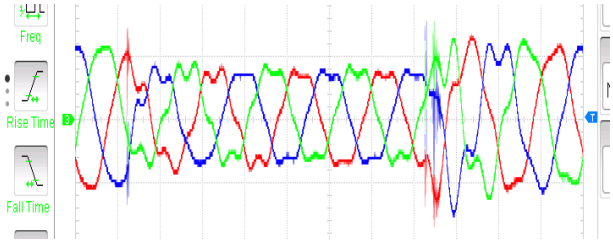

(f) Voltage with Sag and harmonics

Figure 5.8: Three phase real voltage signals with disturbances

Table 5.4: CA (%) of real time three phase signals

CLASS	DWT				MODWT				SGWT				ST			
	MLP	HMMs	DT	RF	MPL	HMMs	DT	RF	MLP	HMMs	DT	RF	MPL	HMMs	DT	RF
R1	81.50	71.32	92.35	94.73	84.34	72.72	92.97	93.98	85.19	78.93	94.92	95.94	84.90	78.74	95.23	96.09
R2	84.09	92.79	96.17	94.68	85.20	93.07	95.66	96.90	85.47	97.98	95.98	97.05	85.07	98.92	97.03	98.20
R3	84.31	0	94.00	95.07	87.95	0	95.90	96.84	88.58	0	96.90	97.33	85.94	0	95.02	96.01
R4	81.06	91.04	93.90	94.21	84.05	91.32	94.13	94.88	84.95	93.10	94.72	95.14	86.98	93.02	95.91	97.90
R5	84.13	89.94	94.97	95.08	84.21	90.07	95.06	95.79	84.87	92.06	96.28	96.15	87.04	93.10	96.12	95.94
R6	87.91	46.63	92.96	94.07	87.99	47.92	97.02	97.94	87.90	48.47	98.08	98.82	84.92	48.87	98.58	98.72
R7	84.90	32.34	96.05	97.52	85.53	33.45	96.90	97.56	86.54	36.62	97.92	97.91	85.62	37.06	97.02	98.01
R8	84.93	87.34	92.74	92.24	85.36	88.05	93.43	96.26	85.92	89.43	97.16	98.50	85.91	89.83	97.46	98.58
R9	82.86	97.61	91.73	92.05	84.67	98.23	92.45	94.38	84.91	95.56	95.93	98.66	86.43	95.96	96.43	98.83
TOTAL %CA	84.31	61.52	94.94	95.46	86.21	62.02	95.47	96.41	87.12	63.32	97.13	98.86	87.31	64.13	96.00	97.89

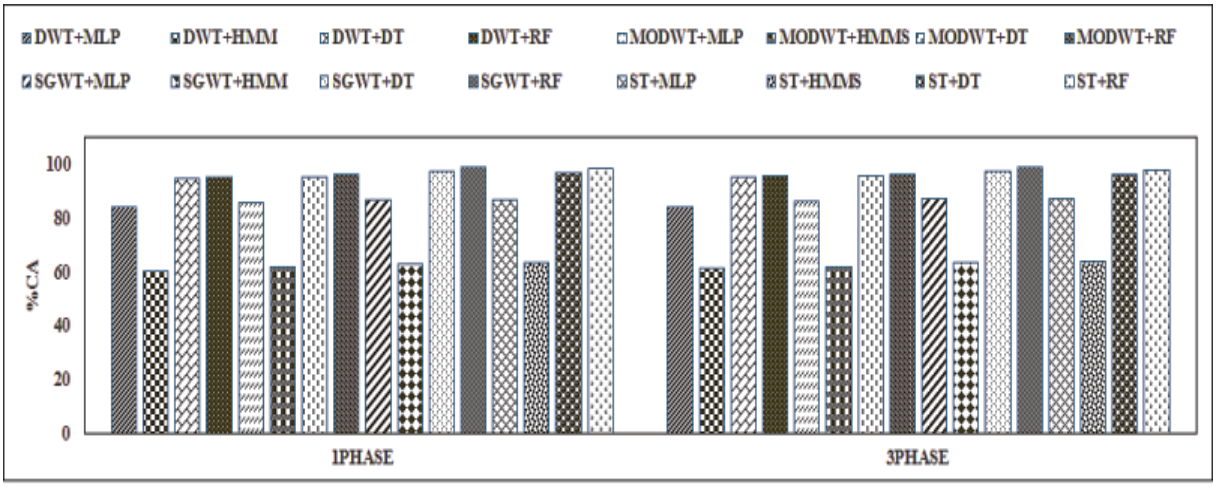

Figure 5.9: Classification rate of real signal

Table 5.5: CA (%) of three phase fault signals

CLASS	DWT				MODWT				SGWT				ST			
	MLP	HMMs	DT	RF	MPL	HMMs	DT	RF	MLP	HMMs	DT	RF	MPL	HMMs	DT	RF
L−G	75.21	80.0	80.90	92.03	80.40	80.71	80.97	93.66	81.66	82.52	90.92	95.94	82.00	84.00	95.0	96.00
L−L	83.76	78.76	81.16	93.08	83.33	83.52	95.0	96.90	85.0	86.66	98.0	98.76	82.01	82.52	95.71	98.85
L−L −G	86.75	88.33	94.00	95.25	85.94	85.70	96.02	96.94	88.76	84.33	96.60	97.42	81.82	83.52	95.52	96.17
L−L− L−G	74.14	81.17	90.0	94.33	89.92	91.58	94.27	94.54	84.42	89.12	94.72	95.0	85.33	89.05	98.33	98.33
L−L −L	91.42	91.94	91.42	96.57	81.21	82.41	95.36	95.09	89.00	90.30	97.72	98.64	88.63	90.25	94.63	95.10
TOTAL %CA	83.51	85.42	94.90	95.06	85.01	87.96	95.49	96.42	87.76	89.33	97.03	98.52	87.35	89.92	96.05	97.81

has consistency with higher $\%CA$ rate in each series of data among all the approaches like the previous Chapter. Similarly, the aforementioned proposed methods have also been implemented on fault classification in order to check suitability of these methods.

5.5.2 Fault Classification

Under normal operating condition, the power system operates under balanced conditions with all the equipments carrying normal currents and voltages within the prescribed limits. This healthy operating condition can be disrupted due to a fault in the system. The power system faults are divided in to three phase balanced fault and unbalanced fault. The different types of unbalanced fault are single line to ground fault(L−G), line to line fault (L−L),double line to ground (L−L−G). The balanced faults are three phase fault which are severe type of fault. These faults can be two types such as line to line to line to ground (L−L−L−G) and line to line to line fault (L−L−L).

Three phase voltage signals with fault are captured from an overhead π modeled

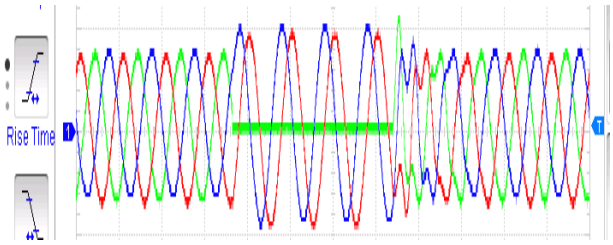

(a) L−G fault

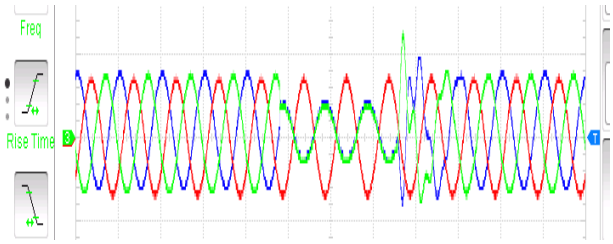

(b) L−L fault

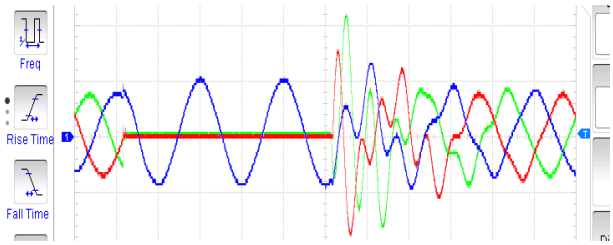

(c) L−L−G fault

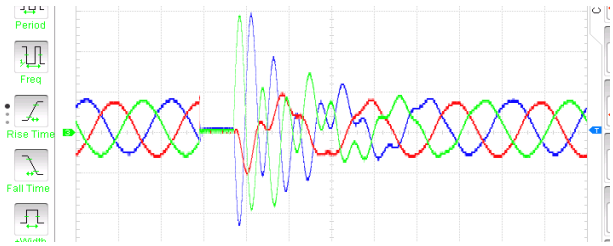

(d) L−L−L−G fault

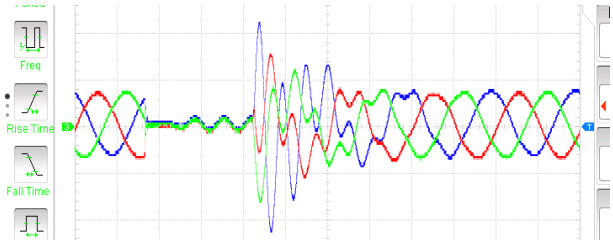

(e) L−L−L fault

Figure 5.10: Three phase real voltage signals fault

transmission line of length 360 (Km) like the other cases. Total five types of fault signals are captured from the panel shown in Figure 5.6. Some of fault signals have been presented in Figure 5.10. Fault signals have been captured from the oscilloscope and fed to MATLAB for analysis like the previous cases. From the details of the WT and the ST contours four features have been extracted and fed to the classifiers in order to recognise the type of fault. The recognition rate in terms of $\%CA$ is given in Table 5.5.

Different approaches have been implemented for calculation of $\%CA$ in Table 5.5. From these tables, it can be observed that all these proposed techniques are working satisfactorily. The HMM has provided good results unlike the PQ disturbance recognition where it failed to recognise slow disturbances perfectly. The RF classifier has given better result than the other classifiers.

5.6 Chapter Summary

In this Chapter, the classifiers have been implemented in the real environment. Seven types of single phase PQ disturbance signals have been captured from a transmission panel and fed to the variants of the WT and the ST in order to extract the features. These extracted features have been fed to the aforementioned classifiers. Similar to the single phase signal classification, nine types of three phase voltage signals have been classified. The classification accuracy of the MPL is poor as was the case of synthesized signals. The HHMs have classified the fast signals successfully, but failed to classify the slow disturbance signals. Hence, the overall $\%CA$ has decreased in both the single and three phase signals. But in case of fault recognition, HMMs have provided satisfactorily result. Hence, the overall classification accuracy has improved in fault classification as compared to the PQ disturbances. However, the DT has been provided satisfactory result but $\%CA$ of the ensemble DT is better than all other classifiers. Though the $\%CA$ of ST based data set is very close to SGWT based data set, the ST requires more time. Similarly, DWT, MODWT and SGWT based data set have more or less same $\%CA$ value, but SGWT is simple, faster than the others. Hence, the SGWT is a suitable method for analysing large data set as compared to the ST and traditional convolution based WT.

Chapters-3,4 and 5 have carried out the PQ detection and classification for both the synthetic and real time data. In the next Chapter various constraints of the islanding, PQ events and faults are detected using the variants of wavelet transform and the S-transform.

Chapter 6

Islanding Detection in an IEEE−14 Bus System Comprising of Conventional and Renewable Photo-Voltaic Generation

6.1 Introduction

The detection and classification of the PQ disturbances with the synthetic data has been carried out in Chapter-3 and Chapter-4. The variants of the wavelet transform and the S−transform have been utilized in Chapter-5 for the detection of the real PQ disturbance signals and three phase fault signals. From Chapter-5, it can be concluded that, though the $\%CA$ of ST based data set is more or less to the SGWT based data set, the SGWT is faster and simpler than the ST. Moreover, the ensemble DT is a good classifier for the recognition of both the PQ disturbance signals and the three phase fault signals. However in recent years the distributed generation has been steadily penetrating in the traditional power system. The major portion of the distributed generation sources are the solar photovoltaic generating units. The islanding issues are the major bottlenecks in the power system having distributed generation. Hence the islanding detection within power quality disturbance condition is one of the major challenges in the distributed generation environment.

The islanding detection methods are categorized in to three groups such as the active, the passive and the communication methods. In case of active methods, small disturbances are injected into the system and the subsequent results are observed in terms of change in the output parameter. The active methods like SMS, APS and AFD may suffer from high non-detection zone (NDZ) with the increase in reactive power [105]. SFS though provides less NDZ, may provide poor PQ [77]. The passive scheme is a low cost method which makes decision based on local measurement of voltage and current signals. The passive methods suffer from the non-detection zone (NDZ) [80]. The communication based islanding detection is also universally accepted approach but somewhat cost effective than the traditional passive methods. In order to minimize NDZ, signal processing techniques such as the Fourier transform (FT), the short term Fourier transform (STFT), the wavelet transform (DWT), S-transform (ST) are implemented in order to improve the detection quality. The fast method FT provides only the frequency component. The commonly used DWT suffers from the computational complexity. However, in some cases, capability of ST degrades during analysis of the nonstationary signals with transients. However, the main limitation of the ST is computational complexity. Similarly, the traditional ANN based classifiers suffers from retraining and increase of training time with the addition of data. The FL consumes more training time. However, the HMMs are only suitable for classification of fast disturbance signals.

This Chapter gives emphasis on the power quality disturbance analysis of $IEEE-14$ bus system. In this $IEEE-14$ bus system a synchronous generator has been replaced with the photovoltaic (PV) system [106], [107]. The PQ disturbances have been injected into the adjacent bus of the PV connected bus. The voltage signals have been captured at the point of common coupling (PCC) and fed to the aforementioned methods in order to discriminate the islanding event from the PQ disturbances. The proposed data mining based classifiers have been implemented for classification of both the PQ and islanding events.

6.2 Important Steps carried out in this Chapter

- Modelling of $IEEE-14$ bus system.

- To inject PQ events in to $IEEE-14$ bus system embedded with renewable based distributed generation.
- To process PCC voltage signal through the proposed method in order to extract the features.
- To discriminate islanding events from the PQ events by implementing the proposed method.
- To classify all the PQ and islanding events with the proposed data mining classifiers.

6.3 Organisation of the Chapter

In this Chapter, the Section-6.4 presents the brief description of the model. The different situation of the Islanding and the PQ events has been explained in Section-6.5. The importance of negative sequence component for islanding detection has been described in Section-6.6. The feature extraction and the data preparation have been described in Section-6.7 and Section-6.8. Simulation results on localization Islanding and PQ events at different situations with the variants of the WT and the ST has been discussed in Section-6.9. Similarly, the threshold values have been selection for discrimination of islanding events from nonislanding events is explained in Section-6.10. In Section-6.11, the proposed data mining based classifiers have been implemented for recognition of all the PQ and islanding events. Finally, the concluding remarks of the chapter are presented in Section-6.12. All these procedures have been presented in the form of flow chart in Figure 6.1.

6.4 Description of the System Model

In order to investigate the performance of the proposed techniques, an $IEEE-14$ bus test system has been simulated in MATLAB/SIMULINK environment that reflects a real system in all the vital parts. Moreover, the performance of the simulated system is quiet similar to what happens in a real situation.

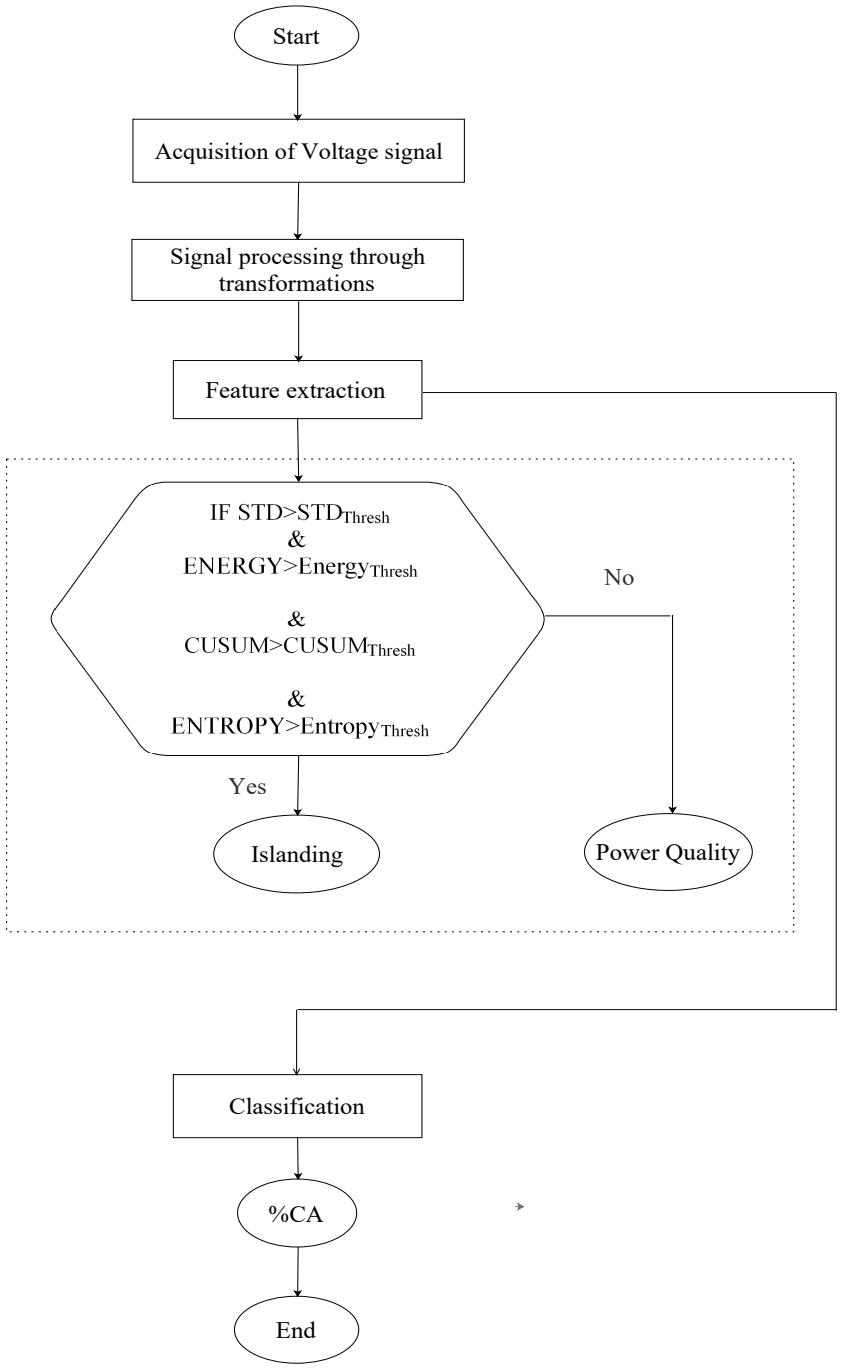

Figure 6.1: Flowchart of the Chapter work

A general description of the standard $IEEE-14$ bus has been presented in this section while the system data is given in Appendix-C. The overall specification is followed by the IEEE-bus system [108]. The considered base power and voltage are 100 MVA and 13.8 kV respectively. Similarly, the system has been designed with frequency 60 Hz and bus-1 as slack bus as per the specification. The parameters are in p.u with respect to the nominal rating of the device. Moreover, $v^{max} = 1.06$ p.u and $v^{min} = 0.94$ p.u are used as the voltage security limits for the optimal power flow analysis. An alternative source, such as the photovoltaic system has integrated to this bus system with the replacement of the DG-3 as shown in Figure 6.2. This integration has made in order to analyse the consequence of the islanding along with the PQ disturbances. The PQ disturbances are injected by varying the load at adjacent bus-4. The voltage signal at the point of common coupling (PCC) has captured and fed for further processing. The model is simulated at 20 kHz (60 Hz base frequency).

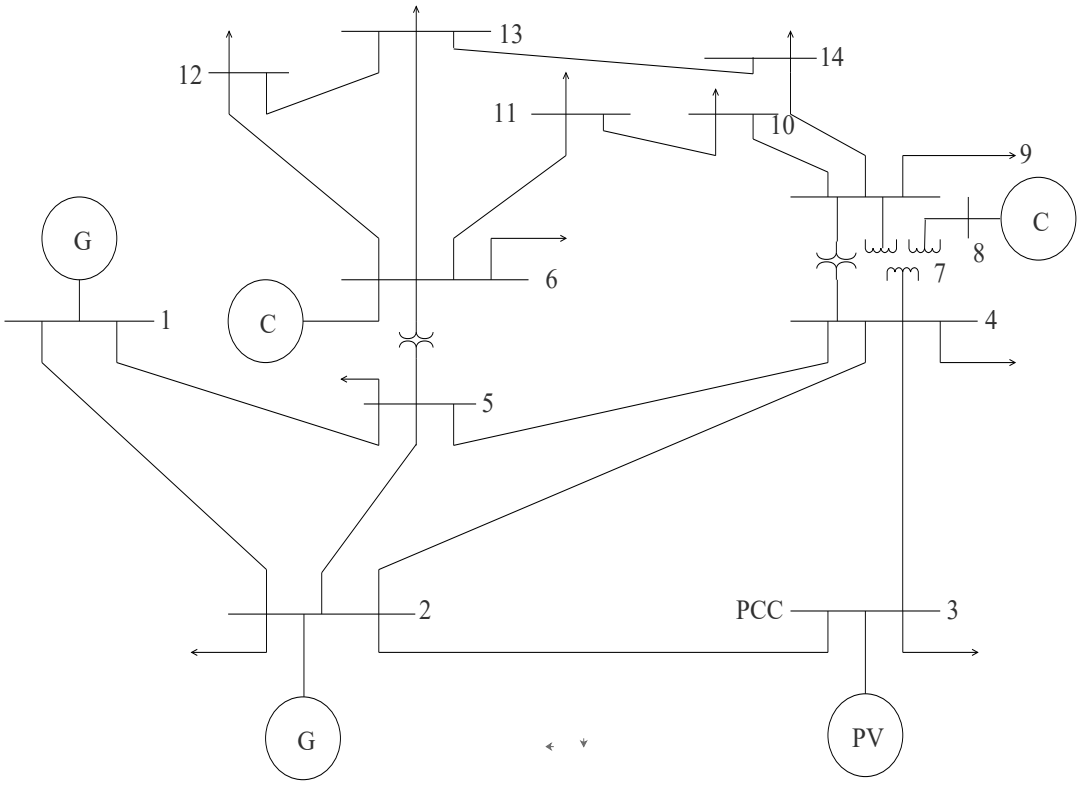

Figure 6.2: IEEE 14-Bus System with PV

6.5 Condition for Islanding and PQ events

The various conditions have bben artificially created with the help of the researchers. Some conditions considered in this thesis are discussed below.

1. **Normal operating condition** : The three phase circuit breaker−1 (connected between PV system and bus−3) is closed condition and the breaker−2 (at bus−4) through which extracted load connected is in open condition permanently. This is the normal state of operation of the model presented here. So the voltage wave form captured at the PCC is purely sinusoidal.

2. **Islanding condition** : The three phase circuit breaker−1 is normally in closed condition and opened at time 0.4 sec. The breaker−2 is open condition like before. This is the islanding condition.

3. **PQ disturbance condition** : The three phase circuit breaker−1 is closed permanently. The circuit breaker−2 which is normally in open condition is closed at time 0.3 sec. Due to this, the load is varied from the normal condition and leads distortion in the voltage signal. This is known as the PQ disturbance. With the variation of type of load connected, the type of PQ disturbance changes.

4. **Islanding with PQ disturbance condition** : The circuit breaker−2 is closed at time 0.3 sec, which creates PQ disturbance. The three phase circuit breaker−1 is opened at time 0.4 sec due to which islanding (islanding for PV) occurred. Both classes of events such as the pure power quality disturbance (PQD) and power quality disturbance with islanding (PQDI) are occurred.

6.6 Negative Sequence Component for the Islanding Detection

Symmetrical components are employed in order to determine unbalanced conditions on a three phase by implementing the single phase calculation. The symmetrical component consists of positive, negative and zero sequence quantities. The positive sequence is generally present in the balanced operation of the system which associates with the

normal voltage and currents of steady state operation. The negative sequence quantities are a measure of the unbalance condition present in a power system. Similarly the zero sequence quantities are accomplished with the ground associated in an unbalanced operating condition. The equation for the calculation of the negative sequence voltage signal is given in (6.1)

$$V_n = \frac{1}{3}\left(V_a + a^2 V_b + a V_c\right) \tag{6.1}$$

where V_a, V_b, V_c are three phase voltages captured at the PCC. Similarly, $a = 1\angle 120$ is the complex operator. The negative sequence voltage signal are passed through the transformations such as the variants of the WT and ST.

6.7 Feature Extraction

In this work, four features have been extracted from the the negative sequence voltage signal captured at the PCC like the PQ classification. These features such as the energy, the standard deviation (STD), the cumulative sum (CUSUM) and the entropy have been discussed in Chapter-3,4. These features are used to set the threshold in order to discriminate the PQD from the islanding. Moreover, these selected features are fed to the data mining based classifiers for classification.

6.8 Data preparation

A wide range of the simulation cases have been executed in order to capture large amount of data to provide solid information to the classifiers, so that all the distortions can be classified properly. The PQ disturbances such as the sag, the swell have been created by changing the resistive and the capacitive load. Similarly the harmonic is injected by adding rectifier loads.

6.9 Simulation Results on Localization Islanding and the PQ events

The various conditions described in Section-6.5 are simulated in this Section. The voltage signals captured at the PCC have been fed trough the signal processing based transforms for the analysis. The signals are decomposed up to four levels of decomposition as carried out for the localization of PQD in Chapter-3. The different cases considered for the localization of the distortion due to the PQ disturbance and islanding events have been presented in this section. The horizontal label represents the samples and the vertical label represents the voltage magnitude in V p.u.

6.9.1 Normal Operating Condition

The normal operation is the distortion free operation that represents the steady state operation of the system. The proposed $IEEE-14$ bus embedded with the renewable based PV system is at the normal operating condition during which the system is free from the extra load. So the three phase circuit breaker-2 (connected at bus-4) is opened. The voltage signal captured at the PCC has been fed for analysis and shown in Figure 6.3. The horizontal axis represents the amplitude in terms of Voltage per unit. By implementing WT variants, the signals have been decomposed up to four decomposition levels. From, Figure 6.3, it can be observed, as the voltage is distortion free, so there is no deviation in the waveforms after the transformations. The S-contours have also no deviation.

6.9.2 Islanding Condition

The islanding operation occurs when the utility grid supply is isolated due to some emergency conditions and the DG feeds power to the local loads. In this case, the PV system has been disconnected from the grid system in order to create the islanding situation. The islanding has been created at bus-3 by disconnecting the PV system from the system at time 0.4 sec. The PCC voltage with the islanding captured at bus-3 has been fed to the transformations. As the previous cases signal has been analysed through the transformations shown in Figure 6.4. Even at the finer decomposition

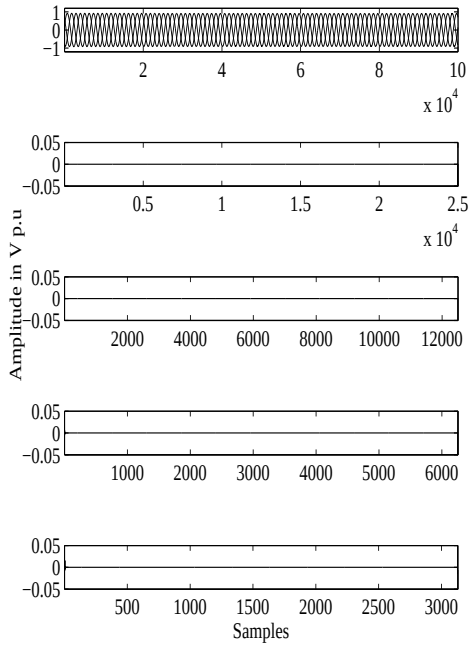

(a) DWT analysis

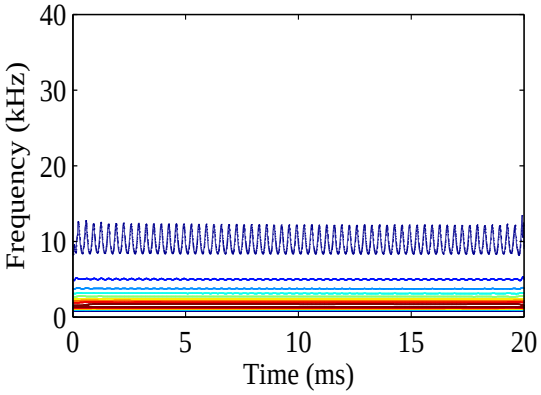

(b) ST analysis

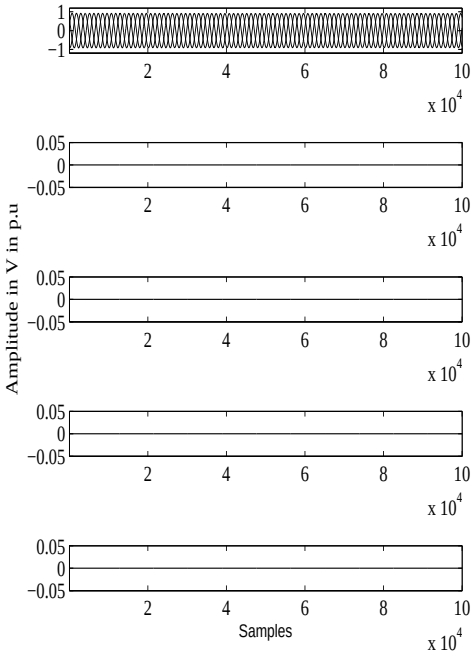

(c) MODWT analysis

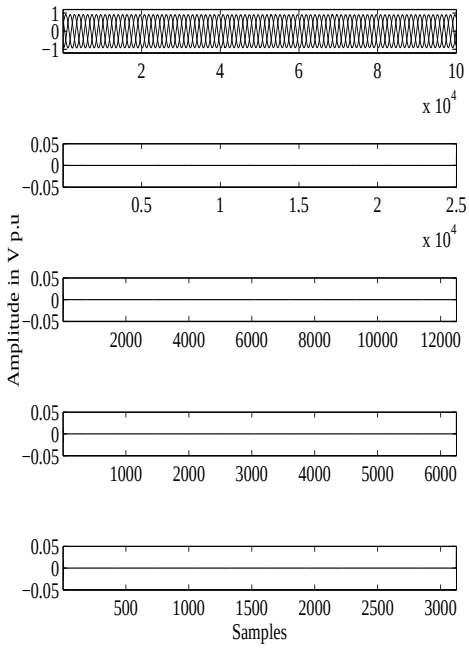

(d) SGWT analysis

Figure 6.3: Localization of pure sinusoidal voltage signal

levels of the WT variants, the islanding occurrence point is clearly detected. In case of ST, the distortion has been detected properly.

6.9.3 PQ Disturbance Condition in Bus System

The PQ disturbances have been injected at bus−4 in order to get PQ disturbance environment artificially in the bus system. In this case two PQ disturbances have been considered. They are the sag and the transient.

6.9.3.1 Sag Injection to the Bus near to the PV Connected Bus

In this case, the sag has been injected at bus−4 during $0.3-0.45$ sec. The PCC voltage has been captured and fed through the transformations in order to get influence of the PQ in adjacent buses shown in Figure 6.5. The signal has been decomposed up to four finer levels in WT transformations like the other cases.

From Figure 6.5 it can be observed that the sag inception point has been precisely found out in each case. The end point of the sag has been clearly found out in every decomposition level of the DWT and the SGWT except MODWT with same amplitude. The ST has provided the proper localization of the sag.

6.9.3.2 Transient at Bus near to the PV Connected Bus

In this case, the transient has been created at same bus like sag case. The duration of transient is $0.4-0.42$ sec. The voltage with the transient captured at PCC is fed for transformations. The transient inception and the end points have been clearly found out in Figure 6.6. The duration of transient can be properly identified.

6.9.4 Islanding within PQ Disturbance Situation

The power quality disturbances have been injected at bus−4 like the previous case. The islanding environment has been artificially created at bus−3 during the presence of PQ disturbances. The influence of islanding within the PQ disturbances at other buses has been observed by analyzing the PCC voltage signal. Different PQ disturbance amid islanding have been analyzed as follows.

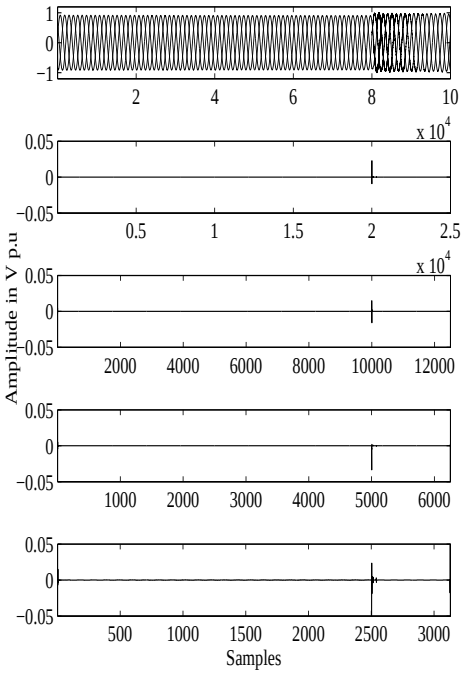

(a) DWT analysis

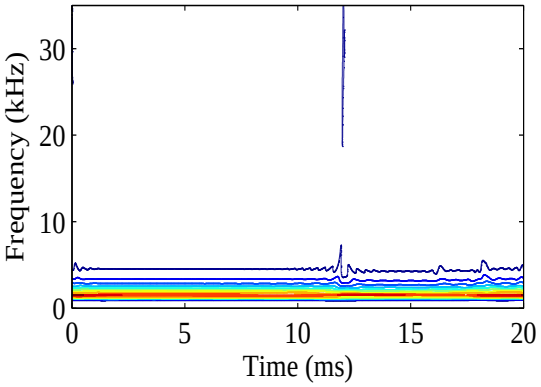

(b) ST analysis

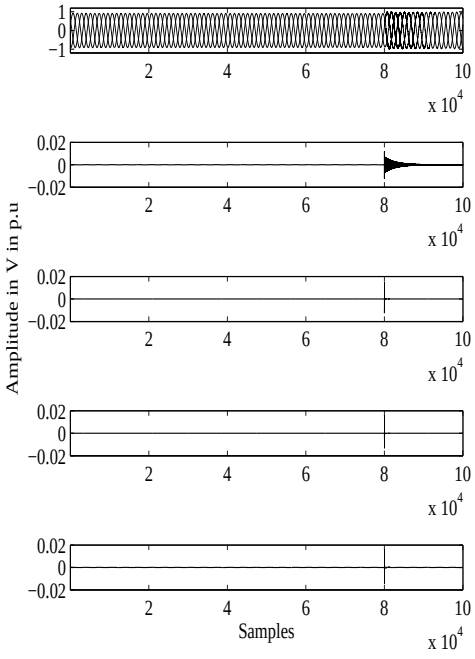

(c) MODWT analysis

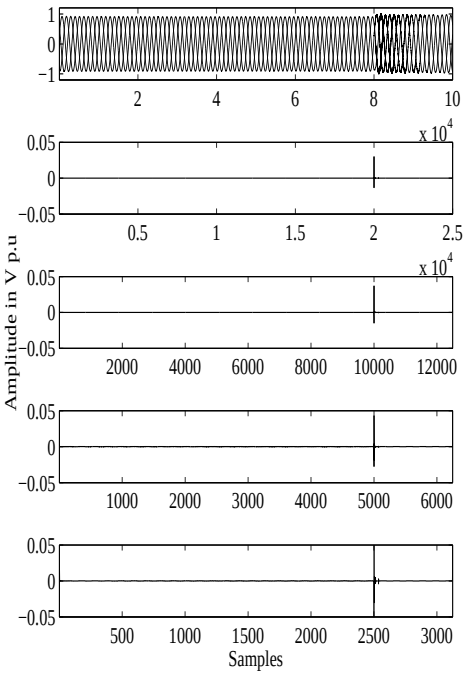

(d) SGWT analysis

Figure 6.4: Localization of islanding

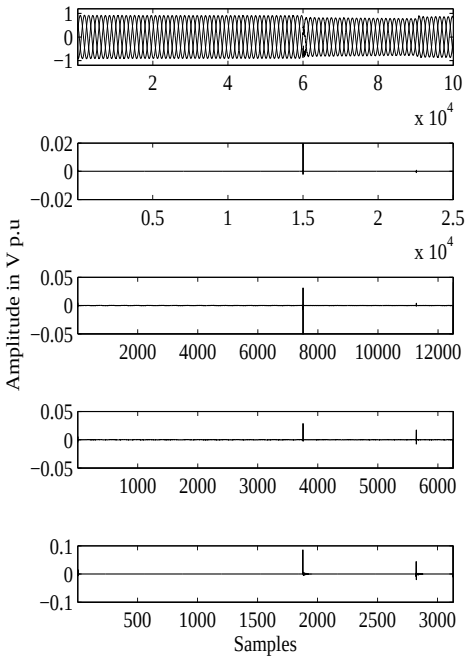

(a) DWT analysis

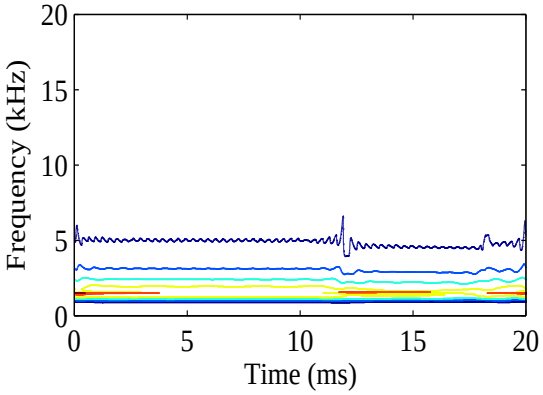

(b) ST analysis

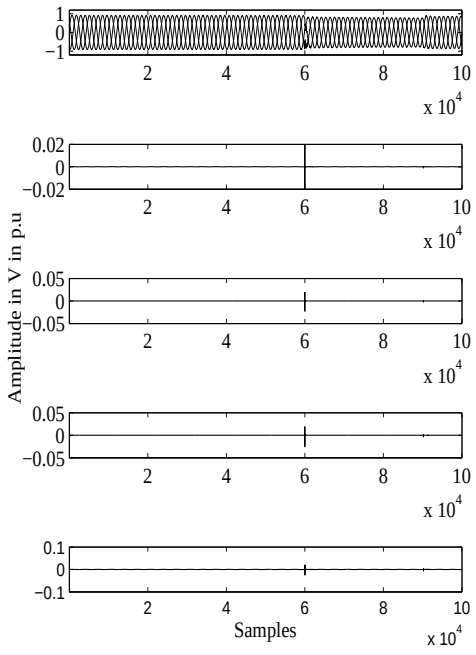

(c) MODWT analysis

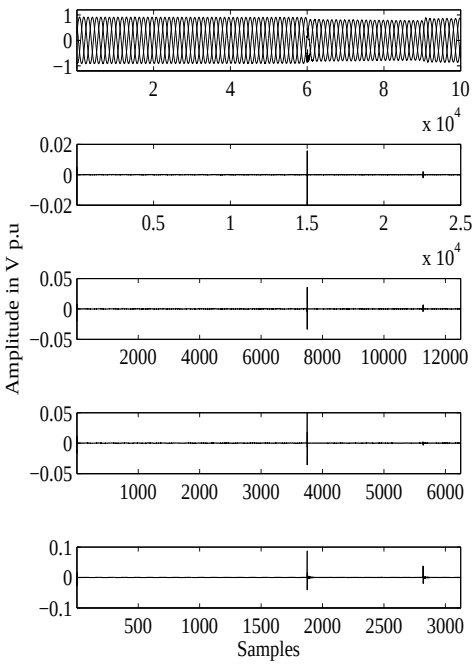

(d) SGWT analysis

Figure 6.5: Localization of sag in pure sinusoidal voltage signal

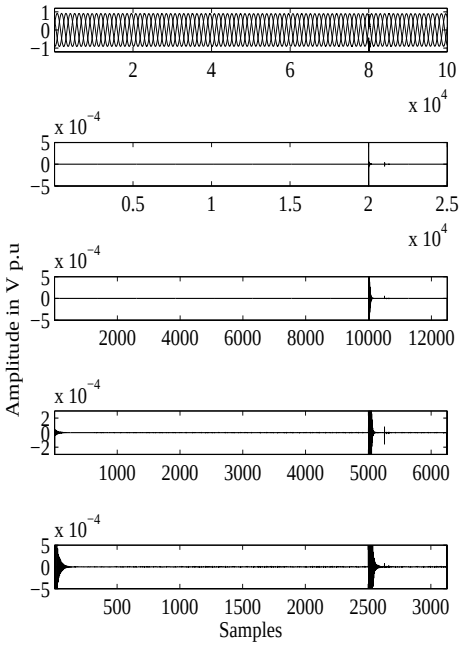

(a) DWT analysis

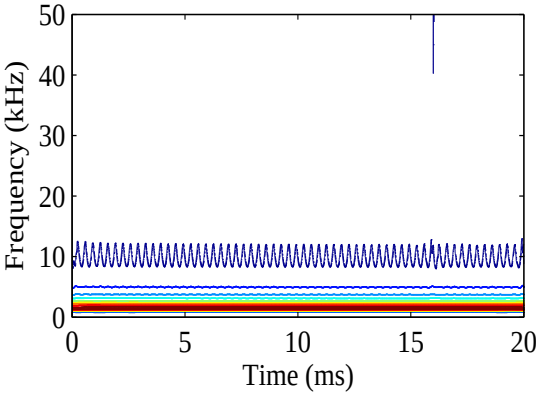

(b) ST analysis

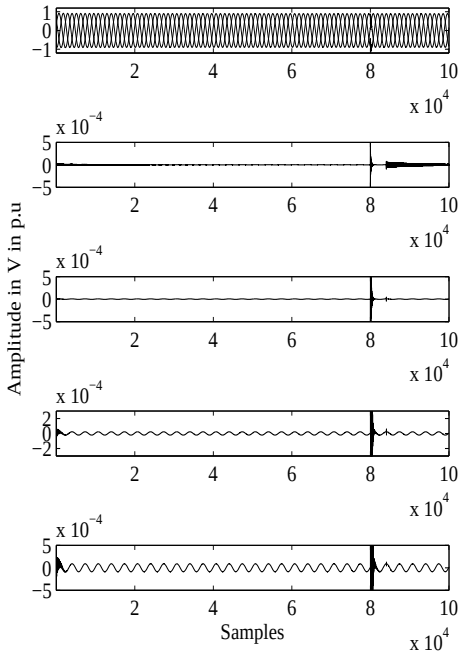

(c) MODWT analysis

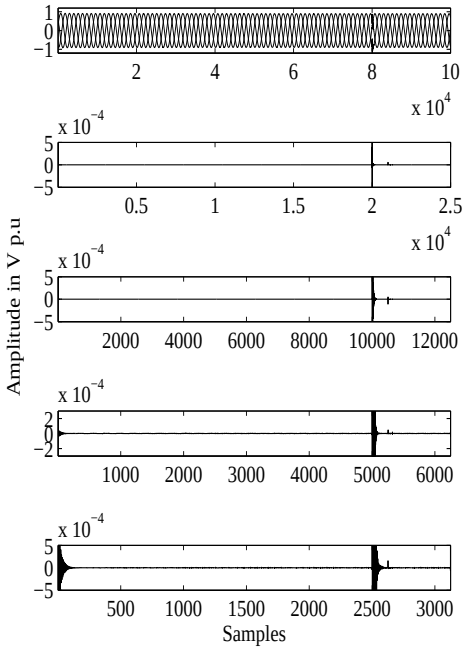

(d) SGWT analysis

Figure 6.6: Localization of transient in pure sinusoidal voltage signal

6.9.4.1 Islanding within Sag

In this situation, the sag has been injected at bus−4 during $0.3 - 0.45$ sec. The islanding environment has been created by disconnecting the bus−3 at 0.4 sec within PQ disturbance. The captured PCC voltage has been fed as the input to the transformations in order to get the influence of islanding within the PQ situation. With the same magnitude, all the distortions i.e the sag initial and the final points along with the islanding inception point have been properly localized by the DWT and the SGWT. From Figure 6.7, it is observed, that as in the previous case, the MODWT has failed to clearly display all the distortion points with same amplitude at respective decomposition levels unlike DWT and SGWT.

6.9.4.2 Islanding along with the Transient

In this case, the islanding environment has been created coinciding with the inception of the transient unlike the sag with the islanding case. The transient has been injected at bus−4 during $0.4-0.42$ sec. The islanding situation has been established at the same instant of inception of transient i.e. at 0.4 sec. All the distortions have been clearly localized at all decomposition levels through all the signal processing transformations shown in Figure 6.8.

6.9.4.3 Islanding along with Harmonic

Harmonics have been injected in to the system by connecting the rectifier load at all the buses. The islanding situation has been established at bus−3 at time 0.4 sec like the other cases. The islanding within the harmonics doped environment has been detected properly through the transformations and is shown in Figure 6.9. From Figure 6.9, it can be observed that the amplitude of islanding is more than the harmonic in all the decomposition levels of the variants of WT.

6.9.4.4 Islanding within Harmonic embedded with Sag

In this case, the islanding has been localized in harmonics doped environment with sag in order to get the combined PQ disturbances situation. Like the previous cases, the harmonics have been injected at all the buses and the sag injected at bus−4

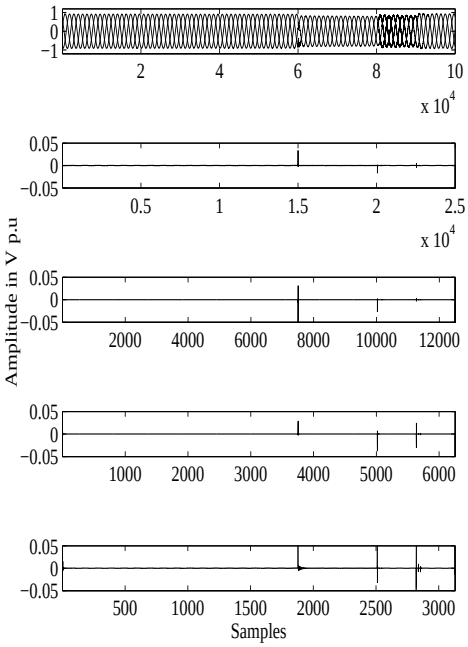

(a) DWT analysis

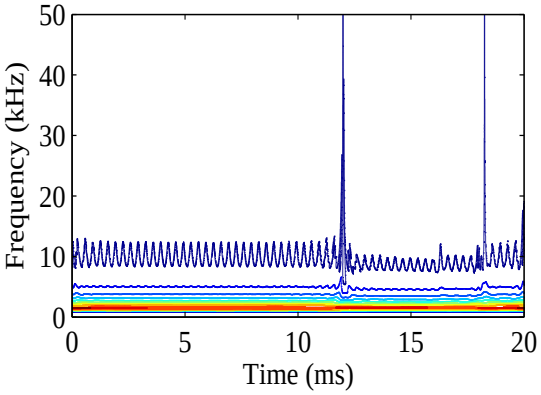

(b) ST analysis

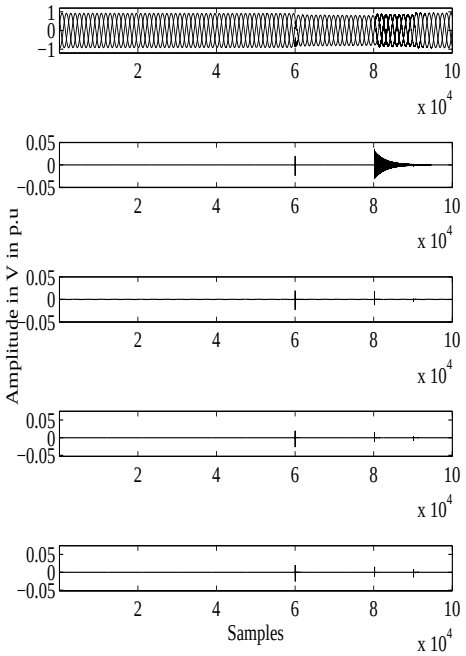

(c) MODWT analysis

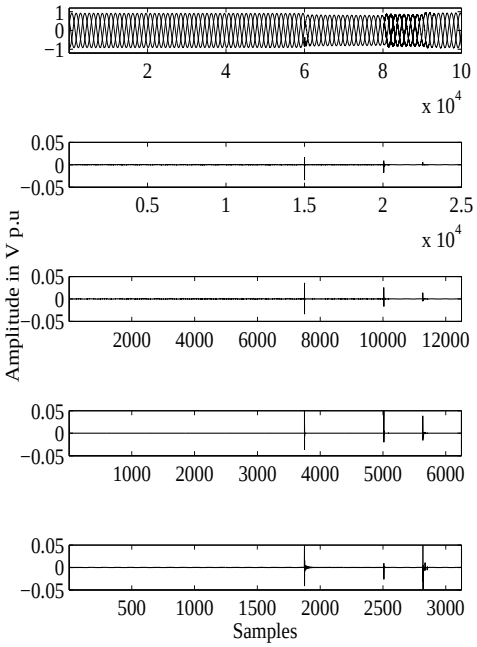

(d) SGWT analysis

Figure 6.7: Localization of islanding within sag

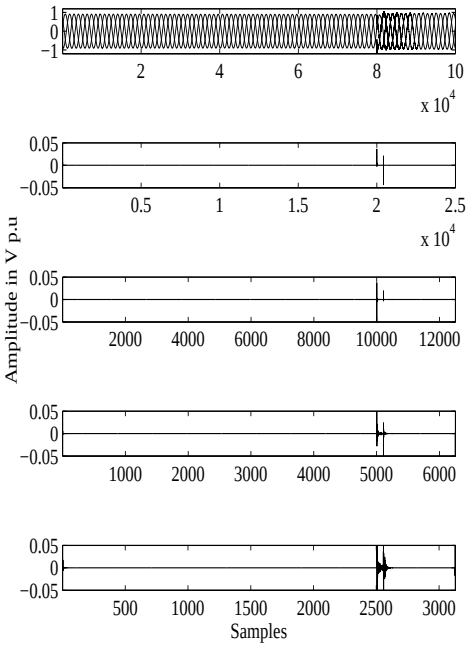

(a) DWT analysis

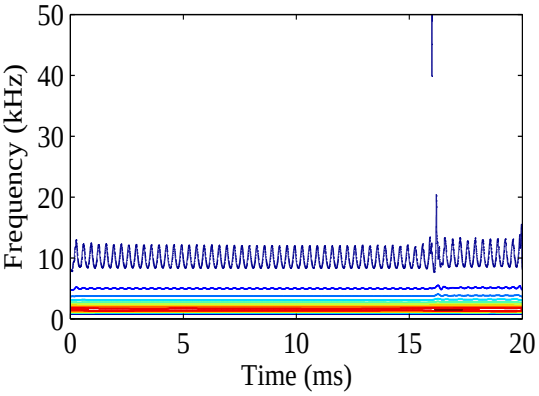

(b) ST analysis

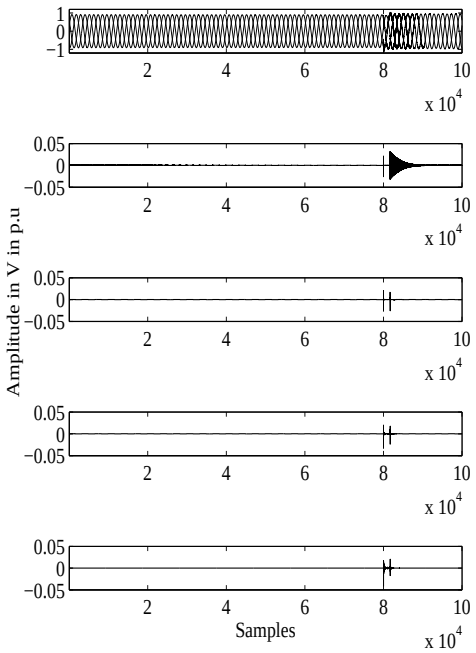

(c) MODWT analysis

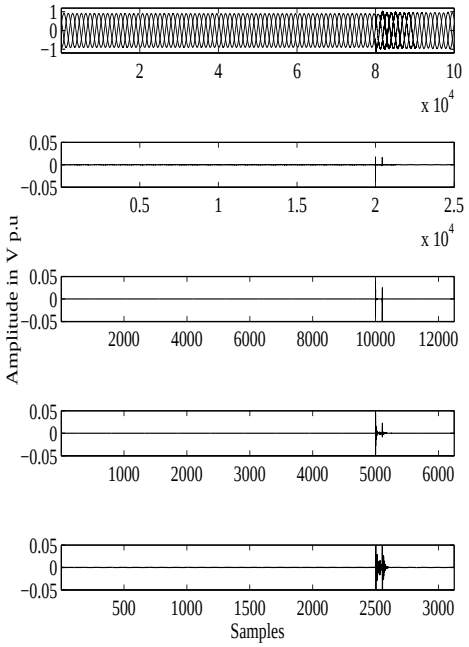

(d) SGWT analysis

Figure 6.8: Localization of islanding along with transient

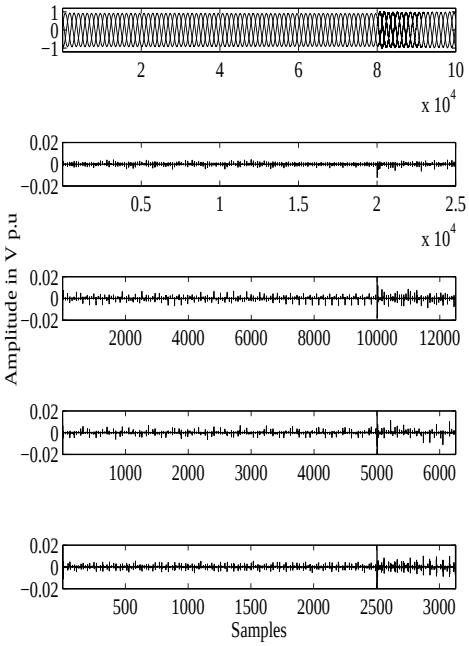

(a) DWT analysis

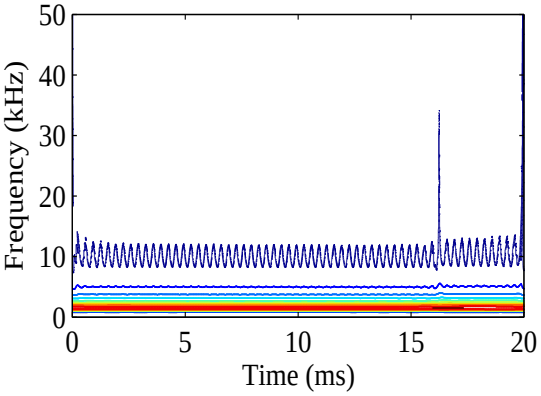

(b) ST analysis

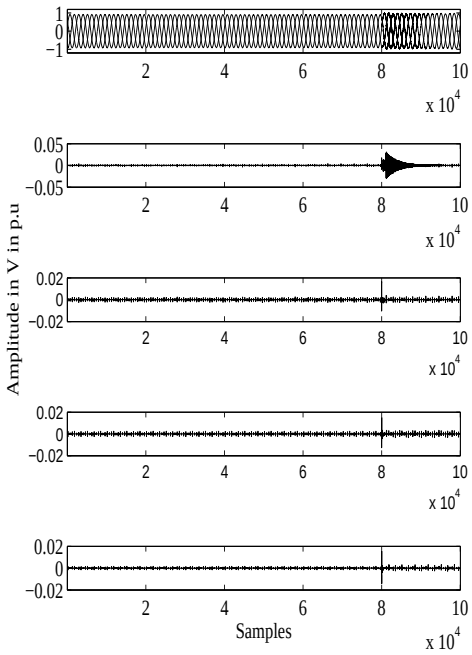

(c) MODWT analysis

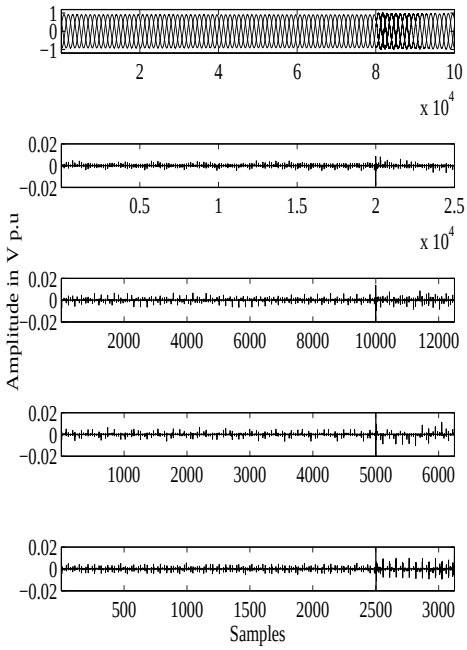

(d) SGWT analysis

Figure 6.9: Localization of islanding amid harmonics

during $0.3 - 0.45$ sec. The analysis of the PCC voltage signal has been presented in Figure 6.11. All the distortions have been clearly properly localized by the Wavelet Transforms (WTs). As the harmonics is filtered in each level, the harmonics have been suppressed in the finer levels of the WTs. As in the previous cases, the DWT and the SGWT have provided better localization than the MODWT at the same amplitude in the respective decomposition levels. The magnitude of the distortion points due to the sag and the islanding is more than the magnitude of the harmonic distortion similar to the islanding within the harmonic case.

In all the cases the islanding has been localized by implementing aforementioned analysis techniques. Similar to the previous cases, all the analysis techniques have been applied for localization of the islanding within faulty environment in next subsequent subsection in order to observe the efficacy of the proposed method.

6.9.5 Islanding localization within Three-phase Fault Environment

The previous subsection has discussed the islanding localization within the PQ environment in a grid-connected PV system, where as in this subsection the islanding has been localized along with the three-phase fault injected to adjacent bus of the PV connected bus i.e., bus-4. The fault has been injected for the time $0.4 - 0.43$ sec. The simultaneous occurrence of the three phase fault and islanding event has been investigated. The PCC voltage signal along with three phase fault has been decomposed by the variants of WT and ST, shown in Figure 6.11. The fault inception point is localized at each decomposition levels. The fault inception and clearance instances have been also localized at all the decomposition levels.

Though all the distortions such as the three phase fault, the islanding and the PQ disturbances have been properly localized in all the aforementioned methods, they fail to properly identify all the distortions. However, the threshold selection method has been employed in the subsequent section in order to discriminate the islanding with PQ events from pure the PQ events.

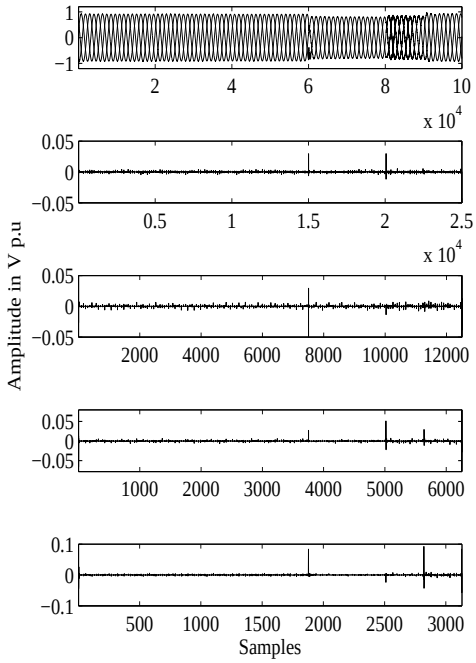

(a) DWT analysis

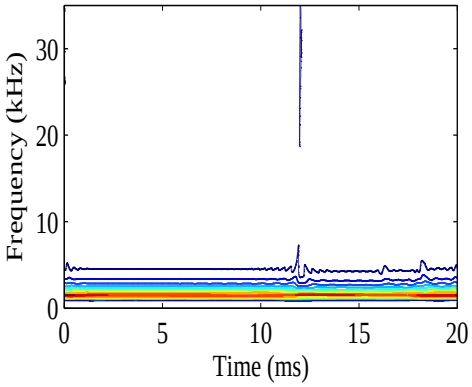

(b) ST analysis

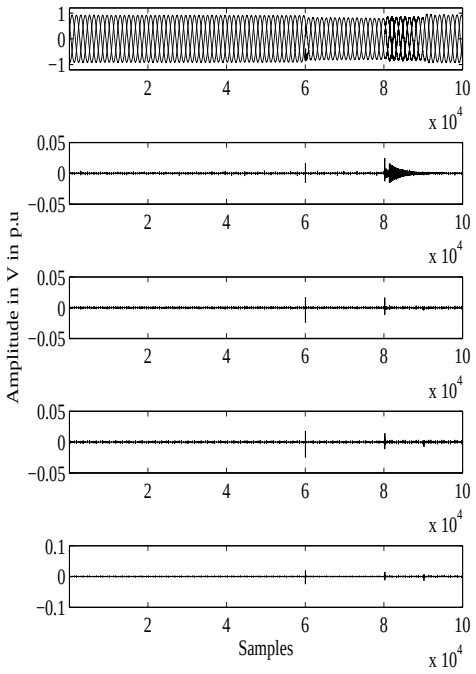

(c) MODWT analysis

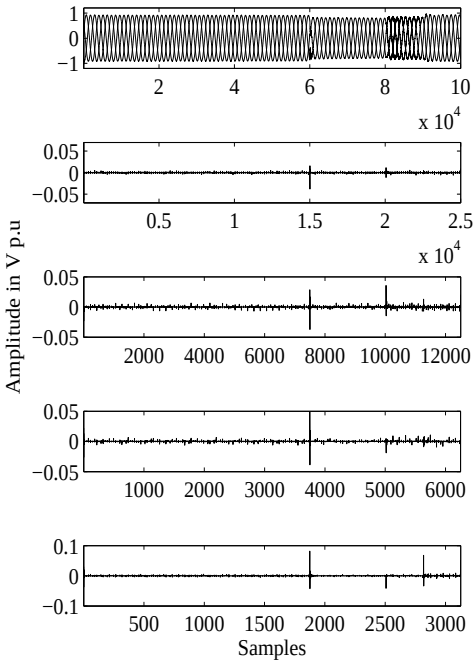

(d) SGWT analysis

Figure 6.10: Localization of islanding within harmonic and sag

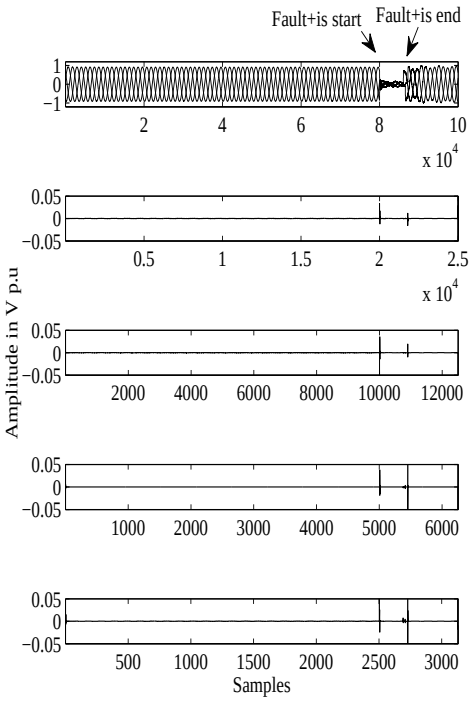

(a) DWT analysis

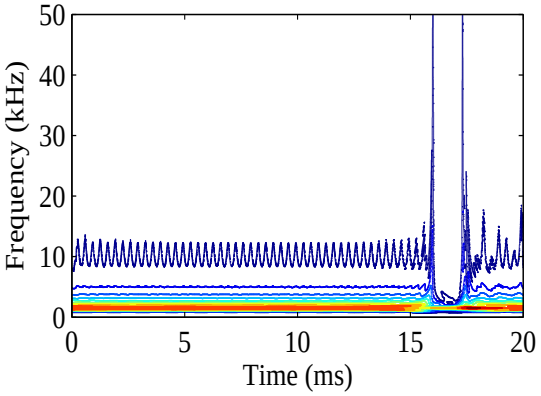

(b) ST analysis

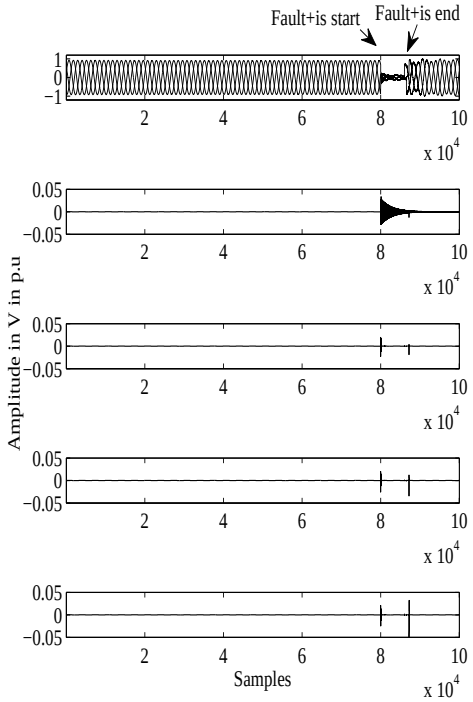

(c) MODWT analysis

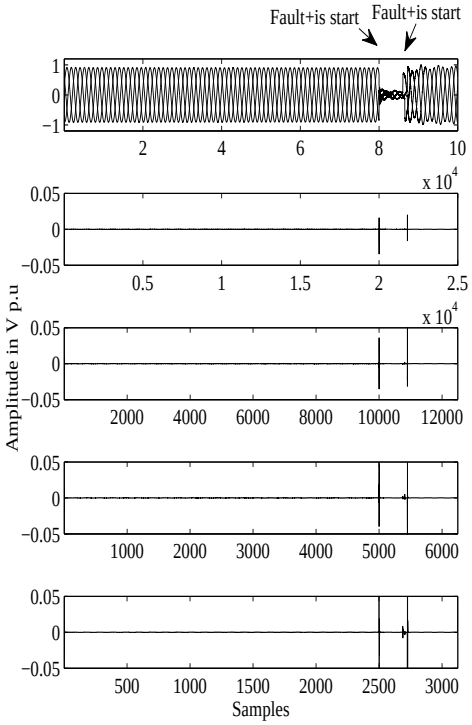

(d) SGWT analysis

Figure 6.11: Localization of islanding along with fault

Table 6.1: Simulation time of DWT,MODWT,SGWT and ST

Signal Name	DWT (Time in sec)	MODWT (Time in sec)	SGWT (Time in sec)	ST (Time in sec)
Normal voltage	0.888714	13.664974	0.877639	223.5075
Islanding	0.709393	13.866876	0.647831	360.0658
Sag	0.691212	14.009237	0.681233	300.1308
Sag+ islanding	0.700812	13.548546	0.656332	310.4855
Fault	0.927177	14.989277	0.837867	320.6541
Fault+islanding	0.728254	14.313309	0.654368	321.7276
Harmonics	0.705359	14.423151	0.575649	439.9520
Harmonics + islanding	0.978505	15.832037	0.663345	325.9520
Transient	0.713990	14.294301	0.690822	309.9298
Transient + islanding	0.729225	14.939197	0.701850	326.2344

6.10 Results on Threshold Selection for Discrimination of Islanding with PQ Events from the Pure PQ Events

This section has presented, the performance of the performance indices (PI) in order to discriminate the PQ disturbances from the islanding events. Similar to the localization case, the PQ disturbances and the fault have been injected at bus−4. The voltage signals have been captured from the PCC and fed through the transformations. Four performance indices such as the Standard Deviation, the Entropy, the CUSUM and the Energy have been extracted at first decomposition level of the WT variants. The brief description of the threshold selections in different situations have been discussed below.

6.10.1 Under Condition of PQ Disturbance

The aforementioned indices are extracted from the negative sequence component of captured PCC voltage. A threshold line (THL) has been drawn in order to discriminate the power quality disturbance (PQD) from the islanding events within the power quality disturbance (PQDI). All these procedures have been presented in the form of flow chart in Figure 6.1. The threshold line for all the performance indices extracted from the DWT has been shown in Figure 6.12. The acronyms given in Figure 6.12, Figure 6.13 and Figure 6.15 represented by Standard dev: Standard deviation, PQD: Power quality disturbance, PQDI: Islanding and power quality disturbance, THL: Threshold line. The threshold value for the PV connected IEEE-14 bus is selected as 75 for CUSUM, 0.05 p.u for energy, $03.02 * 10^5$ for entropy and 0.0007 for STD. When the STD is more than 0.0007, entropy value is more than $03.02 * 10^5$, energy content is more than 0.05 p.u., the CUSUM is more than 75, then the PQDI are detected, otherwise it corresponds to the PQD condition. From the Figures, it can be observed that in islanding situation, the PI value are more than the respective PI value of pure PQ.

Similarly, the THL has been drawn from the coefficients of MODWT shown in Figure 6.13. From Figure 6.12 and Figure 6.13, it can be observed, the threshold value of DWT and MODWT are same at first decomposition. Moreover, the THL in SGWT has been shown in Figure 6.12 which is different from the DWT and MODWT threshold value. The threshold value has been selected as 6 for CUSUM, 0.05 p.u for energy, 0.3 p.u for entropy and 0.001 for STD. When the STD is more than 0.001, the entropy value more than $2*10^6$ p.u., the energy content more than 1.1, the CUSUM more than $2*10^6$, then the PQDI are detected, otherwise it corresponds to the PQD. Moreover, these threshold selection has been discussed under fault condition in subsequent subsection in order to observe the robustness in any abnormal situation.

6.10.2 Under the Fault Condition

The threshold selection has been discussed along with the injection of the fault in to adjacent bus of the PV connected bus like the previous subsection. In this subsection, the different types of fault such as $L-L-L$, $L-L-L-G$, $L-L$, $L-L-G$, $L-G$, and

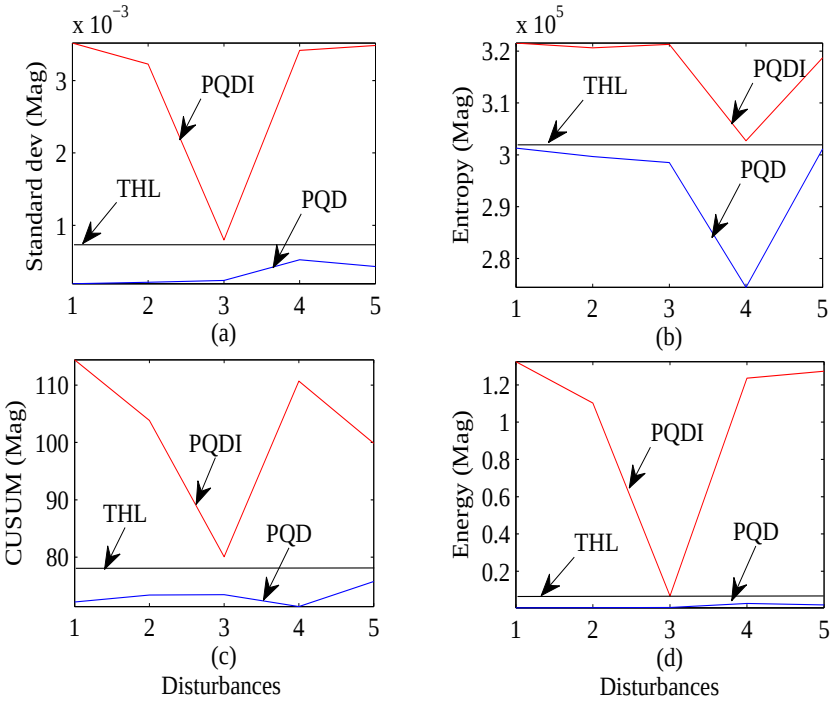

Figure 6.12: Threshold line for DWT extracted performance indices.

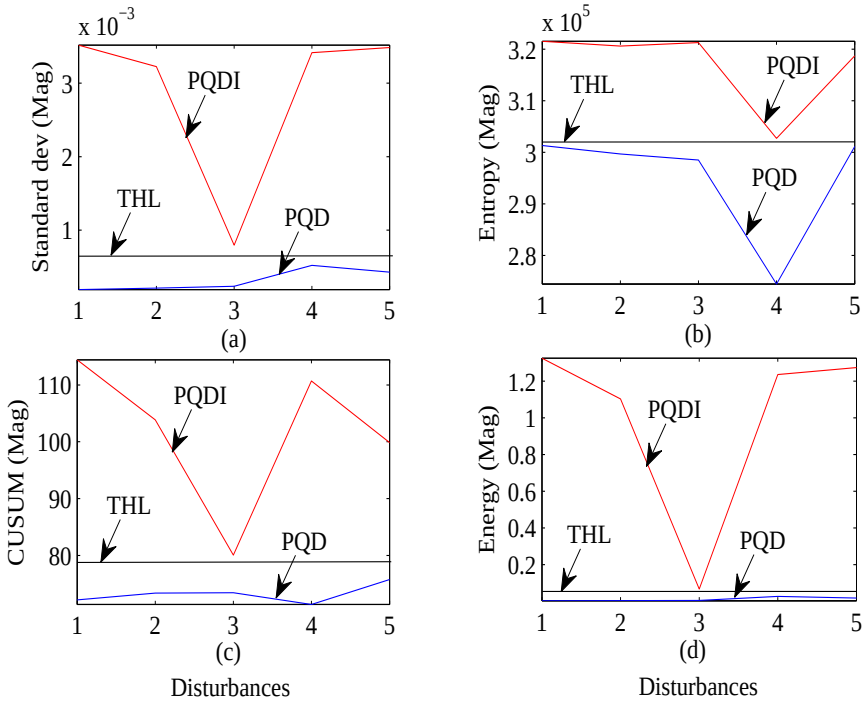

Figure 6.13: Threshold line for MODWT extracted performance indices

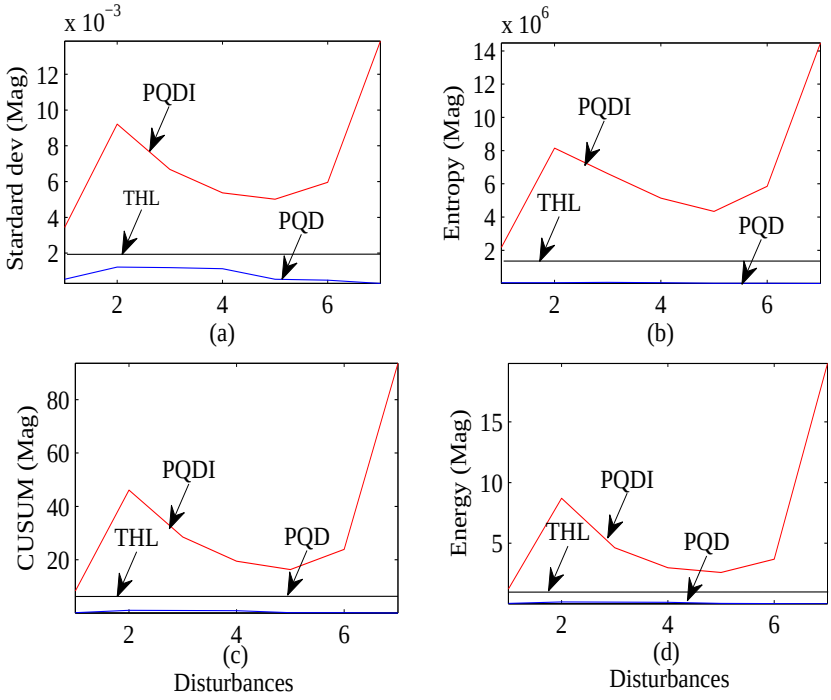

Figure 6.14: Threshold line for SGWT extracted performance indices

finally the single phase faults has been injected at bus−4 at the instant of the islanding at bus−3. The threshold line has been drawn and is shown in Figure 6.15. In this figure, the acronyms are represented by Standard dev: Standard deviation, Fault+is: Fault with islanding, THL: Threshold line like the previous cases. From Figure 6.15, it can be observed that the threshold line properly discriminates the islanding events from the fault condition as in the case of the power quality events. The threshold value can be selected $1.8 * 10^6$ for CUSUM, 1.1 p.u for energy, 3 for entropy and 0.002 for STD. Moreover, irrespective of the type of fault, the islanding events have higher valued performance indices than the pure fault condition like the pure power quality disturbance cases.

The islanding events have been properly discriminated from the nonislanding events with the variants of WT. The simulation time for single signal of each event for the single decomposition level by the WT variants have been presented in Table 6.1. Also the simulation time of ST of these events have been presented in this Table. From Table 6.1, it can be observed that the SGWT is faster than the DWT and MODWT.

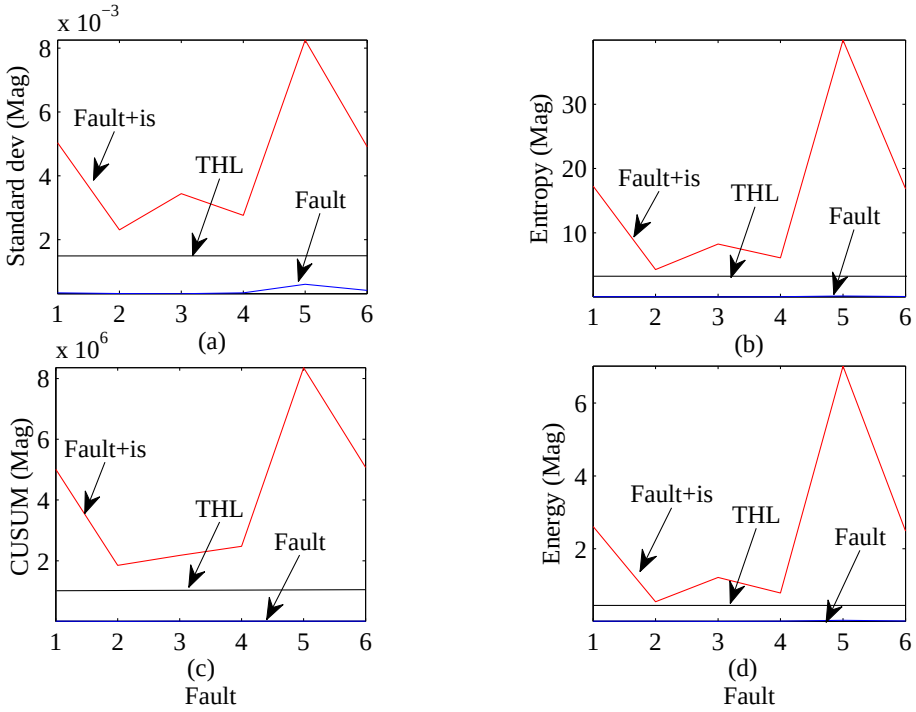

Figure 6.15: Threshold line for SGWT extracted performance indices.

Although the ST has been implemented for the detection, it suffers from the extra memory consumption and the computational burden. This extra memory requirement makes the system sluggish. In DWT and MODWT, with the down sampling, the performance indices values at the first decomposition level remain similar but in ST analysis, the performance indices value changes with the down sampling. In this case ST has not been implemented for threshold selection due to extra requirement of both memory and time.

In the islanding events are segregated from the power quality events. The proper discrimination of each of power quality and islanding events have been carried out in the next subsequent section.

6.11 Recognition Results

In the Chapter-4,5, four different classifiers has been implemented for discrimination of different power quality events and the performance of the classifiers are also compared.

Table 6.2: Assigned Class label

Signal name	Class name
Transient+islanding	CP1
Swell+islanding	CP2
Sag+islanding	CP3
Harmonic+sag+ islanding	CP4
Harmonic+swell+ islanding	CP5
Harmonic+ islanding	CP6
Transient	CP7
Sag	CP8
Swell	CP9
Harmonic+sag	CP10
Harmonic+swell	CP11
Harmonic	CP12

According to their performance, DT and RF have performed satisfactorily in all cases. In this chapter, DT and RF has been applied for classification of power quality and the islanding events. Like the previous chapters, by varying the inception instances, the duration and magnitude of the events total 680 voltage signals are extracted from the PCC. Each signals have been decomposed up to 12 levels by SGWT. Like that of the previous chapter, four features have been extracted for each decomposition levels. So, total $4 * 12$ feature vectors for each signal are formed and fed to the data mining based classifiers for classification. The classification in the form of confusion matrix have been presented in the Table 6.3 and 6.4. The confusion matrix or the error matrix provides the performance of classification model on a set of test data for which true values are known. Each row of the matrix represents the instance in an actual class while each column represents the instances in the predicted class(vice-versa).

The Table 6.2 carries the assigned class labels. The DT performance has been represented in Table 6.3 whereas Table 6.4 enlisted the performance of RF. In DT out of 680 instances, correctly classified instances are 650 and misclassified instances are 30 with the consideration of (60/40)% (60% training data, 40% testing data) data division. In other words, the classification rate of DT is 95.5882. Whereas the recognition rate of RF is 100% i.e all the instance are classified properly with zero misclassification. So the RF is working satisfactorily in islanding as well as power quality environment.

Table 6.3: Confusion matrix of DT

Actual/Predicted	CP1	CP2	CP3	CP4	CP5	CP6	CP7	CP8	CP9	CP10	CP11	CP12
CP1	50	0	0	0	0	0	0	0	0	0	0	0
CP2	10	25	0	0	0	0	0	0	0	0	0	0
CP3	0	0	70	0	0	0	0	0	0	0	0	0
CP4	0	0	0	25	0	0	0	0	0	0	0	0
CP5	0	0	0	0	70	0	0	0	0	0	0	0
CP6	0	0	0	0	0	30	0	0	0	0	0	0
CP7	0	0	0	0	0	0	80	0	0	0	0	0
CP8	0	0	0	0	0	0	0	85	0	0	0	0
CP9	0	0	0	0	0	0	0	10	80	0	0	0
CP10	0	0	0	0	0	0	0	0	0	45	0	10
CP11	0	0	0	0	0	0	0	0	0	0	65	0
CP12	0	0	0	0	0	0	0	0	0	0	0	25

Table 6.4: Confusion matrix of RF

Actual/Predicted	CP1	CP2	CP3	CP4	CP5	CP6	CP7	CP8	CP9	CP10	CP11	CP12
CP1	50	0	0	0	0	0	0	0	0	0	0	0
CP2	0	35	0	0	0	0	0	0	0	0	0	0
CP3	0	0	70	0	0	0	0	0	0	0	0	0
CP4	0	0	0	25	0	0	0	0	0	0	0	0
CP5	0	0	0	0	70	0	0	0	0	0	0	0
CP6	0	0	0	0	0	30	0	0	0	0	0	0
CP7	0	0	0	0	0	0	80	0	0	0	0	0
CP8	0	0	0	0	0	0	0	85	0	0	0	0
CP9	0	0	0	0	0	0	0	0	90	0	0	0
CP10	0	0	0	0	0	0	0	0	0	55	0	10
CP11	0	0	0	0	0	0	0	0	0	0	65	0
CP12	0	0	0	0	0	0	0	0	0	0	0	25

6.12 Chapter Summary

In this Chapter, IEEE-14 bus system has been modelled. The power quality disturbances have been injected at one of the bus. During the PQ events, the islanding environment has been created artificially at the adjacent bus and the captured PCC voltage analyzed with the variants of the WT and the ST. With the variants of the WT such as the DWT, the MODWT and the SGWT, the threshold lines have been drawn in order to discriminate the islanding events from the nonislanding cases according to their performance indices value. Although the DWT, MODWT have provided same threshold value the DWT is faster than the MODWT at the first decomposition level. The SGWT has provided better results than the DWT and the MODWT. Moreover, the SGWT is faster than DWT and MODWT. The SGWT has provided better results in pure fault and fault with islanding events. In general, WT variants have been able to detect the various constraints of islanding, PQ disturbances and faults in reasonable time. Only the S-transform has taken more time to detect the various constrain as it requires large memory size. However, the RF has better performance rate than the DT in classification of both the power quality and islanding events. Hence RF is the best classifier.

Chapter 7

Conclusions and Scope for Future Work

In this chapter, the overall conclusions of the thesis have been presented and the scope for further extension of the research work has been discussed.

7.1 General Conclusion

The thesis has illustrated on selection of suitable and fast techniques for detection and identification of power quality (PQ) disturbances. The research studies presented in this thesis have started with the introduction to the power quality disturbances along with its causes and consequences in the modern power system. The performance of the existing signal analysis methods is discussed. Ten different types of power quality signals have been synthesized in MATLAB Simulation environment. The wavelet transform i.e DWT and ST have been implemented for the analysis of these signals in order to achieve a comparison of the performances of techniques for localization of the distortions presented within the signal. The various drawbacks of these techniques have been encountered during the analysis of the signal. The modified version of DWT known as MODWT has been proposed for the localisation of the distortion within the power quality signal. This down sampling free MODWT is a suitable method to forecast further inception of disturbances. This thesis has also described a new technique termed as second generation wavelet transform for the detection and

localisation of power quality disturbances. The effectiveness of the SGWT has been evaluated by comparing with the variants of WT i.e DWT and MODWT. The SGWT is a simple and fast technique for analysis of the signals. The subsequent segment of the thesis concentrates on the classification of disturbances. The discrimination process needs suitable features for an efficient classification. The classification approaches such as decision tree and ensemble decision tree i.e random forest are discussed. However, decision tree suffers from overfitting problems when large class of data set are required to be classified. The ensemble decision tree is overcomes this overfitting problems. The studies extended towards the real time signal analysis captured from the single phase and three phase transmission panel in ordered to test the suitability of the aforementioned techniques. The variants of the wavelet transforms and ST are also implemented when renewable distributed generation embedded with IEEE−14 bus system. The distortions due to PQ and islanding have been detected and localized. The islanding events are discriminated from the PQ disturbances by the threshold lines drawn from the features extracted from the detail coefficients of WT. The different pure PQ and islanding events have been classified by the data mining classifiers.
The studies performed in this thesis provides following conclusions such as

1. The DWT fails to analyse signal of any length.

2. The ST is based on complex calculations and requires more time.

3. The modified DWT is suitable for the analysis of the signal of any length unlike the DWT. This frequency domain analysis also requires more time.

4. The second generation wavelet transform is a simple method. This lifting based time domain analysis is faster than the frequency domain analysis such as the DWT and the MODWT. So, the SGWT is the best method for localisation of distortions in the signals.

5. The data mining based classification methods are suitable for automatic classification power quality disturbance signals. The DT is simple for the implementation. The RF has classified large class of data set properly. The aforementioned methods has worked satisfactorily in real time environment. From the both simulation and the real time environment, it can be inferred that RF is the best

classifier. Similarly, the efficiency of the RF in terms of classification accuracy is better than the DT. Moreover, the SGWT based data set have better classification rate than the others. The aforementioned methods have performed satisfactorily in noisy environment.

6. Different types of real time fault signals have been discriminated properly with these techniques. This classification process has also followed the same procedure like power quality signal analysis, carried out in Chapter-3,4.

7. The SGWT is also a suitable method which discriminates islanding events from the power quality disturbances efficiently. In order to analyze the signals captured at PCC, the ST requires much more time as compared to SGWT.

8. The DT and RF have been working satisfactorily for classification of all the PQ and islanding events.

7.2 Contribution of the Thesis

The contribution of the thesis are briefly outlined in this section as follows:

1. The maximal overlap discrete wavelet transform has been proposed in Chapter-3 for localisation of power quality disturbances.

2. Similarly, the lifting scheme based wavelet transform has proposed in Chapter-3. This scheme has been detected and localised all the ten type of simulated power quality disturbance signals feaster than the other transforms.

3. Data mining based decision tree and ensemble decision tree named as random forest have been proposed in Chapter-4 for classification of large data set. These classification process requires suitable features which are extracted in this Chapter. Suitable features have been extracted from the detail coefficients of the WT variants.

4. The real time PQ signals captured from the single phase and three phase transmission panels are discriminated with the aforementioned methods in Chapter-5.

The feature extraction is followed by classification. The classification process for real time PQ signals is same as that of the synthesized PQ signals.

5. In Chapter-6 different power quality disturbances are injected to $IEEE-14$ bus embedded with the renewable based PV system. The disturbances have been injected at adjacent bus of PV connected bus. The PCC voltage have been captured and processed through the SGWT. The thresh hold lines have been drawn with the extracted features. These features are extracted from the detail coefficients and the threshold lines assisted in discriminating islanding events from the power quality disturbances. The proposed data mining classifiers have been employed for classification of the all the PQ as well as islanding events.

7.3 Scope for Future Research

This research work has looked into some valuable interpretations in the power quality environment. The realisation obtained from this work requires for further investigation as

- **Detection of power quality disturbances** : The work has been based on the power quality disturbance signal analysis which attempts to implement different detection methods for the localization of the disturbance in the signal properly. As the power system operation is instantaneous, so more suitable techniques can be implemented for proper and faster detection of the disturbances.

- **Classification of power quality disturbances** : The classification process can be simple and time effective by reducing features with selection of suitable features. Moreover, different techniques like the Hilbert transform, the extreme machine learning method etc can be developed for the analysis of power quality signals.

- **Discrimination of power quality from others** : The threshold line has been selected for discrimination of power quality events from the islanding events in IEEE−14 bus system embedded with photovoltaic system. So the threshold selection can be implemented for other bus system for the discrimination of power quality events from others.

Appendix A

Specification of Transmission line-1

Table A.1: Specification of Transmission line Simulation Panel for Single phase data collection

Name	Specification
Sending end Transformer	Primary: $0-110-220V$, Secondary: $220V, VA:1250$
Receiving end Transformer	Primary: $0-220V$, Secondary: $110V, 130, 160, 210, 220, 240.VA:1000$
Number of π section	Five each section : $80KMS$
Each section	$L=35.0mH(5Amax)$
Resistance	$R=2.6E$
Capacitance	$C=1.6\mu fd$
Line parameters	$R=0.0325E/KM, L=0.4375mH/KM, C=0.015Mfd/KM, 0.02Mfd$
Line parameters for $400KM$	$R=13E, L=175mH, C=6Mfd, 8Mfd$
Resistance bank	$SW1:2K/20W, SW2:969E/50W, SW3:484E/100W, SW4:242E/200W, SW5:141E/400W$
Inductor Bank	$SW1:15VA, SW2:30VA, SW3:60VA, SW4:60VA, SW5:10mH(unitypf)$
Capacitor Bank	$SW1:1.2Mfd, SW2:3.15Mfd, SW3:6Mfd, SW4:8Mfd, SW5:12.5Mfd$
External Potential Transformer	Primary: $440V$, Secondary: $220V, VA:25$
External Current Transformer	Primary: $10A$, Secondary: $5A, VA:5$
Sending end Power Analyzer :SE1	PT:NIL(Maximum rms is $300V$),PT: primary$-10A$, Secondary$-5A, VA:5$
MCB'S	$MainMCB:20A, 2Poles, ControlMCB:2A,$
Variac	Sending end: $6A$, receiving end: $6A$
Meters	Voltmeter: $0-750VAC$, ammeter: $0-20A$

Appendix B

Specification of Transmission line-2

Table B.1: Specification of Transmission line Simulation Panel for Three phase signal collection

Name	Specification
Mains voltage	$3 \times 380V \pm 10$, $50Hz$
Line parameters	$R = 13ohm, L = 290mH, mutualcapacitanceC_l = 0.5\mu fd,$
Earth return parameter	$R_e = 11$ ohm, $L_e = 250mH$, $C_e = 1\mu fd$
Resistance bank	$46W, 65W, 110W, 160W, 230W, 330W, 400W$
Inductor Bank (power per phase)	$34Var, 48VAr, 83VAr, 121VAr, 171VAr, 242VAr, 297VAr$
Capacitor Bank	$2\mu fd, 3\mu fd, 5\mu fd, 7\mu fd, 10\mu fd, 13\mu fd, 18\mu fd$

Appendix C

IEEE 14-Bus System Data

Table C.1: Transmission line and transformer data

Line number	From bus #	To bus #	Type	r_{hk} p.u	x_{hk} p.u	$b_h = b_k$ p.u	m_{tap} (p.u/p.u)
1	1	2	Line	0.01938	0.05917	0.0528	-
2	1	5	Line	0.05403	0.22304	0.0492	-
3	2	3	Line	0.04699	0.19797	0.0438	-
4	2	4	Line	0.05811	0.17632	0.0374	-
5	2	5	Line	0.05695	0.17388	0.34	-
6	3	4	Line	0.06701	0.17103	0.0346	-
7	4	5	Line	0.01335	0.04211	0.0128	-
8	4	7	Transf.	0	0.20912	0	0.978
9	4	9	Transf.	0	0.55618	0	0.969
10	5	6	Transf.	0	0.25202	0	0.932
11	6	11	Line	0.09498	0.19890	0	-
12	6	12	Line	0.12291	0.25581	0	-
13	6	13	Line	0.06615	0.13027	0	-
14	7	8	Transf.	0	0.17615	0	1.0
15	7	9	Line	0	0.11001	0	-
16	9	10	Line	0.03181	0.08450	0	-
17	9	14	Line	0.12711	0.27038	0	-
18	10	11	Line	0.08205	0.19207	0	-
19	12	13	Line	0.22092	0.19988	0	-
20	13	14	Line	0.17093	0.34802	0	-

Table C.2: Synchronous machine data

Parameter	Unit	Mech.1	Mech.2	Mech.3	Mech.4	Mech.5
Bus Model	#	1	2	3	6	8
S_n	MVA	615	60	60	25	25
x_l	p.u	0.02396	0	0	0.135	0.135
r_a	p.u	0	0.0031	0.0031	0.0041	0.0041
x_d	p.u	0.8979	1.05	1.05	1.25	1.25
$x_d^{'}$	p.u	0.2995	0.185	0.185	0.232	0.232
$x_d^{"}$	p.u	0.23	0.13	0.13	0.12	0.12
$T_{d0}^{'}$	s	7.4	6.1	6.1	4.75	4.75
$T_{d0}^{"}$	s	0.03	0.04	0.04	0.06	0.06
x_q	p.u	0.646	0.98	0.98	1.22	1.22
$x_q^{'}$	p.u	0.646	0.36	0.36	0.715	0.715
$x_q^{"}$	p.u	0.4	0.13	0.13	0.12	0.12
$T_{q0}^{'}$	s	0	0.3	0.3	1.5	1.5
$T_{q0}^{"}$	s	0.033	0.099	0.099	0.21	0.21
D	p.u	2	2	2	2	2
H	MWs/MVA	5.148	6.54	6.54	5.06	5.06

Table C.3: Bus,real,reactive power and shunt data

Bus #	Voltage Rating (kV)	p_l p.u	q_l p.u	b_{sh}
1	69.0	-	-	-
2	69.0	0.217	0.217	-
3	69.0	0.942	0.19	-
4	69.0	0.478	-0.039	-
5	69.0	0.076	0.016	-
6	13.8	0.112	0.075	-
7	13.8	-	-	-
8	18.0	-	-	-
9	13.8	0.295	0.166	0.19
10	13.8	0.09	0.058	-
11	13.8	0.035	0.018	-
12	13.8	0.061	0.016	-
13	13.8	0.135	0.058	-
14	13.8	0.149	0.05	-

Table C.4: Static generator data

Bus #	Type	p_G p.u	v_G p.u	q_G^{max} p.u	q_G^{min} p.u
1	Slack	2.324	1.06	9.9	-9.9
2	pv	0.4	1.045	0.5	-0.4
3	pv	0	1.01	0.4	0
6	pv	0	1.07	0.24	-0.06
8	pv	0	1.09	0.24	-0.06

References

[1] R. C. Dugan, M. F. McGranaghan, and H. W. Beaty, "Electrical power systems quality," *New York, NY: McGraw-Hill*, vol. 1, 1996.

[2] M. E. Meral, *Voltage quality enhancement with custom power park*. PhD thesis, Phd Thesis, Cukurova University, 2009.

[3] "Recommended practice for monitoring electric power quality," tech. rep., Technical report, Draft 5, 1994.

[4] C. Zhao, X. Zhao, and X. Jia, "System innovation for solving power quality problems based on environmental economic," in *Power Systems Conference and Exposition*, pp. 41–45, IEEE PES, 2004.

[5] J. Arrillaga, N. R. Watson, and S. Chen, *Power system quality assessment*. Wiley, 2000.

[6] M. Bollen, "What is power quality?," *Electric Power Systems Research*, vol. 66, no. 1, pp. 5–14, 2003.

[7] P. Janik and T. Lobos, "Automated classification of power-quality disturbances using svm and rbf networks," *IEEE Transactions on Power Delivery*, vol. 21, no. 3, pp. 1663–1669, 2006.

[8] S. Khokhar, A. Mohd Zin, A. Mokhtar, and N. Ismail, "Matlab/simulink based modeling and simulation of power quality disturbances," in *IEEE Conference on Energy Conversion (CENCON)*, pp. 445–450, IEEE, 2014.

[9] D. O. Koval, "Power system disturbance patterns," *IEEE Transactions on Industry Applications*, vol. 26, no. 3, pp. 556–562, 1990.

[10] G.-J. Lee, M. M. Albu, and G. T. Heydt, "A power quality index based on equipment sensitivity, cost, and network vulnerability," *IEEE Transactions on Power Delivery*, vol. 19, no. 3, pp. 1504–1510, 2004.

[11] X. Ma, C. Zhou, and I. Kemp, "Interpretation of wavelet analysis and its application in partial discharge detection," *IEEE Transactions on Dielectrics and Electrical Insulation*, vol. 9, no. 3, pp. 446–457, 2002.

[12] B. K. Panigrahi, A. Baijal, P. Krishna Chaitanya, and P. P. Nayak, "Power quality analysis using complex wavelet transform," in *Joint International Conference on Power Electronics, Drives and Energy Systems (PEDES) and 2010 Power India*, pp. 1–5, IEEE, 2010.

[13] F. Choong, M. Reaz, and F. Mohd-Yasin, "Advances in signal processing and artificial intelligence technologies in the classification of power quality events: a survey," *Electric Power Components and Systems*, vol. 33, no. 12, pp. 1333–1349, 2005.

[14] D. Gabor, "Theory of communication. part 1: The analysis of information," *Journal of the Institution of Electrical Engineers-Part III: Radio and Communication Engineering*, vol. 93, no. 26, pp. 429–441, 1946.

[15] P. S. Wright, "Short-time fourier transforms and wigner-ville distributions applied to the calibration of power frequency harmonic analyzers," *IEEE Transactions on Instrumentation and Measurement*, vol. 48, no. 2, pp. 475–478, 1999.

[16] T. Zhu, "Detection and characterization of oscillatory transients using matching pursuits with a damped sinusoidal dictionary," *IEEE Transactions on Power Delivery*, vol. 22, no. 2, pp. 1093–1099, 2007.

[17] T. Lin and A. Dom, "On power quality indices and real time measurement," *IEEE Transactions on Power Delivery*, vol. 20, no. 4, pp. 2552–2562, 2005.

[18] Y. Shin, A. C. Parsons, E. J. Powers, and W. Grady, "Time-frequency analysis of power system disturbance signals for power quality," in *Power Engineering Society Summer Meeting*, vol. 1, pp. 402–407, IEEE, 1999.

[19] F. Jurado and J. R. Saenz, "Comparison between discrete stft and wavelets for the analysis of power quality events," *Electric Power Systems Research*, vol. 62, no. 3, pp. 183–190, 2002.

[20] S. G. Mallat, "A theory for multiresolution signal decomposition: the wavelet representation," *IEEE Transactions on Pattern Analysis and Machine Intelligence,*, vol. 11, no. 7, pp. 674–693, 1989.

[21] R. Aggarwal and C. Kim, "Wavelet transforms in power systems," *Power Engineering Journal*, pp. 81–87, 2000.

[22] R. Polikar, "The engineer's ultimate guide to wavelet analysis-the wavelet tutorial," 1996.

[23] S. Santoso, E. J. Powers, and W. Grady, "Power quality disturbance data compression using wavelet transform methods," *IEEE Transactions on Power Delivery*, vol. 12, no. 3, pp. 1250–1257, 1997.

[24] O. Poisson, P. Rioual, and M. Meunier, "Detection and measurement of power quality disturbances using wavelet transform," *IEEE Transactions on Power Delivery*, vol. 15, no. 3, pp. 1039–1044, 2000.

[25] B. Perunici, M. Mallini, Z. Wang, and Y. Liu, "Power quality disturbance detection and classification using wavelets and artificial neural networks," in *8th International Conference on Harmonics and Quality of Power Proceedings*, vol. 1, pp. 77–82, IEEE, 1998.

[26] A. Gaouda, M. Salama, M. Sultan, and A. Chikhani, "Power quality detection and classification using wavelet-multiresolution signal decomposition," *IEEE Transactions on Power Delivery*, vol. 14, no. 4, pp. 1469–1476, 1999.

[27] F. Costa and B. A. Souza, "Fault-induced transient analysis for realtime fault detection and location in transmission lines," in *International Conference on Power Systems Transients*, 2011.

[28] F. Bezerra Costa, "Fault-induced transient detection based on real-time analysis of the wavelet coefficient energy," *IEEE Transactions on Power Delivery*, vol. 29, no. 1, pp. 140–153, 2014.

[29] P. Dash, B. Panigrahi, and G. Panda, "Power quality analysis using s-transform," *IEEE Transactions on Power Delivery*, vol. 18, no. 2, pp. 406–411, 2003.

[30] C. Bhende, S. Mishra, and B. Panigrahi, "Detection and classification of power quality disturbances using s-transform and modular neural network," *Electric Power Systems Research*, vol. 78, no. 1, pp. 122–128, 2008.

[31] I. W. Lee and P. K. Dash, "S-transform-based intelligent system for classification of power quality disturbance signals," *IEEE Transactions on Industrial Electronics*, vol. 50, no. 4, pp. 800–805, 2003.

[32] P. Dash and M. Chilukuri, "Hybrid s-transform and kalman filtering approach for detection and measurement of short duration disturbances in power networks," *IEEE Transactions on Instrumentation and Measurement*, vol. 53, no. 2, pp. 588–596, 2004.

[33] P. Dash and M. Chilukuri, "Hybrid s-transform and kalman filtering approach for detection and measurement of short duration disturbances in power networks," *IEEE Transactions on Instrumentation and Measurement*, vol. 53, no. 2, pp. 588–596, 2004.

[34] B. K. Panigrahi, P. K. Dash, and J. Reddy, "Hybrid signal processing and machine intelligence techniques for detection, quantification and classification of power quality disturbances," *Engineering Applications of Artificial Intelligence*, vol. 22, no. 3, pp. 442–454, 2009.

[35] M. E. Salem, A. Mohamed, and S. A. Samad, "Rule based system for power quality disturbance classification incorporating s-transform features," *Expert Systems with Applications*, vol. 37, no. 4, pp. 3229–3235, 2010.

[36] R. Brown, R. Frayne, *et al.*, "A fast discrete s-transform for biomedical signal processing," in *30th Annual International Conference of the IEEE Engineering in Medicine and Biology Society*, pp. 2586–2589, IEEE, 2008.

[37] B. Biswal, P. K. Dash, and B. K. Panigrahi, "Non-stationary power signal processing for pattern recognition using hs-transform," *Applied Soft Computing*, vol. 9, no. 1, pp. 107–117, 2009.

[38] A. G. Hafez and E. Ghamry, "Geomagnetic sudden commencement automatic detection via modwt," *IEEE Transactions on Geoscience and Remote Sensing,*, vol. 51, no. 3, pp. 1547–1554, 2013.

[39] G. P. Nason and B. W. Silverman, "The stationary wavelet transform and some statistical applications," *LECTURE NOTES IN STATISTICS-NEW YORK-SPRINGER*, pp. 281–281, 1995.

[40] R. Coifman and D. Donoho, "Translation-invariant de-noising, in wavelets and statistics," 1995.

[41] J.-C. Pesquet, H. Krim, and H. Carfantan, "Time-invariant orthonormal wavelet representations," *IEEE Transactions on Signal Processing*, vol. 44, no. 8, pp. 1964–1970, 1996.

[42] D. B. Percival and H. O. Mofjeld, "Analysis of subtidal coastal sea level fluctuations using wavelets," *Journal of the American Statistical Association*, vol. 92, no. 439, pp. 868–880, 1997.

[43] T. Zafar and W. Morsi, "Power quality and the un-decimated wavelet transform: An analytic approach for time-varying disturbances," *Electric Power Systems Research*, vol. 96, pp. 201–210, 2013.

[44] D. Alves, C. Neto, F. Costa, and R. Ribeiro, "Power measurement using the maximal overlap discrete wavelet transform," in *11th IEEE/IAS International Conference on Industry Applications (INDUSCON)*, pp. 1–7, IEEE, 2014.

[45] S. Ahmad, A. Popoola, and K. Ahmad, "Wavelet-based multiresolution forecasting," *Technical Report University of Surrey*, 2005.

[46] A. Kumar, L. K. Joshi, A. Pal, and A. Shukla, "Modwt based time scale decomposition analysis of bse and nse indexes financial time series," *International Journal of Mathematical Analysis*, vol. 5, no. 27, pp. 1343–1352, 2011.

[47] W. Sweldens, "The lifting scheme: A custom-design construction of biorthogonal wavelets," *Applied and Computational Harmonic Analysis*, vol. 3, no. 2, pp. 186–200, 1996.

[48] I. Daubechies and W. Sweldens, "Factoring wavelet transforms into lifting steps," *Journal of Fourier Analysis and Applications*, vol. 4, no. 3, pp. 247–269, 1998.

[49] X. Song, C. Zhou, D. M. Hepburn, G. Zhang, and M. Michel, "Second generation wavelet transform for data denoising in pd measurement," *IEEE Transactions on Dielectrics and Electrical Insulation,*, vol. 14, no. 6, pp. 1531–1537, 2007.

[50] K. Andra, C. Chakrabarti, and T. Acharya, "A vlsi architecture for lifting-based forward and inverse wavelet transform," *IEEE Transactions on Signal Processing*, vol. 50, no. 4, pp. 966–977, 2002.

[51] T. Zhu, S. Tso, and K. Lo, "Wavelet-based fuzzy reasoning approach to power-quality disturbance recognition," *IEEE Transactions on Power Delivery*, vol. 19, no. 4, pp. 1928–1935, 2004.

[52] B. Biswal, M. Biswal, S. Mishra, and R. Jalaja, "Automatic classification of power quality events using balanced neural tree," *IEEE Transactions on Industrial Electronics*, vol. 61, no. 1, pp. 521–530, 2014.

[53] B. Panigrahi and V. R. Pandi, "Optimal feature selection for classification of power quality disturbances using wavelet packet-based fuzzy k-nearest neighbour algorithm," *IET Generation, Transmission and Distribution*, vol. 3, no. 3, pp. 296–306, 2009.

[54] H. Eristi, A. Ucar, and Y. Demir, "Wavelet-based feature extraction and selection for classification of power system disturbances using support vector machines," *Electric Power Systems Research*, vol. 80, no. 7, pp. 743–752, 2010.

[55] C.-Y. Lee and Y.-X. Shen, "Optimal feature selection for power-quality disturbances classification," *IEEE Transactions on Power Delivery*, vol. 26, no. 4, pp. 2342–2351, 2011.

[56] A. S. Yilmaz, A. Subasi, M. Bayrak, V. M. Karsli, and E. Ercelebi, "Application of lifting based wavelet transforms to characterize power quality events," *Energy Conversion and Management*, vol. 48, no. 1, pp. 112–123, 2007.

[57] A. K. Ghosh and D. L. Lubkeman, "The classification of power system disturbance waveforms using a neural network approach," *IEEE Transactions on Power Delivery*, vol. 10, no. 1, pp. 109–115, 1995.

[58] Y. Shi *et al.*, "Particle swarm optimization: developments, applications and resources," in *Proceedings of the 2001 Congress on Evolutionary Computation*, vol. 1, pp. 81–86, IEEE, 2001.

[59] M. E. El-Hawary, *Electric power applications of fuzzy systems.* Wiley-IEEE Press, 1998.

[60] W. A. Ibrahim, M. Morcos, and D. Kreiss, "An adaptive neuro-fuzzy intelligent tool and expert system for power quality analysis. i. an introduction," in *IEEE Power Engineering Society Summer Meeting*, vol. 1, pp. 493–498, IEEE, 1999.

[61] P. Dash, S. Mishra, M. Salama, and A. Liew, "Classification of power system disturbances using a fuzzy expert system and a fourier linear combiner," *IEEE Transactions on power Delivery*, vol. 15, no. 2, pp. 472–477, 2000.

[62] S. Hasheminejad, S. Esmaeili, and S. Jazebi, "Power quality disturbance classification using s-transform and hidden markov model," *Electric Power Components and Systems*, vol. 40, no. 10, pp. 1160–1182, 2012.

[63] M. B. I. Reaz, F. Choong, M. S. Sulaiman, F. Mohd-Yasin, and M. Kamada, "Expert system for power quality disturbance classifier," *IEEE Transactions on Power Delivery*, vol. 22, no. 3, pp. 1979–1988, 2007.

[64] T. Abdel-Galil, E. El-Saadany, A. Youssef, and M. Salama, "Disturbance classification using hidden markov models and vector quantization," *IEEE Transactions on Power Delivery*, vol. 20, no. 3, pp. 2129–2135, 2005.

[65] J. Chung, E. J. Powers, W. M. Grady, and S. C. Bhatt, "Power disturbance classifier using a rule-based method and wavelet packet-based hidden markov model," *IEEE Transactions on Power Delivery*, vol. 17, no. 1, pp. 233–241, 2002.

[66] H. Dehghani, B. Vahidi, R. Naghizadeh, and S. Hosseinian, "Power quality disturbance classification using a statistical and wavelet-based hidden markov model with dempster–shafer algorithm," *International Journal of Electrical Power and Energy Systems*, vol. 47, pp. 368–377, 2013.

[67] S. R. Safavian and D. Landgrebe, "A survey of decision tree classifier methodology," 1990.

[68] S. Samantaray, "Decision tree-initialised fuzzy rule-based approach for power quality events classification," *IET Generation, Transmission and Distribution*, vol. 4, no. 4, pp. 530–537, 2010.

[69] M. Biswal and P. K. Dash, "Measurement and classification of simultaneous power signal patterns with an s-transform variant and fuzzy decision tree," *IEEE Transactions on Industrial Informatics*, vol. 9, no. 4, pp. 1819–1827, 2013.

[70] R. Kumar, B. Singh, D. Shahani, A. Chandra, and K. Al-Haddad, "Recognition of power-quality disturbances using s-transform-based ann classifier and rule-based decision tree," *IEEE Transactions on Industry Applications*, vol. 51, no. 2, pp. 1249–1258, 2015.

[71] L. Breiman, "Random forests," *Machine learning*, vol. 45, no. 1, pp. 5–32, 2001.

[72] S. Samantaray, I. Kamwa, and G. Joos, "Ensemble decision trees for phasor measurement unit-based wide-area security assessment in the operations time frame," *IET Generation, Transmission and Distribution*, vol. 4, no. 12, pp. 1334–1348, 2010.

[73] V. Menon and M. H. Nehrir, "A hybrid islanding detection technique using voltage unbalance and frequency set point," *IEEE Transactions on Power Systems*, vol. 22, no. 1, pp. 442–448, 2007.

[74] S.-I. Jang and K.-H. Kim, "An islanding detection method for distributed generations using voltage unbalance and total harmonic distortion of current," *IEEE Transactions on Power Delivery*, vol. 19, no. 2, pp. 745–752, 2004.

[75] H. Wang, F. Liu, Y. Kang, J. Chen, and X. Wei, "Experimental investigation on non detection zones of active frequency drift method for anti-islanding," in *33rd Annual Conference of the IEEE Industrial Electronics Society IECON*, pp. 1708–1713, IEEE, 2007.

[76] F. Liu, X. Lin, Y. Kang, Y. Zhang, and S. Duan, "An active islanding detection method for grid-connected converters," in *3rd IEEE Conference on Industrial Electronics and Applications*, pp. 734–737, IEEE, 2008.

[77] S. R. Mohanty, N. Kishor, P. K. Ray, and J. P. Catalo, "Comparative study of advanced signal processing techniques for islanding detection in a hybrid distributed generation system," *IEEE Transactions on Sustainable Energy*, vol. 6, no. 1, pp. 122–131, 2015.

[78] W. Freitas, W. Xu, C. M. Affonso, and Z. Huang, "Comparative analysis between rocof and vector surge relays for distributed generation applications," *IEEE Transactions on Power Delivery*, vol. 20, no. 2, pp. 1315–1324, 2005.

[79] H. Zeineldin and J. L. Kirtley Jr, "Performance of the ovp/uvp and ofp/ufp method with voltage and frequency dependent loads," *IEEE Transactions on Power Delivery*, vol. 24, no. 2, pp. 772–778, 2009.

[80] X. Zhu, C. Du, G. Shen, M. Chen, and D. Xu, "Analysis of the non-detection zone with passive islanding detection methods for current control dg system," in *Twenty-Fourth Annual IEEE Applied Power Electronics Conference and Exposition, APEC*, pp. 358–363, IEEE, 2009.

[81] C.-T. Hsieh, J.-M. Lin, and S.-J. Huang, "Enhancement of islanding-detection of distributed generation systems via wavelet transform-based approaches," *International Journal of Electrical Power and Energy Systems*, vol. 30, no. 10, pp. 575–580, 2008.

[82] M. Hanif, M. Basu, and K. Gaughan, "Development of en50438 compliant wavelet-based islanding detection technique for three-phase static distributed generation systems," *IET Renewable Power Generation*, vol. 6, no. 4, pp. 289–301, 2012.

[83] P. K. Ray, S. R. Mohanty, and N. Kishor, "Disturbance detection in grid-connected distributed generation system using wavelet and s-transform," *Electric Power Systems Research*, vol. 81, no. 3, pp. 805–819, 2011.

[84] R. A. Brown and R. Frayne, "A fast discrete s-transform for biomedical signal processing," in *30th Annual International Conference of the IEEE Engineering in Medicine and Biology Society*, pp. 2586–2589, IEEE, 2008.

[85] K. C. Hwan and R. Aggarwal, "Wavelet transform in power systems: Part 1 general introduction to the wavelet transform," *IEE–Power Engineering Journal*, vol. 14, no. 2, pp. 81–87, 2000.

[86] L. Satish and B. Nazneen, "Wavelet-based denoising of partial discharge signals buried in excessive noise and interference," *IEEE Transactions on Dielectrics and Electrical Insulation*, vol. 10, no. 2, pp. 354–367, 2003.

[87] S. Santoso, E. J. Powers, W. M. Grady, and P. Hofmann, "Power quality assessment via wavelet transform analysis," *IEEE Transactions on Power Delivery,*, vol. 11, no. 2, pp. 924–930, 1996.

[88] M. Misti, Y. Misti, G. Oppenheim, and J. Poggi, "Wavelet toolbox manualusers guide," *The Math Works Inc., USA*, 1996.

[89] X. Zhou, C. Zhou, and I. Kemp, "An improved methodology for application of wavelet transform to partial discharge measurement denoising," *IEEE Transactions on Dielectrics and Electrical Insulation,*, vol. 12, no. 3, pp. 586–594, 2005.

[90] R. G. Stockwell, L. Mansinha, and R. Lowe, "Localization of the complex spectrum: the s transform," *IEEE Transactions on Signal Processing,*, vol. 44, no. 4, pp. 998–1001, 1996.

[91] D. B. Percival and A. T. Walden, "Wavelet methods for time series analysis (cambridge series in statistical and probabilistic mathematics)," 2000.

[92] A. Manjunath and H. Ravikumar, "Comparison of discrete wavelet transform (dwt), lifting wavelet transform (lwt) stationary wavelet transform (swt) and s-transform in power quality analysis," *European Journal of Scientific Research*, vol. 39, no. 4, pp. 569–576, 2010.

[93] M. Masoum, S. Jamali, and N. Ghaffarzadeh, "Detection and classification of power quality disturbances using discrete wavelet transform and wavelet networks," *IET Science, Measurement and Technology*, vol. 4, no. 4, pp. 193–205, 2010.

[94] M. B. I. Reaz, F. Choong, M. S. Sulaiman, F. Mohd-Yasin, and M. Kamada, "Expert system for power quality disturbance classifier," *IEEE Transactions on Power Delivery*, vol. 22, no. 3, pp. 1979–1988, 2007.

[95] S. Mohanty, A. Pradhan, and A. Routray, "A cumulative sum-based fault detector for power system relaying application," *IEEE Transactions on Power Delivery*, vol. 23, no. 1, pp. 79–86, 2008.

[96] R. Chattamvelli, *Data mining methods*. Alpha Science International, Ltd, 2009.

[97] R. Kohavi and J. R. Quinlan, "Data mining tasks and methods: Classification: decision-tree discovery," in *Handbook of Data Mining and Knowledge Discovery*, pp. 267–276, Oxford University Press, Inc., 2002.

[98] G. Williams, *Data mining with Rattle and R: the art of excavating data for knowledge discovery*. Springer Science and Business Media, 2011.

[99] J. Han, M. Kamber, and J. Pei, *Data mining: concepts and techniques*. Elsevier, 2011.

[100] N. Poona and R. Ismail, "Using boruta-selected spectroscopic wavebands for the asymptomatic detection of fusarium circinatum stress," 2014.

[101] S. Kalyani and K. S. Swarup, "Classification and assessment of power system security using multiclass svm," *IEEE Transactions on Systems, Man, and Cybernetics, Part C: Applications and Reviews*, vol. 41, no. 5, pp. 753–758, 2011.

[102] M. Chilukuri, P. Dash, and K. Basu, "Time-frequency based pattern recognition technique for detection and classification of power quality disturbances," in *IEEE Region 10 Conference TENCON*, vol. 100, pp. 260–263, IEEE, 2004.

[103] H. Zhang, P. Liu, and O. Malik, "Detection and classification of power quality disturbances in noisy conditions," in *IEE Proceedings-Generation, Transmission and Distribution*, vol. 150, pp. 567–572, IET, 2003.

[104] F. Zhao and R. Yang, "Power-quality disturbance recognition using s-transform," *IEEE Transactions on Power Delivery*, vol. 22, no. 2, pp. 944–950, 2007.

[105] S. R. Mohanty, N. Kishor, P. K. Ray, and J. P. Catalão, "Comparative study of advanced signal processing techniques for islanding detection in a hybrid distributed generation system," *IEEE Transactions on Sustainable Energy*, vol. 6, no. 1, pp. 122–131, 2015.

[106] B. S. Kumar and K. Sudhakar, "Performance evaluation of 10 mw grid connected solar photovoltaic power plant in india," *Energy Reports*, vol. 1, pp. 184–192, 2015.

[107] R. O. Gonzalez, J. C. S. Saavedra, O. C. Castillo, and V. G. Ortega, "Comparison controllers for inverter operating in island mode in microgrids with linear and nonlinear loads," *IEEE Latin America Transactions*, vol. 12, no. 8, pp. 1441–1448, 2014.

[108] F. Milano, *Power system modelling and scripting*. Springer Science and Business Media, 2010.

Dissemination

Journals

1. S. Upadhyaya, S. Mohanty, and C.N. Bhende, "Hybrid methods for fast detection and characterization of power quality disturbances ," *Journal of Control, Automation and Electrical Systems*, vol. 26, pp. 556–566, 2015.

2. S. Upadhyaya and S. Mohanty, "Fast Methods for Power Quality Analysis ," *International Journal of Emerging Electric Power Systems*,(Communicated)

3. S. Upadhyaya and S. Mohanty, "Power quality disturbance localization using maximal overlap discrete wavelet transform," in *IEEE Transactions on Industry Applications*,(Communicated)

4. S. Upadhyaya, S. Mohanty, and C.N. Bhende, "Islanding and Power Quality Disturbance Detection Using Wavelet Based Signal Processing," *IET Electric Power Applications*,(Communicated)

Conference

1. S. Upadhyaya and S. Mohanty, "Power quality disturbance detection using wavelet based signal processing," in *2013 Annual IEEE India Conference (INDICON)*. IEEE, Dec 2013, pp. 1–6.

2. S. Upadhyaya and S. Mohanty, "Power quality disturbance localization using maximal overlap discrete wavelet transform," in *IEEE India Conference (INDICON)*. IEEE, Dec 2015, pp. 1–6. (Recommonded for review in IEEE Transactions on Industry Applications)

3. S. Upadhyaya and S. Mohanty, "Localization and Classification of Power Quality Disturbances using Maximal Overlap Discrete Wavelet Transform and Data Mining based Classifiers," in *IFAC-Papers On Line*. Elsevier, Feb. 2016, pp. 437–442.

Author's Biography

Swarnabala Upadhyaya was born to Mr. Purnachandra Upadhyaya and Mrs. Sabitri Upadhyaya in Balasore, Odisha, India. She completed her B.Tech degree in Electrical Engineering from Orissa school of Mining Engineering (Government College of Engineering, Keonjhar), Odisha in 2008. Then she joined as Lecturer in Seemanta Engineering College, Baripada for one year. She obtained M.tech degree in Veer Surendra Sai University of Technology, Burla, Odisha in 2011 with the same stream. Then she joined as Asst.Prof. in Eastern College of Science and Technology. After six month she took admission for Ph.D at National Institute of Technology Rourkela in 2012. Her research area of interests include power quality, power systems, wavelet transform and data mining techniques.

Communication Details:
*A*ddress: Department of Electrical Engineering, National
Institute of Technology Rourkela,
Odisha, PIN: 769008.
e-mail: swarnabala.u@gmail.com